Investigating quantum phenomena in nano- and micromechanical oscillators

Chaitanya Joshi, M.Sc. Physics*

Submitted for the degree of Doctor of Philosophy

Heriot-Watt University

EPS/IPaQS

Group of Quantum Information Theory

and

Quantum Optics and Cold Atoms Group

October 2012

ABSTRACT

This thesis theoretically investigates quantum features in nano- and micromechanical oscillators. The thesis aims at proposing novel schemes to prepare mesoscopic mechanical systems in non-classical states including entangled states. The main emphasis of the work is to understand genuine quantum features in coupled harmonic oscillators with infinite dimensional Hilbert spaces. With the recent experimental breakthroughs in achieving the ground state of mesoscopic mechanical systems, the time is now ripe to investigate in detail a full quantum description of such mesoscopic mechanical systems. Thus, the main emphasis of the thesis is on probing salient quantum features in coupled mechanical systems that are assumed to be prepared in vibrational states close to their quantum ground states. A major part of the thesis makes use of various theoretical techniques widely used in quantum optics and quantum information. The majority of the results reported in this thesis involves analytical calculations augmented with numerical investigations. We believe many of the results obtained will be of interest to researchers with background in quantum optics and quantum information and with research interest in the quantum-classical crossover in continuous variable systems.

DEDICATION

...To my parents, my brother and my *Papaji****, who by no doubt are best in the world***

ACKNOWLEDGEMENT

The work accomplished in this thesis has been made possible only because of constant support and encouragement of my thesis supervisors Dr. Patrik Öhberg and Dr. Erika Andersson, who always stood by me over the last three years. The years spent during my doctoral degree will always be cherished by me as one of the most enriching years of my life, both professionally and personally. Needless to say this would have not been made possible without the guidance of Patrik and Erika. Patrik and Erika always gave me the freedom to explore my own research interests and thus helped me made myself more self-dependent. During any of those days of distress and disbelief (believe me there were few of them !), Patrik and Erika always had open doors for me. This included any advice on Physics or life in general. I thank them whole heartedly for all their support, kindness, generosity and above all believing in me for all these years.

There are many other people who have immensely contributed towards the completion of this thesis. In particular I am indebted to Prof. Mats Jonson, Dr. Michael Hall, Dr. Jonas Larson for numerous discussions on Physics. I thank all of them for teaching me some wonderful Physics along with enlightening me with their rich professional and personal experiences. I am extremely grateful to Prof. G. J. Milburn and Dr. Brendon Lovett for kindly agreeing to examine my thesis and for all the constructive

criticisms and extremely useful feedback. I am also indebted to the QUISCO group for organising many insightful and thought provoking meetings over the last three years. I would like to thank Overseas Research Student Award Scheme for providing me with the financial support during my PhD. I would also like to thank Prof. A. H. Greenaway for providing me with some additional financial grants and Prof. Rebecca Cheung for kindly agreeing to be my secondary supervisor. I am also indebted to Dr. Sankalpa Ghosh for being a constant source of motivation and guidance. My gratitude to my high school teacher Mr. Virender for all the encouragement and support.

At this stage I would like to thank the organisers of the Les Houches Summer School on 'Quantum Machines' for providing me with an opportunity to learn some interesting physics amidst the blissful Alps. I would also like to thank Prof. D. Bouwmeester for inviting me to attend the workshop on 'Quantum to classical transition in mechanical systems' in Leiden. I am also grateful to Prof. G. J. Milburn for providing me with a very warm hospitality during my research visit to the University of Queensland. I am also grateful to Michael and Robyn for providing me with a lovely hospitality during my stay in Brisbane. I also owe many thanks to all the wonderful people I have met in various conferences and summer schools I attended over the last three years.

During my stay in Edinburgh, I met some wonderful people and made few life long friends. I am thankful to all my friends and colleagues whose constant support and encouragement helped me to keep running this doctoral marathon. I am thankful to Adetunmise, Akhil, Ankur Raj, Ankur Pandey, Aurora, Frauke, Kusum, Laura, Massimo, Matthew, Nabin, Nathan and Vedran for sharing a wonderful time with me. I am thankful to Giuseppe and Francesca for all those lovely Italian dinners and the warm hospitality bestowed on me. Best of luck mates for your future inning. Special thanks to Mr. Mundo for always being *too much* (not true !) and for all those late afternoon long *discussions*. Something important will be missing without the mentioning of Ms. Butera, for always being kind, supportive and helpful. Ms. Butera, thank you for being one of the best friend and for sharing as well as keeping

all those *secrets*, the quality time spent with you will always be cherished by me.

Last but certainly not the least, I would like to thank my parents, brother Ujjwal, Chacha and my whole family for all the support, warmth, love and care. It is only because of their unconditional love, sacrifices and support it has become possible for me to reach up to this level. I pray to almighty that I shall always live up to their expectations in life. My sincere regards to my dearest *Papaji* for being one of the strongest pillars of my life and always infusing me with confidence and motivation. This thesis will be incomplete without the mentioning of my dearest *Baboo*, *Chotti Bua* and my loving *Badi Mummy*, whose everlasting sweet memories will always provide me with the warm tender touch in my life. Thank you all !

CONTENTS

LIST OF FIGURES

LIST OF PUBLICATIONS

The work carried out in this thesis resulted in following publications:

1. C. Joshi, A. Hutter, F. E. Zimmer, M. Jonson, E. Andersson and P. Öhberg: Quantum entanglement of nanocantilevers, *Phys. Rev. A* **82**, 043846 (2010).

2. C. Joshi, M. Jonson, E. Andersson and P. Öhberg: Quantum entanglement of anharmonic oscillators, *J. Phys. B: At. Mol. Opt. Phys.* **44**, 245503 (2011).

3. C. Joshi, J. Larson, M. Jonson, E. Andersson and P. Öhberg: Entanglement of distant optomechanical systems, *Phys. Rev. A* **85**, 033805 (2012).

CHAPTER 1

QUANTUM-CLASSICAL BORDER ?

It is commonly believed that classical mechanics governs the macroscopic world while the microscopic world comes under the paradigm of quantum mechanics. This assertion is not very convincing, especially in the light of the fact that there is nothing intrinsic in quantum mechanics that forbids it from governing the macroscopic world. Over the years, this particular notion has been very strongly debated and there are long standing arguments to ascertain the validity of quantum mechanics in the macroscopic world [1].

However, we all agree that normally we do not see quantum superpositions at everyday length scale and this might prompt us to question the validity of quantum mechanics in our 'classical' world. A widely accepted notion of quantum-classical crossover is the concept of environment-induced decoherence [2]. Decoherence induced by the environment is widely assumed to be the cause of degradation of any quantum system to its classical counterpart. Another interpretation from Penrose rules out the possibility of macroscopic superpositions, which he attributes to the gravitation induced state collapse [3]. He argues that a massive object that exists in two or more places simultaneously interacts with itself through gravity in a way that 'tugs' it to one place or the other. Many world-leading physicists including Penrose have had serious

disagreements with some of the postulates of quantum theory, but for the sake of the present work we assume that the quantum theory *is* correct. Building on this assertion, in the present work we want to explore the possibility to see genuine quantum effects in the mesoscopic domain.

It is now commonly believed that the vanishing of quantum superpositions is a result of our inability to perfectly isolate the system of interest from its surroundings and this gives rise to decoherence. Decoherence thus mainly arises as a result of interaction of a quantum system with its environment which 'entangles' the two and redistributes the quantum coherence over so many degrees of freedom so as to render it unobservable [4].

Mesoscopic or even macroscopic systems could be the excellent candidates to study the unavoidable effect of decoherence. This is mainly because of the available many degrees of freedom, these big systems can store a large amount of energy, which eventually undergoes decoherence and gets dissipated as thermal radiation. Such experimental studies on macroscopic molecules such as C_{70} have already been carried out, and found to be in good conformity with theoretical predictions [4]. Nonetheless, in most cases, the negative influence of an environment on any quantum system becomes magnified at the macroscopic scale, which eventually results in reducing any quantum coherence to an incoherent mixture.

This motivates us to ask ourselves a difficult but interesting question about the limits of the quantum theory : Is it really possible to conceive a situation where we can see a quantum superposition state in the mesoscopic or macroscopic domain, and if not, then what are the 'boundaries' of the quantum theory ? Precisely setting the boundary between the quantum and the classical world has remained one of the most difficult conundrums for the physicists for a long time.

Over the past few years, probing of quantum-classical border has developed into an exciting research area with high impetus both from theory and experiments. To quote

Zurek, "...small gaps in the landscape of the border territory between the quantum and the classical were actually not that small after all and that they presented excellent opportunities for further advances" [2]. Thus studies related to understanding quantum-classical crossover are important not only from a theoretical point of view, but also have huge potential to improve our understanding of various experimental results and most importantly to understand the mysteries of Nature.

Recently we have witnessed some fascinating experimental realisations confirming some of the strange quantum effects [5, 6]. This fray of studying the quantum properties of mesoscopic systems includes proposals for entanglement generation between Bose-Einstein condensates [7] and quantum coherence between atomic ensembles [8]. The unprecedented level of sophistication achieved in manipulating and controlling mesoscopic and even macroscopic systems has resulted in a far better understanding of their inherent quantum nature.

In this quest for studying the level of 'quantumness' present in mesoscopic objects, tremendous progress has been achieved in exploring the quantum regime of nano- and micromechanical systems [9]. Physical systems as diverse as nanomechanical oscillators, mirrors, micro cavities and nano-membranes are excitingly being explored to study their quantum properties. These mechanical systems offer a very promising playground to study the quantum-classical crossover. This is mainly because these miniaturised vibrating systems contain macroscopic number of atoms and can be fabricated to have very high resonant frequencies and exceedingly large quality factors [10], thereby guarding against the effects of decoherence.

If quantum mechanics is to be believed then a vibrating mechanical system should lose or gain energy in discrete dollops proportional to its fundamental vibrational frequency. But, with the commonly encountered temperatures of the surroundings and low vibrational frequencies of mechanical oscillators, normally the thermal energy overpowers the quantum contribution. Thus at ordinary ambience, mechanical systems wiggle under the action of thermal energy and thereby making it hard to

notice any interesting quantum phenomenon.

Nevertheless, with the nanomechanical oscillators' frequencies approaching GHz range and their length scale entering in the nano-regime, the man made nanomechanical systems needs to be cooled to temperatures $\sim$ mK. In this temperature regime, the quantum energy $\hbar\omega$ will be comparable to the thermal energy k_BT. Such temperatures should allow one to observe truly quantum mechanical phenomena, such as preparing mechanical oscillators in number states [11], squeezed states [12, 13] and Schrödinger's cat states [14, 15, 16]. Mesoscopic mechanical systems could thus be the ideal candidates with the potential to help us solve the puzzle of the quantum-classical transition.

With the fast paced developments in the fabrication and manipulation techniques of nano- and micromechanical systems, it appears very likely that soon we will enter in an era where the dynamics of nano- and micromechanical systems will be fully governed by the laws of quantum mechanics and classical description will thus become inadequate. Although there have already been attempts to envisage quantum mechanical phenomena on a mesoscopic scale, the possibility to achieve the quantum ground state of a mesoscopic mechanical system has remained one of the prerequisite to explore its 'quantum-world' any further. The advancement in techniques such as laser cooling of mechanical resonators [17, 18, 19, 20] has brought quantum state preparation within experimental reach. Very recently, O'Connell and co-workers were able to cryogenically cool a mechanical resonator to its quantum ground state, and were also successful in strongly coupling it to a superconducting qubit to read out the motion of the resonator [21]. They were triumphant in controllably creating a single phonon excitation in the resonator, thereby setting a first step in attaining a complete quantum control of a mechanical system. Adding another milestone to the rapidly progressing field of nano- and micromechanical oscillators, Jaspen and co-workers have recently demonstrated the laser cooling of the vibrational motion of a nanomechanical oscillator to its quantum ground state [22]. These successful ex-

perimental results heralds a new era in investigating the quantum behaviour of nano- and micromechanical systems.

The advancements in techniques for ground state cooling of mechanical resonators has not only favoured the quantum state preparation of nano- and micromechanical systems, but has also fuelled a surge of interest in physically coupling nano- and micromechanical systems to other quantum optical systems with better quantum control. The list include trapped ions in a nano-trap [23], atomic Bose-Einstein condensates [24], Cooper pair boxes (CPB) [25] and electronic spin degrees of freedom [26]. A strong motivation to fabricate hybrid quantum systems is to realise the idea of constructing quantum interfaces and quantum memories for quantum information processing [27, 28] and quantum limited displacement measurements [29]. From a fundamental point of view, testing EPR type [30] non-local correlations in mesoscopic mechanical systems is of great interest too.

Entanglement is one of *the* characteristic traits of quantum mechanics. An entangled state of a composite quantum system possesses so strong correlations that cannot be explained by a classical theory. Entanglement is a weird concept where two particles remain intimately connected, even when separated over vast distances. To ensure the existence of quantum mechanical correlations and distinguish them from classical correlations the entangled pair must be measured in different bases. In response to Einstein, Podolsky and Rosen (EPR) argument that quantum mechanics was incomplete [30], in a groundbreaking work, John S. Bell came up with a restriction which all classically correlated states must satisfy [31]. After providing a mathematical formulation of locality and realism, Bell showed specific cases where the main idea propounded in [30] would be inconsistent with the predictions of quantum mechanics.

According to the Copenhagen interpretation of quantum mechanics, the entangled state is indefinite until measured. Quantum entanglement is a form of quantum superposition. When a measurement is made and it causes one member of an entangled pair to take on a definite value (e.g., right circular polarization), the other member

of this entangled pair will at any subsequent time be found to have taken the appropriately correlated value (e.g., left circular polarization). Thus, there is a correlation between the results of measurements performed on entangled pairs, and this correlation is observed even though the entangled pair may have been separated by arbitrarily large distances. Entangled states of composite quantum systems play a crucial role in quantum communication [32], quantum cryptography [33] and quantum computing [34].

So far, entanglement and quantum superpositions with mesoscopic systems have been experimentally demonstrated such as the interference of molecules [4, 35] and entangling of atomic ensembles [36]. The study of entanglement of macroscopic objects is of prime interest. For instance, Treutlein and coauthors [24] have presented a scheme to couple the vibrational mode of a nanocantilever with the collective spin degrees of freedom of an ultra-cold Bose Einstein condensate (BEC) while Bose and Agarwal have proposed a scheme to entangle the vibrational modes of two nanocantilevers through a Cooper pair box (CPB) [25]. The scheme presented in [25] prepares two nano-mechanical oscillators in a non-Gaussian entangled state through a CPB; in addition they were also able to show that a similar principle can be used to entangle two CPBs and have proposed a teleportation experiment to read-out the entanglement present between the two cantilevers. The proposal discussed in [25] thus leads to an interesting scheme that can entangle two continuous variable systems (two nanomechanical oscillators) and as well as two discrete variable systems (two CPBs). Singh and coauthors have proposed a scheme to couple a nanomechanical oscillator to a dipolar crystal [37]. In their scheme a nanomechanical oscillator is fabricated with a ferroelectric tip and it interacts with the array of ultra-cold dipolar molecules via the dipole-dipole interactions [37]. This interaction is predicted to produce single-mode squeezing of the center of mass motion of an isolated trapped molecule and two-mode squeezing of the phonons of an array of molecules.

Apart from the above-mentioned schemes, recently there has been a huge interest

in studying the quantum features of optomechanical systems. Radiation pressure induced strong coupling between an optical cavity mode and the vibrational mode of a nanomechanical system has already been experimentally achieved [38]. In most of the optomechanical schemes that exploit the coupling between the vibrational motion of a nanocantilever with the optical cavity mode, the cantilever forms a part of the cavity. This can be realised by constructing a Fabry-Pérot cavity with one fixed mirror and one movable mirror. The movable mirror, under the action of radiation pressure coupling and thermal fluctuations, executes small displacement around its equilibrium value. As a result of the small displacement of the movable mirror, the length of the cavity becomes a function of the position of the movable mirror. The resonance frequency of the cavity thus becomes a function of the position of the vibrating mirror and hence coupling is achieved between the two modes. Along the same lines a strong dispersive coupling of a cavity mode with a micromechanical membrane has been reported in [39].

In most of the suggested optomechanical schemes that exploit the interaction between the optical and the mechanical modes, the main ingredient is the cavity-enhanced radiation pressure coupling between the optical and mechanical degrees of freedom. This in turn allows quantum-limited position measurements and gives rise to dynamical back-action, enabling amplification and even cooling of the state of the mechanical oscillator.

Among all the proposals to study the quantum properties of nanomechanical systems the scheme suggested in [24] is particularly interesting. In [24], a proposal is laid out to couple the vibrational mode of a nanocantilever to the collective spin of an ultra-cold BEC. This scheme allows one to couple two nanocantilevers independently to a common cloud of ultra-cold BEC, through which both of the nanocantilevers can interact with each other. This interesting coupling mechanism allows one to entangle the vibrational mode of two spatially separated mesoscopic mechanical systems [40].

Apart from mediating interactions between the oscillators, the ultra-cold BEC can

be used as an indirect probe to infer the state of the two nanocantilevers. The two nanocantilevers can also be directly coupled to one another. However, achieving indirect coupling between the two nanocantilevers has its own advantage. An indirect coupling between the two nanocantilevers, mediated via the collective excitations of the ultra-cold BEC, can be engineered to generate entangled 'dark states' of the two mechanical systems. The details of this scheme is presented in chapter 3.

It will be shown later in chapter 3 that if the total number of excitations in the ultra-cold BEC is much smaller than the total number of atoms N in the BEC, then the interaction mechanism between two indirectly coupled nanocantilevers can be mapped onto a much simpler physical problem of an open chain of three coupled harmonic oscillators. This new physical scenario, where the indirect interaction between the oscillators is mediated via another oscillator, can shed important light on the generation of quantum correlations in coupled harmonic oscillators. A lot is known in the literature about the quantum features of two directly coupled harmonic oscillators or even about many coupled harmonic oscillators in the thermodynamical limit [41]. But a detailed investigation exploiting quantum features of two indirectly coupled harmonic oscillators is lacking. In the present thesis we cater our attention to this interesting yet unexplored regime of two indirectly coupled harmonic oscillators when the interaction is mediated via another oscillator. This forms the motivation for later sections of chapter 3 and chapter 6.

There also exists a proposal to use an array of mechanical resonators to enhance the spin-spin interaction [42] and thereby utilising this hybrid architecture for quantum computing. The chief principle in this proposed scheme is to magnetically couple the vibrational motion of a resonator to the magnetic moment of a spin qubit. Due to their weak coupling to the environment, spin systems are ideal for realising the idea of quantum computing. But, for the same reason spin-spin interaction is also very weak to achieve entanglement over long distances. In [42], Rabl and coauthors propose to overcome this difficulty by coupling the spin qubits to array of resonators, which in

turn are coupled electrically. Thus effectively a long range spin-spin interaction is built which can potentially be used for realising the various ideas of quantum computing and other quantum architectures.

Efficient interaction between a nanomechanical oscillator and other quantum optical system requires avoiding losses while maintaining large coupling between the two and also mitigating thermal effects. This is one of the prerequisites for most of the existing schemes that can possibly couple such diverse systems. This strong coupling regime can be obtained if the nanomechanical system can be coupled to other quantum optical system within a coupling time much shorter than the decoherence time scale. In [24] this regime can be obtained by using a strong magnetic field gradient to strongly couple the atomic spin with the vibrational motion of the cantilever, whereas in [38, 39] the strong coupling regime requires an ultra high-finesse optical cavity along with nano-oscillators with exceedingly large Q factors.

In most of the schemes proposed for physically coupling a mechanical systems to other quantum optical systems [24, 26], the Hamiltonian governing the dynamics is reminiscent of the Jaynes Cummings Hamiltonian [43]. The Jaynes Cummings model is one of those few models in quantum optics which can be exactly solved under certain conditions. In its original form the Jaynes Cummings model was proposed to describe the dynamics of a single two-level system interacting with a single quantised electromagnetic field. There also exists generalisations of the Jaynes Cummings model such as the Tavis Cummings Hamiltonian which describe the interaction between a collection of two-level atoms and a single quantised field [44]. In many of the existing schemes which deals with studying the quantum properties of nanomechanical systems, the nano resonator is modelled as a quantum harmonic oscillator which has been cooled near to its ground state and thus occupying the low lying excited states in its vibrational spectrum. The nanomechanical system, modelled as a quantum harmonic oscillator, then gets coupled via electromagnetic interaction to other quantum optical systems.

In many of the existing schemes that explore the quantum dynamics of nanomechanical systems, the mechanical systems are treated as *harmonic* oscillators. Interestingly, there are also proposals to model a nanomechanical system as an anharmonic oscillator [45]. The prime motivation of studying nonlinearities in nanomechanical systems is the fact that quantum dynamics of passively coupled mechanical oscillators initially prepared in coherent (classical) states and evolving under a time-independent harmonic potential always remains classical [46]. Therefore an external nonlinearity is essential to see interesting quantum features in passively coupled mechanical oscillators which are initially prepared in coherent (classical) states.

The physics of anharmonic oscillators has been studied in great detail by several authors both in the classical and quantum domain [47, 48, 49, 50]. In particular, Milburn has investigated the quantum and classical dynamics of an anharmonic oscillator in phase space [48] and has shown that decoherence induced state reduction results in quantum to classical crossover in a nonlinear oscillator. In [49], a quantum master equation is derived for a doubly clamped driven nonlinear beam.

Another recent interest in studying the nonlinear properties of mechanical oscillators is to do with the fact that under certain conditions, an external nonlinearity can lead to stronger entanglement between two quantum mechanical systems as compared to their linear counterparts [51]. It is shown in [51] that two qubits interacting via a nonlinear resonator may lead to maximally entangled state of the two qubits. In this way, a nanomechanical oscillator can act as a quantum bus to enhance the interactions between the two qubits. There has also been continued interest in studying the squeezing properties of nonlinear mechanical oscillators. For instance, in [12] a possibility of squeezing the in-phase quadrature of a nanomechanical system has been presented. They have shown that it is possible to squeeze the in-phase quadrature of a nano-oscillator prepared in its ground state or a coherent state.

An *anharmonic* (nonlinear) oscillator in the quantum regime offers a number of intriguing new possibilities for quantum state preparation and manipulation. One of

the many motivations for studying nonlinear oscillators is that by active cooling techniques, such as laser cooling, the thermal fluctuations of a nanomechanical system can only be reduced to the standard quantum limit. If a reduction in noise is sought beyond this limit, then squeezing one of the quadratures of a mechanical oscillator is required and for this one typically relies on nonlinearities. There already exists many feasible schemes that explore the possibility of squeezing the state of a mechanical oscillator [12, 13, 52]. Moreover, coherent nonlinear effects are of great interest as they turn out to be important resources for processing universal quantum information with continuous variables [53]. In this direction a theoretical investigation probing salient quantum features in coupled nonlinear oscillators has been carried out in [54]

With the recent emergence of the novel field of optomechanics, probing quantum correlations in mesoscopic systems has taken a new turn. Optomechanics is a promising research avenue that combines the interaction between optics and mechanics [55]. In a simplest optomechanical setup exploiting optomechanical interaction, the main component is a cavity with a movable mirror. Light in the cavity and the movable mirror interact due to radiation pressure coupling. Under the action of radiation pressure and thermal fluctuations, the movable mirror executes simple harmonic motion around its equilibrium value, which in turn changes the cavity resonance frequency. This eventually results in coupling between light and mechanics. A scheme exploiting this radiation pressure coupling to generate optomechanical correlations between two distant cavities is discussed in [56].

In spite of the various exciting theoretical and experimental advances in quantum state preparation of nano- and micromechanical systems, the chief difficulty lies in inferring the degree of entanglement present in such mesoscopic systems. Experimentally estimating the degree of inseparability is difficult even for microscopic systems and this difficulty becomes magnified for macroscopic systems. Another concern lies in the fact that there is no universal test of entanglement which might hold for all the states. Entanglement measures which disclose entanglement for a class of states

but may fail to do so for other states. Most of the theoretical measures of entanglement [57, 58] are not directly accessible in experiments but in recent experiments it has become possible to observe a pure state entanglement measure [59]. The non-local character present in the nanomechanical systems can be ascertained in principle from experiments involving Bell's inequality violations [60], but as pointed out in [25], the difficulty in analysing the degree of entanglement in mechanical systems is the fact that experiments involving Bell's inequality violation requires measurements in Schrödinger cat like basis, which is certainly not an easy task for mesoscopic mechanical systems. Moreover, there are classes of entangled mixed states which do not necessarily violate Bell's inequality.

Therefore, other novel techniques need to be developed for quantifying the entanglement present between the mechanical oscillators. A possible tool to measure the quantum state of such mechanical systems is the full state quantum tomography [61] but these techniques are experimentally very demanding. There is also a recent work suggesting an experimentally friendly measure of quantum correlations between two arbitrary qubit states [62]. In [62], a parameter has been defined in terms of which quantum correlations can be experimentally quantified by measuring the expectation value of a small set of observables without the need for a full quantum state tomography. Also there has been a scheme proposed to measure the quantum state of a nanomechanical oscillator cooled near to the vibrational ground state [63]. In [63], the proposal is aimed at determining the Wigner function of a mechanical cantilever cooled near its ground state and involves a detector atom coupled to the cantilever's vibrational mode and to a pair of optical fields, which induce a Raman transition between the ground and excited states of the atom. It has been proposed that the probability for the atom to be found in the excited state is a direct measure of the Wigner characteristic function of the nanomechanical oscillator.

In the context of optomechanics there are other interesting schemes to detect the non-classical states of a mechanical oscillator through indirect measurements [64, 65].

The central idea behind these schemes is to transfer the mechanical state onto the optical modes. By measuring the quantum correlations in the initially uncorrelated optical modes, non-local correlations in the mechanical state of the oscillator can be inferred [64, 65].

Given all the theoretical and experimental advances in this exciting research field involving the study of nano- and micromechanical systems, the future prospects seems very promising. All these stimulating theoretical and experimental studies heralds a new era in investigating various quantum phenomena in mesoscopic systems and has brought us closer than ever to test the foundations of quantum mechanics. With recent experiments coming within just an order of magnitude away from the ability to observe quantum zero-point motion, ideas about the quantum to classical transition may soon become experimentally accessible, and then it shall be very interesting to see the test of the famous Schrödinger's cat paradox [14] on objects of macroscopic scale.

Even though there has been impeccable success in exploring the quantum features of mesoscopic mechanical systems, there is still a lot to be done to fully probe the 'quantum in mechanics' [9]. A strong impetus is needed from both theoretical and experimental studies to fully understand the intriguing dynamics of mechanical oscillators. The biggest challenge is a careful readout of the quantum state with a minimum perturbation. Novel techniques and ideas needs to be brought in for inferring entanglement and other non-classical correlations in mechanical systems. Methods also needs to be developed for minimising the effects of decoherence in mesoscopic mechanical systems, which might degrade their quantum properties.

The thesis thus consists of a detailed theoretical treatment of novel schemes to prepare mesoscopic mechanical systems in non-classical states including entangled states. The thesis is outlined as follows. In chapter 2 we provide a brief introduction to some of the essential concepts that will be used throughout the thesis. In chapter 3, a physical system of two nano-cantilevers coupled to a cloud of ultra-cold atoms is discussed.

Chapter 4 discusses a possibility to induce a quartic nonlinearity to the motion of a harmonic oscillator, which is further explored to generate non-classical states of the mechanical oscillator. In chapter 5 a scheme to generate distant optomechanical correlations is studied while in chapter 6 Markovian evolution of strongly coupled bosonic modes is studied. We conclude the thesis with discussions and a future outlook in chapter 7.

CHAPTER 2

BASICS

2.1 Introduction

In this chapter we shall review some basic theoretical concepts that will be essential in building the framework of the thesis. We shall briefly discuss some preliminary topics including number states, coherent states, thermal states, quantum characteristic functions, and various quasi-probability distributions including the P-function, Wigner function and the Q-function. We shall also briefly dwell on the essentials of Gaussian continuous variables (CV) states by describing the covariance matrix, which is sufficient to fully characterise any Gaussian state.

2.1.1 Number states

Consider a bosonic mode described by a creation ($\hat{a}^\dagger$) and an annihilation ($\hat{a}$) operator respectively. Single-mode number states or Fock states are then defined as the eigenstates of the number operator $\hat{n}$ ($\hat{a}^\dagger\hat{a}$) so that

$$\hat{a}^\dagger\hat{a}|n\rangle = n|n\rangle. \tag{2.1}$$

The number states form an orthonormal complete basis set such that $\langle n|m\rangle = \delta_{n,m}$ and can be seen as the energy eigenstates of the free field Hamiltonian $H_{\text{free}} \sim \hat{a}^\dagger\hat{a}$. Similar to the case of a single-mode number state, one can also define a two-mode number state which is the joint eigenstate of the respective number operators

$$\hat{a}^\dagger\hat{a}\ \hat{b}^\dagger\hat{b}|n_a, n_b\rangle = n_a n_b|n_a, n_b\rangle = n_a n_b|n_a\rangle|n_b\rangle. \tag{2.2}$$

By virtue of the definition of number states, the vacuum state is the zero energy eigenstate of the number operator. The action of creation and annihilation operators on any general number states is

$$\hat{a}^\dagger|n\rangle = \sqrt{n+1}|n+1\rangle, \tag{2.3}$$

$$\hat{a}|n\rangle = \sqrt{n}|n-1\rangle. \tag{2.4}$$

Number states or Fock states are one of the most important non-classical states featuring in quantum optics and forms the basis of non-Gaussian continuous variables quantum computing. It is worthwhile to point out that among the class of number states, vacuum state $|0\rangle$ is the only state with a Gaussian wave function and is thus characterised by a positive Wigner function which is Gaussian in character.

2.1.2 Coherent states

Coherent states are the closest approximation to classical states and are one of the most naturally occurring states in quantum optics. Coherent states, as described by Zurek, are the 'pointer' (eigen) states of the environment. The inevitable coupling of a quantum system to its environment results in a loss of quantum coherence. The details will be provided later, but the main result is that an initial coherent state evolving under a purely dissipative channel, remains a coherent state, but with an exponentially decaying amplitude. In this sense, coherent states are called the 'pointer' (eigen) states of the environment.

Single-mode coherent states are generated by the action of the Glauber displacement operator $\hat{D}(\alpha)$=$e^{\alpha\hat{a}^\dagger-\alpha^*\hat{a}}$ on a vacuum state

$$|\alpha\rangle = \hat{D}(\alpha)|0\rangle = e^{\alpha\hat{a}^\dagger-\alpha^*\hat{a}}|0\rangle, \tag{2.5}$$

where α is a complex number in general with magnitude $|\alpha|$. The Glauber displacement operator $\hat{D}(\alpha)$ is unitary and to see this we shall first make use of the operator ordering theorem

Theorem 1. *For two operators $\hat{A}$ and $\hat{B}$ which commute with their commutator so that $[\hat{A},[\hat{A},\hat{B}]]$=$[\hat{B},[\hat{A},\hat{B}]]$=0, then $exp(\theta(\hat{A}+\hat{B})) = exp(\theta\hat{A})exp(\theta\hat{B})exp(-(\theta^2/2)[\hat{A},\hat{B}])$*

Making use of the fact that $[\hat{a},\hat{a}^\dagger] = 1$, the Glauber displacement operator can be rewritten as $\hat{D}(\alpha) = e^{\alpha\hat{a}^\dagger}e^{-\alpha^*\hat{a}}e^{-|\alpha|^2/2}$ and from which it easily follows that $\hat{D}^\dagger(\alpha)$=$e^{-\alpha\hat{a}^\dagger}$ $e^{\alpha^*\hat{a}}e^{-|\alpha|^2/2} = \hat{D}(-\alpha)$. Unitarity of the displacement operator is guaranteed by the fact that for any operator $\hat{o}$, $e^{\hat{o}}e^{-\hat{o}} = 1$. Coherent states have many interesting features and some of them can be summarised here :

- A coherent state can be expanded in a number state basis as $|\alpha\rangle$= $e^{-|\alpha|^2/2}\sum_{n=0}^{\infty}\frac{\alpha^n}{\sqrt{n!}}|n\rangle$.
- A coherent state is the right eigenstate of the annihilation operator with eigenvalue α so that $\hat{a}|\alpha\rangle$= $\alpha|\alpha\rangle$.
- A coherent state is the left eigenstate of the creation operator with eigenvalue α^* so that $\langle\alpha|\hat{a}^\dagger$= $\alpha^*\langle\alpha|$.
- A coherent state obeys the Poisson photon number probability distribution, P(n)=$|\langle n|\alpha\rangle|^2$=exp($-|\alpha|^2$)$|\alpha|^{2n}/n!$. The mean and the variance of the photon number probability distribution is given by $\langle\hat{n}\rangle = |\alpha|^2$ and $\Delta n^2 = \langle\alpha|n^2|\alpha\rangle -$ $(\langle\alpha|\hat{n}|\alpha\rangle)^2$=$|\alpha|^2 + |\alpha|^4 - |\alpha|^4$=$|\alpha|^2$ respectively.
- A coherent state is a minimum uncertainty state. This follows by defining the position and momentum quadrature operators as $\hat{x} = (\hat{a} + \hat{a}^\dagger)/\sqrt{2}$ and $\hat{p} = i(\hat{a}^\dagger - \hat{a})/\sqrt{2}$. For an initial coherent state, the variance in the position and

momentum quadratures can then be computed as $\Delta x^2 = \langle\alpha|x^2|\alpha\rangle - (\langle\alpha|\hat{x}|\alpha\rangle)^2$ $=1/2$ and $\Delta p^2 = \langle\alpha|p^2|\alpha\rangle - (\langle\alpha|\hat{p}|\alpha\rangle)^2=1/2$. This confirms the bound set by Heisenberg uncertainty relation $\Delta x^2\ \Delta p^2 \geq 1/4$.

- Coherent states are not mutually orthogonal and for two coherent states with amplitude α and β, the overlap between them is given by $\langle\alpha|\beta\rangle=e^{-|\alpha-\beta|^2}$.

- Coherent states form an over complete basis and the identity can be resolved in terms of the coherent states $(1/\pi)\int_{-\infty}^{\infty} d^2\alpha|\alpha\rangle\langle\alpha| = \mathbf{1}$. This is a useful resolution of identity as it allows one to compute expectation value of any quantum mechanical observable as
$\mathrm{Tr}(\hat{A})=\sum_{m=0}^{\infty}\langle m|\hat{A}|m\rangle=(1/\pi)\int_{-\infty}^{\infty} d^2\alpha \sum_{m=0}^{\infty}\langle\alpha|m\rangle\langle m|\hat{A}|\alpha\rangle=(1/\pi)\int_{-\infty}^{\infty} d^2\alpha\langle\alpha|\hat{A}|\alpha\rangle$.

2.1.3 Thermal states

The inevitable coupling of a system of interest to its environmental degrees of freedom results in a class of states known as mixed states where a thermal state is a prime example of it. We have minimal knowledge about such states and thus can no longer assign a wave function to such states. Such states can only be described in terms of a density matrix $\hat{\rho}$. In thermal equilibrium, the state of a system with Hamiltonian $\hat{H}$ is represented by a density matrix

$$\rho = \frac{\exp(-\beta\hat{H})}{\mathrm{Tr}[\exp(-\beta\hat{H})]}, \tag{2.6}$$

where $\beta = 1/k_B T$. A single mode bosonic field with frequency ω in thermal equilibrium at temperature T takes the form

$$\rho = \frac{\exp(-\beta\hbar\omega\hat{n})}{\mathrm{Tr}[\exp(-\beta\hbar\omega\hat{n})]}. \tag{2.7}$$

The above density matrix is diagonal in the number state basis and can be rewritten as

$$\rho = \sum_{n=0}^{\infty} \frac{\exp(-\beta\hbar\omega n)}{\mathrm{Tr}[\exp(-\beta\hbar\omega n)]} |n\rangle\langle n|. \tag{2.8}$$

Defining the mean thermal occupancy as $\bar{n} = 1/(\exp(\beta\hbar\omega) - 1)$, the density matrix representing a single mode thermal state can be written as

$$\rho = \sum_{n=0}^{\infty} \frac{\bar{n}^n}{(\bar{n}+1)^{n+1}} |n\rangle\langle n|. \tag{2.9}$$

2.1.4 Squeezed states

Squeezed states are a class of non-classical states arising mainly in non-linear processes which includes parametric oscillation and four wave mixing. Squeezed states have an important property that the variance of one of its quadrature , say $\hat{x}$, is less than the value 1/2 associated with coherent or vacuum states. In order to obey the Heisenberg uncertainty relation, the variance in the complementary quadrature exceeds the value 1/2. A single-mode squeezed state is described by the action of one-mode squeezing operator $|\zeta\rangle = \exp(-\frac{\zeta}{2}\hat{a}^{\dagger 2} + \frac{\zeta^*}{2}\hat{a}^2)$ on a vacuum state

$$|\zeta\rangle = \exp(-\frac{\zeta}{2}\hat{a}^{\dagger 2} + \frac{\zeta^*}{2}\hat{a}^2)|0\rangle, \tag{2.10}$$

where $\zeta = r\exp(i\phi)$ is the complex squeezing parameter. As required, the squeezing operator $S(\zeta)$ is unitary and under the action of above squeezing transformation the single mode annihilation and creation operators transforms as

$$\hat{S}(\zeta)\hat{a}\hat{S}^{\dagger}(\zeta) = \hat{a}\mathrm{cosh}r + \hat{a}^{\dagger}\exp(i\phi)\mathrm{sinh}r; \tag{2.11}$$

$$\hat{S}(\zeta)\hat{a}^{\dagger}\hat{S}^{\dagger}(\zeta) = \hat{a}^{\dagger}\mathrm{cosh}r + \hat{a}\exp(-i\phi)\mathrm{sinh}r. \tag{2.12}$$

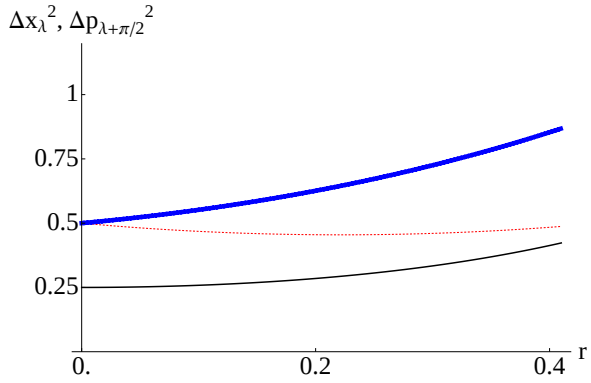

(a)

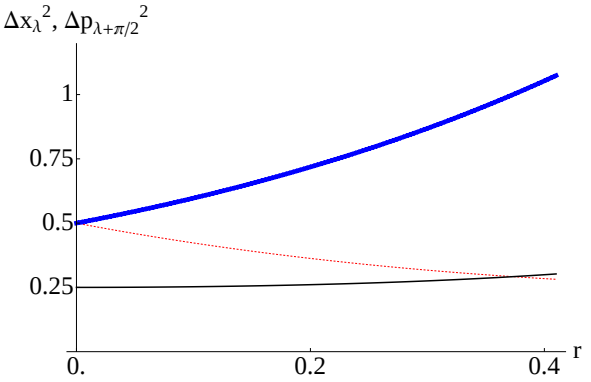

(b)

Figure 2.1: (a) Variance in the $\hat{x}_\lambda$ (red, dotted) and the $\hat{x}_{\lambda+\pi/2}$ (blue, thick solid) quadratures as a function of the squeezing parameter r for (a) $\lambda = 1$, $\phi = \pi$, and (b) $\lambda = 0$, $\phi = \pi/6$. The product of the variance of the quadratures is also shown (black, thin solid).

Defining the quadrature operators $\hat{x}_\lambda$ and $\hat{x}_{\lambda+\pi/2}$ as

$$\hat{x}_\lambda = (1/\sqrt{2})(\hat{a}\exp(-i\lambda) + \hat{a}^\dagger\exp(i\lambda)) \tag{2.13}$$

$$\hat{x}_{\lambda+\pi/2} = (1/\sqrt{2})(\hat{a}\exp(-i(\lambda+\pi/2)) + \hat{a}^\dagger\exp(i(\lambda+\pi/2))), \tag{2.14}$$

the product of the variance in the quadratures comes out as

$$\Delta x_\lambda^2 \Delta x_{\lambda+\pi/2}^2 = \frac{1}{4}(\sin^4(\lambda-\phi/2)+\cos^4(\lambda-\phi/2)+2\sin^2(\lambda-\phi/2)\cos^2(\lambda-\phi/2)\cosh 4r). \tag{2.15}$$

As shown in Fig. 2.1(a) and Fig. 2.1(b), the variance in one of the quadratures of a

squeezed state may drop below the limit set by the coherent and vacuum states, but only at the expense of increased fluctuations in the other quadrature. As required, the Heisenberg uncertainty relation is still obeyed by squeezed states. Similar to the case of single-mode squeezed states, a two-mode squeezed state is defined by the action of the following squeezing operator on a two-mode vacuum state

$$|\zeta_{\mathrm{AB}}\rangle = \exp(-\zeta \hat{a}^{\dagger}\hat{b}^{\dagger} + \zeta^{*}\hat{b}\hat{a})|0\rangle_{\mathrm{A}}|0\rangle_{\mathrm{B}}. \tag{2.16}$$

As expected, the two-mode squeezing operator is also unitary and an important observation is that the two-mode squeezed state $|\zeta_{\mathrm{AB}}\rangle$ is inseparable in terms of the individual single mode states. This leads to inter-mode correlations and the state $|\zeta_{\mathrm{AB}}\rangle$ is thus referred to as an entangled state.

2.1.5 Schrödinger, Heisenberg and interaction pictures

For a closed quantum system, the complete information can be obtained by solving the Schrödinger equation. For a system prepared in a pure state $|\Psi\rangle$, the unitary evolution is governed by the Schrödinger equation

$$i\hbar\frac{d|\hat{\Psi}(t)\rangle}{dt} = \hat{H}_{\mathrm{sys}}|\hat{\Psi}(t)\rangle, \tag{2.17}$$

where $\hat{H}_{\mathrm{sys}}$ is the system Hamiltonian. For a mixed state described by the density matrix ρ, the time evolution is given by

$$\frac{d\rho}{dt} = -\frac{i}{\hbar}[\hat{H}, \rho]. \tag{2.18}$$

The solution of the Schrödinger equation is $|\Psi(t)\rangle = \hat{U}(t)|\Psi(0)\rangle$, where $\hat{U}(t)$ is a unitary operator also satisfying the Schrödinger equation. In the Schrödinger representation, the state evolves as a function of time and the operators remain stationary in time.

An equivalent way of describing the dynamics is to work in the Heisenberg picture. In the Heisenberg picture the state remains stationary in time $|\Psi(t)\rangle = |\Psi(0)\rangle$, while the operator follows the time-dependent equation of motion

$$\frac{d\hat{A}(t)}{dt} = \frac{i}{\hbar}[\hat{H}, \hat{A}(t)] + \frac{\partial}{\partial t}\hat{A}(t). \tag{2.19}$$

For an operator with no explicit time-dependence, the time evolved operators can be expressed as $\hat{A}(t) = \hat{U}(t)\hat{A}\hat{U}^{\dagger}(t)$. The expectation value of any quantum mechanical operator is same in both the representations $\langle\hat{A}\rangle = \langle\psi(t)|\hat{A}(0)|\psi(t)\rangle = \langle\psi(0)|\hat{A}(t)|\psi(0)\rangle$.

Sometimes it is better to move to an interaction picture which is somewhat intermediary between the Schrödinger and the Heisenberg representations. In the interaction picture, dynamics associated with the free evolution part of the Hamiltonian is usually contained with the operators while the evolution due to the interaction part of the Hamiltonian is contained with in the state. This interaction picture is termed as the Schrödinger interaction picture. On the other hand, if the state carries the dynamical evolution due to the free evolution of the Hamiltonian and the operators carry the time evolution associated with the coupling, the interaction picture is termed as the Heisenberg interaction picture.

The transformation to the Schrödinger interaction picture can be achieved by a unitary transformation such that $|\psi_I\rangle = \hat{U}|\psi\rangle$. In this interaction picture, $|\psi_I\rangle$ satisfies the following Schrödinger equation

$$i\hbar\frac{\partial}{\partial t}|\psi_I\rangle = \hat{H}_I|\psi_I\rangle, \tag{2.20}$$

where $\hat{H}_I$ is the interaction picture Hamiltonian given by

$$\hat{H}_I = i\hbar\dot{\hat{U}}\hat{U}^{\dagger} + \hat{U}\hat{H}\hat{U}^{\dagger}. \tag{2.21}$$

We can make use of an example to further clarify the transformation of a Hamiltonian

to its corresponding interaction picture. Consider two coupled bosonic modes labelled a and b, with corresponding resonance frequencies ω_a and ω_b respectively. The two modes are assumed to be coupled through a beam-splitter interaction with interaction strength κ and coupled as $H_{\rm int} = \hbar\kappa(\hat{a}^\dagger\hat{b} + \hat{b}^\dagger\hat{a})$. Thus the closed system dynamics of the two coupled modes is governed by the Hamiltonian

$$\begin{aligned} H &= \hbar\omega_a\hat{a}^\dagger\hat{a} + \hbar\omega_b\hat{b}^\dagger\hat{b} + \hbar\kappa(\hat{a}^\dagger\hat{b} + \hat{b}^\dagger\hat{a}), \qquad (2.22)\\ H &= H_0 + H_{\rm int}, \end{aligned}$$

where $H_0/\hbar = \omega_a\hat{a}^\dagger\hat{a} + \omega_b\hat{b}^\dagger\hat{b}$ describes the free evolution of the two coupled bosonic modes. Now making use of (2.21) where $\hat{U} = e^{iH_0t/\hbar}$ we get

$$\begin{aligned} \hat{H}_I &= i\hbar\dot{\hat{U}}\hat{U}^\dagger + \hat{U}\hat{H}\hat{U}^\dagger \qquad (2.23)\\ \hat{H}_I &= -H_0 + H_0 + \hbar\kappa(\hat{a}^\dagger\hat{b}e^{i(\omega_a-\omega_b)t} + \hat{b}^\dagger\hat{a}e^{-i(\omega_a-\omega_b)t}) \qquad (2.24)\\ \hat{H}_I &= \hbar\kappa(\hat{a}^\dagger\hat{b}e^{i(\omega_a-\omega_b)t} + \hat{b}^\dagger\hat{a}e^{-i(\omega_a-\omega_b)t}), \qquad (2.25) \end{aligned}$$

which is the corresponding form of the Hamiltonian (2.22) in the interaction picture of the free evolution Hamiltonian H_0.

2.1.6 Quantum characteristic function

Although the complete information about a quantum system can be obtained either in terms of the wave function or the density matrix, an equivalent description exists in terms of the quantum characteristic function. Specifying the quantum characteristic function gives us complete statistical information about the state. A p-ordered quantum characteristic function is defined as

$$\chi(\epsilon, p) = \mathrm{Tr}[\hat{\rho}\ \exp(\epsilon\hat{a}^\dagger - \epsilon^*\hat{a})]\exp(p|\epsilon|^2/2), \qquad (2.26)$$

where p = 1, 0, and -1 correspond to normal, symmetric and antinormal ordered characteristic functions. The quantum characteristic function $\chi(\epsilon, p)$ is a complex valued function in general and it achieves its maximum value of 1 at the origin (ϵ=0). From the quantum characteristic function it is easy to find the p-ordered product of annihilation and creation operators. From the characteristic function one can obtain the expectation values of quantum mechanical observables, e.g. $\langle \hat{a}^{\dagger m} \hat{a}^n \rangle_p = (\frac{\partial}{\partial \epsilon})^m (-\frac{\partial}{\partial \epsilon^*})^n \chi(\epsilon, p)|_{\epsilon=0}$. Normal-ordered characteristic function shall be used often in many parts of the thesis and thus we summarise the results for the normal-ordered characteristic function for some of the important classes of states :

- Normal-ordered characteristic function for a number state is $\chi(\epsilon, 1) = \langle n|\exp(\epsilon \hat{a}^\dagger) \exp(-\epsilon^* \hat{a})|n\rangle = L_n(|\epsilon|^2)$, where L_n is the Laguerre polynomial of order n.
- Normal-ordered characteristic function for a coherent state is $\chi(\epsilon, 1) = \langle \alpha|\exp(\epsilon \hat{a}^\dagger) \exp(-\epsilon^* \hat{a})|\alpha\rangle = \exp(\epsilon\alpha^* - \epsilon^*\alpha)$.
- Normal-ordered characteristic function for a thermal state with average thermal occupancy $\bar{n}$ is $\chi(\epsilon, 1) = \mathrm{Tr}[\sum_{n=0}^{\infty} \frac{\bar{n}^n}{(\bar{n}+1)^{n+1}} \exp(\epsilon \hat{a}^\dagger) \exp(-\epsilon^* \hat{a})|n\rangle\langle n|] = \exp(-\bar{n}|\epsilon|^2)$.

2.1.7 Quasi-probability distributions

Other than using the quantum characteristic function to get the full statistical description of a quantum system, an equivalent description can be obtained in terms of a quasi-probability distribution. A quasi-probability distribution can be defined by taking the Fourier transform of a quantum characteristic function. In conformity with a true probability distribution, the quasi-probability distribution so obtained is a real valued function. However, the positivity of the quasi-probability distribution is not always guaranteed and thus it is not always possible to interpret it as a true probability distribution function. For a p-ordered quantum characteristic function the

corresponding quasi-probability distribution takes the form

$$W_\beta(p) = \frac{1}{\pi^2}\int_{\infty}^{-\infty} d^2\epsilon\chi(\epsilon,p)\exp(\beta\epsilon^* - \beta^*\epsilon). \tag{2.27}$$

Some of the important properties of a quasi-probability distribution function can be summarised here :

- The Fourier transform of a normal ordered characteristic function is termed as the Glauber-Sudarshan P- function. In general P-function can be highly singular and the positivity of the P-function guarantees the classical nature of any state.
- The corresponding quasi-probability distribution function for the symmetric ordered characteristic function is termed as the Wigner function. Wigner function is always well behaved but can also attain negative values, which is widely considered as a signature of the non-classical character of the corresponding state.
- Q-function is the quasi-probability distribution function associated with the antinormal ordered characteristic function. Q-function is always positive semi-definite and unlike the P-function and the Wigner function, Q-function can be regarded as representing a true probability distribution function.
- For instance, for a photon number state $|n\rangle$, the quasiprobability distribution corresponding to the p-ordered characteristic function (for $p < 1$ and $p \neq -1$) turns out to be $W_\beta(p) = \frac{2}{\pi(1-p)}(-1)^n(\frac{1+p}{1-p})^n\exp(-2\frac{|\beta|^2}{1-p})L_n(\frac{4|\beta|^2}{1-p^2})$, where L_n is the Laguerre polynomial of order n. For p=-1, the Q-function corresponding to the number state $|n\rangle$ takes the form $Q_\beta = \frac{|\beta|^{2n}}{n!\pi}\exp(-|\beta|^2)$. For a number state other than the vacuum state, the P-function can only be expressed in terms of delta functions and its derivatives. A plot of the Wigner function and the Q function for a number state is shown in Fig. 2.2(a) and Fig. 2.2(b) respectively.

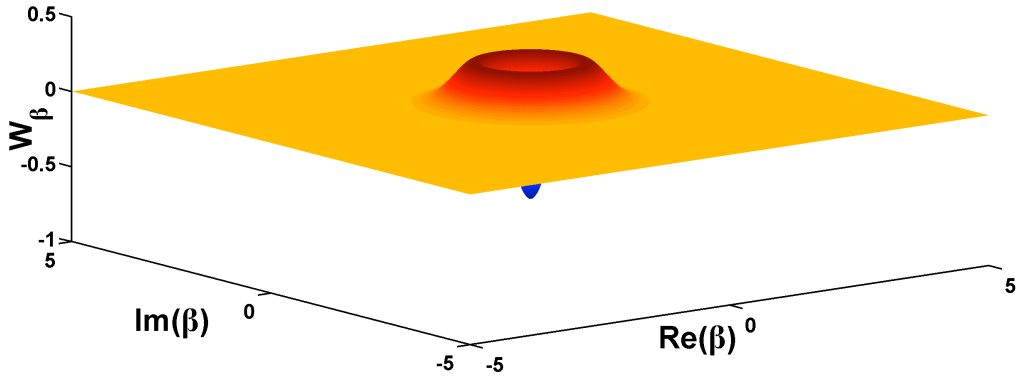

(a)

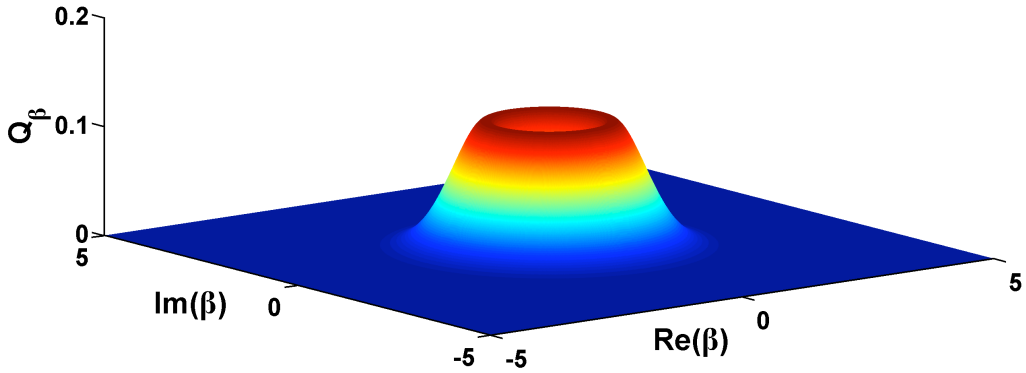

(b)

Figure 2.2: Phase space distribution of (a) the Wigner function W_β and (b) the Q-function Q_β for a number state $|n\rangle$, with n=1. The negativity of the Wigner function is a characteristic of the non-classical nature of the number state while the Q-function always maintains its positive character.

2.1.8 Identities

Other useful identities that will be of relevance throughout the thesis:

- $[\hat{a},\hat{h}]=\frac{\partial}{\partial a^\dagger}\hat{h}$, where $\hat{h}$ is a differentiable function of the creation operator $\hat{a}^\dagger$.
- $[\hat{a}^\dagger,\hat{f}]=-\frac{\partial}{\partial a}\hat{f}$, where $\hat{f}$ is a differentiable function of the destruction operator $\hat{a}$.
- Baker-Campbell-Hausdorff expansion is another useful expansion which will be used in various sections of the thesis. For two arbitrary operators $\hat{A}$ and $\hat{B}$, the Baker-Campbell-Hausdorff expansion is $e^{\hat{A}}\hat{B}e^{-\hat{A}} = \hat{B} + [\hat{A},\hat{B}] + \frac{[\hat{A},[\hat{A},\hat{B}]]}{2!} + ...$

2.1.9 Covariance matrix

Gaussian states including vacuum, coherent, squeezed and thermal states are one of the most commonly encountered states in physical systems. It is known that in absence of photon counting non-Gaussian continuous variable states are required for universal continuous variable (CV) quantum computing. Moreover Gaussian states have positive Wigner functions, so sometimes they can be interpreted as classical. In this respect, the study of non-Gaussian states becomes more important. In spite of this shortcoming Gaussian states have an added advantage that they can be routinely prepared in laboratories these days and can be fully specified in terms of their first and second order moments. Studying quantum aspects of infinite dimensional systems is hard in general, but with Gaussian states this difficulty can be overcome. Gaussian states can be fully characterised in terms of their first and second order moments and which can be arranged in the form of a symmetric and real covariance matrix.

For an initial two-mode Gaussian state, it is sufficient to fully characterise the quantum correlations between the two coupled modes in terms of their Wigner covariance matrix. In this case, the covariance matrix $\mathbf{V}$ is a 4×4 real symmetric matrix $V_{i,j} = (\langle R_i R_j + R_j R_i \rangle)/2$, where $i, j \epsilon \{a, b\}$ and $R^T = (\hat{q}_a, \hat{p}_a, \hat{q}_b, \hat{p}_b)$. Here $\hat{q}_i$ and $\hat{p}_i$ are the position and momentum quadratures of the ith mode. From the expression of

the normal ordered quantum characteristic function $\chi(x,y,t) = \langle e^{x\hat{a}^\dagger} e^{-x^*\hat{a}} e^{y\hat{b}^\dagger} e^{-y^*\hat{b}} \rangle$ it is straightforward to extract the Wigner covariance matrix. This can be seen by noting, $\langle \hat{a}^{\dagger m} \hat{b}^n \rangle = (\frac{\partial}{\partial x})^m (-\frac{\partial}{\partial y^*})^n \chi(x,y,t)|_{x=0,y=0}$.

For a two-mode Gaussian continuous variable system, the covariance matrix $\mathbf{V}$ can be written as

$$\mathbf{V} = \begin{pmatrix} \mathbf{A} & \mathbf{C} \\ \mathbf{C}^T & \mathbf{B} \end{pmatrix}, \tag{2.28}$$

where T denotes a matrix transpose; and

$$\begin{aligned}
\mathbf{A} &= \begin{pmatrix} \langle (\hat{c}+\hat{c}^\dagger)^2 \rangle/2 & \langle [\hat{c}+\hat{c}^\dagger, i(\hat{c}^\dagger - \hat{c})]_+ \rangle/2 \\ \langle [\hat{c}+\hat{c}^\dagger, i(\hat{c}^\dagger - \hat{c})]_+ \rangle/2 & \langle (i(\hat{c}^\dagger - \hat{c}))^2 \rangle/2 \end{pmatrix}, \\
\mathbf{B} &= \begin{pmatrix} \langle (\hat{d}+\hat{d}^\dagger)^2 \rangle/2 & \langle [\hat{d}+\hat{d}^\dagger, i(\hat{d}^\dagger - \hat{d})]_+ \rangle/2 \\ \langle [\hat{d}+\hat{d}^\dagger, i(\hat{d}^\dagger - \hat{d})]_+ \rangle/2 & \langle (i(\hat{d}^\dagger - \hat{d}))^2 \rangle/2 \end{pmatrix}, \\
\mathbf{C} &= \begin{pmatrix} \langle (\hat{c}+\hat{c}^\dagger)(\hat{d}+\hat{d}^\dagger) \rangle/2 & \langle i(\hat{c}+\hat{c}^\dagger)(\hat{d}^\dagger - \hat{d}) \rangle/2 \\ \langle i(\hat{c}^\dagger - \hat{c})(\hat{d}+\hat{d}^\dagger) \rangle/2 & \langle -(\hat{c}^\dagger - \hat{c})(\hat{d}^\dagger - \hat{d}) \rangle/2 \end{pmatrix},
\end{aligned}$$

and $\hat{c}$, $\hat{d}$ are two arbitrary bosonic operators with $\langle [\hat{r}_i, \hat{r}_j]_+ \rangle = (\langle \hat{r}_i \hat{r}_j + \hat{r}_j \hat{r}_i) \rangle)/2$. Once we have the covariance matrix, all the quantum statistical properties of Gaussian continuous variable states can be constructed. Also worth mentioning is the important fact that a state evolving under a Hamiltonian which is quadratic in the position and momentum coordinates maintains its Gaussian character.

A brief introduction provided in this chapter will be of much use in illustrating various results presented in this thesis. In the chapters to follow we shall discuss in detail novel schemes to prepare mesoscopic mechanical systems in non-classical states along with providing the necessary theoretical background.

CHAPTER 3

NANOCANTILEVERS COUPLED TO ULTRA-COLD ATOMS: A HYBRID-QUANTUM DEVICE

3.1 Introduction

The study of ultra-cold atoms has been a subject of intense theoretical and experimental interest for the past two decades. From the very first realisation of an ultra-cold Bose-Einstein condensate (BEC) in the lab [66], the ultra-cold atoms community has seen some pathbreaking discoveries including the Mott-superfluid phase transition in ultra-cold atoms [67], simulation of a spin-chain in an optical lattice [68] and a recent interesting possibility to use ultra-cold atoms as quantum simulators of intractable and open problems in physics [69]. If realised, such a quantum simulator has the potential to explore various unsolved problems in many-body physics including quantum magnetism and high temperature superconductivity.

Ultra-cold atoms in the Bose-Einstein condensed phase provides us with a rare example where quantum coherence can be observed on a mesoscopic scale. Recent theoretical and experimental advances have confirmed the quantum nature of ultra-cold atoms. Using ultra-cold atoms as a toolbox, it may now become possible to test

the limits of the quantum theory. On the other hand, nano- and micromechanical systems are typical condensed matter systems, long considered as lying deep in the classical realms. However, if cooled near to their ground states, such mechanical systems exhibit quantum mechanical motion to a very good approximation. A novel possibility is to explore the interesting physics that might emerge by coupling a quantum optical system to a mechanical system both of which are endowed with vastly different attributes.

One out of many motivations behind engineering a hybrid-quantum device is to explore the possibility of constructing a device which is mesoscopic but yet has quantum attributes. Such hybrid-quantum devices may help us in improving our understanding about various questions of decoherence, understanding the quantum-classical crossover, and may have potential applications in precision measurement and quantum information technology.

A possibility of constructing such a hybrid-quantum device is discussed in [24], where a proposal is laid out to couple the fundamental vibrational mode of a cantilever to the collective spin degrees of freedom of an ultra-cold BEC. In [40], we have extended the idea presented in [24] to couple the vibrational modes of two nanocantilevers to the collective spin degrees of freedom of a cloud of ultra-cold BEC. The scheme presented in [40] forms the basis of this chapter. In the present chapter, starting from building the necessary theoretical background we illustrate in detail the basis of the scheme presented in [40] and shall conclude the chapter with a brief discussion [1].

[1]The scheme presented in this chapter to entangle the vibrational modes of two distant nanocantilevers will work identically the same if the BEC is replaced with an ensemble of ultra-cold atoms to mediate indirect interaction between the two nanocantilevers. Therefore throughout this thesis the words 'BEC' and 'ultra-cold atoms' will be used quite interchangeably. However the added advantage of using a BEC over an ensemble of cold atoms in establishing indirect coupling between two nanocantilevers lies in the fact that all the atoms in the BEC are in the same quantum state and the BEC atomic cloud has a small spatial extent and thus has a very large atomic density. This small spatial confinement of the atoms in the BEC results in identical coupling strength between all the atoms in the BEC and the vibrational modes of distant nanocantilevers.

3.2 Theoretical model

Recently there has been a surge of interest in exploring the quantum regime of mesoscopic mechanical oscillators by coupling them to vastly different physical systems. These include nanomechanical systems coupled to electrical circuits (NEMS) [42], microwave resonators coupled to superconducting qubits [70], or in the setting of an optomechanical cavity with an optical mode coupled to a movable mirror [16].

After many years of sheer hard work it has now become possible to cool a nanomechanical resonator using quantum techniques [71]. It has also recently become possible to realise the ground state of a nano- or micromechanical system either by cryogenically cooling an ultra-high frequency mechanical oscillator [21] or by employing laser cooling to cool an optomechanical device [22, 72]. Such promising experimental advances have opened a new era in which genuine quantum effects in mesoscopic mechanical systems can be seen. A natural next step is to explore further the quantum behaviour of mechanical systems with the ultimate goal to realise their potential applications in quantum information technologies, tests of the quantum theory and ultra-precise sensing technology.

Inspired by recent theoretical and experimental advances in the quantum state preparation of nano- and micromechanical systems, in [40] we theoretically investigated a novel possibility of entangling the vibrational modes of two nanocantilevers which are indirectly coupled via an ensemble of ultra-cold atoms. In the present chapter we shall discuss in detail the scheme presented in [40] to entangle the vibrational modes of two spatially separated mechanical oscillators.

We consider a physical system comprising of two nanocantilevers, modelled as harmonic oscillators with fundamental flexural modes labelled a and b. The two nanocantilevers are assumed to be coupled to a cloud of ultra-cold atoms, modelled as a collection of N two-level atoms. We shall neglect any direct interaction between the nanomechanical systems but allow them to interact via the ultra-cold atoms only. We

shall explain below, that for the particular physical geometry we have in mind, the direct interaction between the nanocantilevers can be neglected without qualitatively changing the main findings of the present chapter.

With the advancement in fabrication techniques of nano- and micromechanical systems, they can now be fabricated with exceedingly large oscillation frequencies and very large quality factors [73]. When pre-cooled near to their quantum ground states, their mechanical motion appears quantised. We shall assume that the two nanocantilevers have been cooled to their near ground states so that the average thermal occupancy of each cantilever is close to zero *i.e.* $\langle n_{\rm thermal}\rangle \ll 1$. We also assume that both cantilevers are vibrating in their fundamental mechanical modes which can be well separated from other vibrational modes [74]. The quantum nanocantilevers have their discrete eigenenergy spectrum well described by the Fock states $(|0\rangle, |1\rangle, ...|n\rangle)$, and quantised energy spacings denoted by $\hbar\omega_a$, $\hbar\omega_b$, where ω_a and ω_b are the resonant frequencies of the two nanocantilevers. In the discussion to follow we shall assume that both the nanocantilevers are vibrating with an identical fundamental resonance frequency ω_0.

In the scheme to follow we shall propose to couple different spin levels of the ultra-cold atoms to the vibrational modes of two identical nanocantilevers. The atomic ensemle is described as a collection of N two-level atoms and can be well approximated by the Dicke model [75, 76]. The justification behind this approximation will soon become clear. At low enough temperature and due to the cooperative effect of the two-level atoms, individual excitations of the two-level atoms becomes the collective excitations in the ultra-cold atoms. Dicke states are defined as the simultaneous eigenstates of the Hermitian operators $\hat{J}_z$ and $\hat{J}^2$ such that

$$\begin{aligned} \hat{J}_z|M,J\rangle &= M|M,J\rangle, \\ \hat{J}^2|M,J\rangle &= J(J+1)|M,J\rangle. \end{aligned} \tag{3.1}$$

The Dicke states can be mathematically constructed by operating $\hat{J}^+$ on the state

$|-J, J\rangle$, $(M+J)$ times. In the above notation, $|M, J\rangle$ represents an atomic ensemble where out of $2J$ atoms, $J+M$ atoms are in the excited state and $J-M$ atoms are in the collective ground state. The set of Dicke states $|M, J\rangle$ span the space of the angular momentum quantum number J. In this representation, $|-J, J\rangle$ refers to the ground state and $|J, J\rangle$ the highest possible excited state. The action of atomic raising and lowering operators on a general state is,

$$\begin{aligned} \hat{J}^{+}|M, J\rangle &= \sqrt{J(J+1) - M(M+1)}|M+1, J\rangle, \\ \hat{J}^{-}|M, J\rangle &= \sqrt{J(J+1) - M(M-1)}|M-1, J\rangle. \end{aligned} \tag{3.2}$$

In terms of individual atomic ground ($\downarrow$) and excited ($\uparrow$) states, the collective ground state and the first excited state of all the atoms in the atomic ensemble can be denoted as

$$|-J, J\rangle = |\downarrow, \downarrow, ... \downarrow\rangle, \tag{3.3}$$

$$|-J+1, J\rangle = \frac{1}{\sqrt{N}}(|\uparrow, \downarrow, ... \downarrow\rangle + |\downarrow, \uparrow, ... \downarrow\rangle + ... + |\downarrow, \downarrow, ... \uparrow\rangle). \tag{3.4}$$

To begin with, we shall restrict the maximum number of excitations in the ensemble of ultra-cold atoms to one and thus will only consider two global states of the atomic ensemble $|-J, J\rangle$ and $|-J+1, J\rangle$ respectively. Here $|-J, J\rangle$ denotes the collective ground state of the ultra-cold atoms and $|-J+1, J\rangle$ denotes a global state with exactly one excitation equally shared between any one of the N two-level atoms. The action of collective atomic raising and lowering operators on these two global states is

$$\begin{aligned} \hat{J}^{+}|-J, J\rangle &= \sqrt{N}|-J+1, J\rangle, \\ \hat{J}^{-}|-J+1, J\rangle &= \sqrt{N}|-J, J\rangle, \\ \hat{J}^{-}|-J, J\rangle &= 0, \\ \hat{J}^{+}|-J+1, J\rangle &= 0, \end{aligned}$$

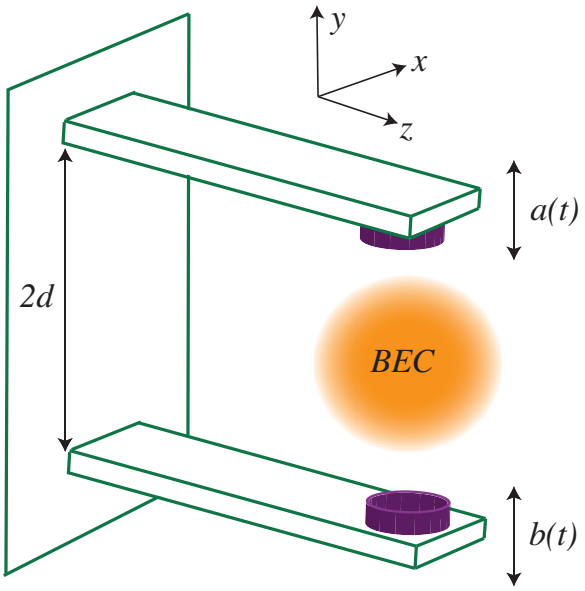

Figure 3.1: Physical setup for our proposed scheme for entangling two nanocantilevers. Two identical nanocantilevers, integrated with an atom chip, have strong ferromagnets attached to their tips. The cantilevers are placed equidistant from an ultra-cold gas of atoms, which is confined to a microtrap. Each nanomagnet couples the vibrational motion of a nanocantilever to the collective spin of the ultra-cold gas.

where $J = \frac{N}{2}$.

In the discussion to follow we shall denote the collective ground state of the ultra-cold atoms as $|g\rangle$ and the next excited state as $|e\rangle$. To model the interaction between the two nanocantilevers and the ultra-cold atoms, we follow the scheme suggested in [24] and subsequently extended in [40]. The physical setup is shown in Fig. 3.1. The two identical nanocantilevers, separated by a distance $2d$ along the y-axis, are assumed to be fabricated on an atom chip with strong ferromagnets attached to their tips. Equidistant from the tips, at a distance d, an ensemble of ultra-cold atoms is confined in a microtrap. The magnetic moment $\boldsymbol{\mu}$ of each ferromagnet is pointing in the x-direction. Under the dipole approximation, the x-component of the magnetic field at the centre of the trap, produced by the ferromagnet on the tip of cantilever a, is

$$B_x = -\frac{\mu_0 \mu}{4\pi y^3} = -\frac{\mu_0 \mu}{4\pi [d + y_a(t)]^3}\,, \tag{3.5}$$

where μ_0 is the vacuum permeability and $y_a(t)$ is the time dependent deflection of the tip of nanocantilever a. For small displacements of the cantilever this expression can be expanded to linear order in $y_a(t)$, so that

$$B_x = -\frac{\mu_0 \mu}{4\pi d^3}\left[1 - 3\frac{y_a(t)}{d}\right]. \tag{3.6}$$

Thus $y_a(t)$ transduces the vibrational motion of cantilever a to an oscillating magnetic field given by

$$\mathbf{B} = G_m y_a(t)\hat{x} \tag{3.7}$$

at the location of the ultra-cold atoms, where $G_m{=}3\mu\mu_0/4\pi d^4$ is the magnitude of the magnetic field gradient in the y-direction.

We now consider a transition between two trapped atomic states $|0\rangle \leftrightarrow |1\rangle$. In a magnetic trap, hyperfine states $(|F, m_F\rangle)$ $|0\rangle \equiv |2,1\rangle$ and $1 \equiv |2,2\rangle$ can be used. However, the different trap frequencies lead to entanglement between internal and motional atomic degrees of freedom. For the simpler situation of an optical or electrodynamic microtrap [77], identical trapping potentials for all hyperfine states is provided. In such a trap, all atoms couple simultaneously to the resonator [2]. To mitigate collisional losses one can use $F = 1$, we choose $|0\rangle \equiv |1,0\rangle$ and $|1\rangle \equiv |1,-1\rangle$. The transition $|0\rangle \leftrightarrow |1\rangle$ can be decoupled from other m_F levels by making use of the quadratic Zeeman effect or by using microwaves to induce m_F-dependent energy shifts [78].Transitions from $|F = 1, m = 0\rangle \equiv |0\rangle$ to $|F = 1, m = -1\rangle \equiv |1\rangle$ can, for instance, be resonantly coupled to the quantised bending motion of the cantilever by tuning the Larmor frequency. Thus our assumption of treating the atomic cloud as a collection of N two-level atoms can be justified under the above conditions.

The cantilevers oscillates in the y direction while the magnetic dipole moment of each magnet is pointing in the x direction. The magnets on the oscillating cantilevers

[2] A trap geometry similar to an Ioffe-Pritchard trap would also be possible, in which case the ferromagnets would be aligned along the z-direction and B_0 along the long trap axis in the x-direction.

creates an oscillating magnetic field $\mathbf{B} = G_m y_a(t)\hat{x}$ in the x direction. This field interacts with the collective atomic spin $\vec{J}$ via the interaction Hamiltonian. Due to the field the quantization axis of the atoms is along x direction. Coupling is thus achieved between the fundamental bending mode of cantilever a and the collective spin of the ultra-cold gas through the Zeeman interaction

$$-\mu_{\rm atom} \cdot \mathbf{B}(\mathbf{t}) = -\mu^x_{\rm atom} G_m y_a(t) = \hbar\kappa_a \frac{1}{\sqrt{N}} \hat{J}_x(\hat{a} + \hat{a}^\dagger) = \hbar\kappa_a \frac{1}{\sqrt{N}} (\hat{J}^+ + \hat{J}^-)(\hat{a} + \hat{a}^\dagger), \tag{3.8}$$

where $\boldsymbol{\mu}^{\ x}_{\rm atom}$ is the x component of the collective magnetic moment of the ultra-cold gas and $\kappa_a = \mu_B G_m \sqrt{N} a_0/\sqrt{8}\hbar$ is the coupling constant for the collective atomic spin coupled to a single vibrational mode of cantilever a. Here N is the number of ultra-cold atoms and $a_0 = \sqrt{\hbar/2m_{\rm eff}\omega_0}$ is the amplitude of the zero-point fluctuations of cantilever a, which has effective mass $m_{\rm eff}$ and angular oscillation frequency ω_0. The coupling between cantilever b and the ensemble of ultra-cold atoms is described by an analogous term.

In the strong coupling regime between the collective spin of the atomic cloud and the vibrational motion of two nanocantilevers, the system is analogous to a conventional cavity-QED setup. For a nanocantilever with mass $m \sim 10^{-16}$ kg and resonance frequency $\omega_0/2\pi \sim$1 MHz, which is separated from an atomic cloud of $N \sim 100$ atoms by a distance of $d \sim 250$ nm, the interaction produced by a small [3] disk-shaped magnet containing $N_{\rm mag} \sim 10^6$ nickel atoms corresponds to a coupling constant $\kappa_a \sim 100$ Hz.

In the particular geometry we envisage for physically entangling the two nanomechanical oscillators, direct interaction between the magnetic dipoles on the two cantilever tips can be neglected. To see this, one can compare the two interaction strengths, one due to the direct interaction between the magnetic cantilever tips and the other due to the interaction between either cantilever magnet and the collective spin of the

[3] If the finite size of the magnet is taken into account the coupling constant κ is reduced by a factor ~ 2. The strong coupling regime can still be achieved by increasing the number of atoms in the trap centre.

atomic cloud. The ratio between these interaction terms is

$$\frac{H_{\text{ Zeeman}}}{H_{\text{ direct}}} \approx 4\frac{d\sqrt{N}}{a_0 N_{\text{mag}}} \sim 25\,. \tag{3.9}$$

However, even if this direct interaction is included, the qualitative behaviour of the system does not change. We must stress, though, that as shown later in the chapter the role of the atomic ensemble is essential for generating a time independent statistical mixture of *dark* (entangled) states of the two nanocantilevers. In the absence of an atomic cloud, a pair of nanocantilevers interacting directly via the dipole-dipole interaction may well exhibit time-dependent entanglement. It would, however, be difficult to use or capture these states because one would have to, for instance, be able to control the direct interaction between the two cantilevers such that it could be switched off at a chosen time when the entanglement between the two cantilevers is maximal.

The collective magnetic dipole moment of the ultra-cold atoms experience the electromagnetic field generated by the quantised motion of the two nanocantilevers. If we assume that the atomic cloud can be represented by a single quantised mode of frequency ω_a, which can be tuned to resonate with the identical fundamental oscillation frequency ω_0 of each nano-resonator, then the dynamics of the two nanocantilevers interacting via the atomic cloud is well described by the Jaynes-Cummings Hamiltonian [43]. The Jaynes Cummings model, which has been well studied in the quantum optics community, approximates the atom-light interaction by treating the atom as a dipole placed in an external field. Although the Jaynes Cummings model is based on a simple assumption of light matter interaction, it has proved to be quite successful in studying phenomena like trapping of atoms (Lie et al.,1998), electro-magnetically indued transparency and enhancement of refractive index (Scully et. al.,1997) etc. A very useful feature of the Jaynes Cummings model is that it is symmetric with respect to the interchange of atom and field quanta.

Under the dipole and the rotating wave approximations (RWA) [79], and taking

κ_a=κ_b=κ, the Hamiltonian describing the coupled system of two nanocantilevers interacting with a cloud of ultra-cold atoms takes the form

$$\begin{aligned} \frac{H}{\hbar} &= \omega_0(\hat{J}_z + \hat{a}^\dagger\hat{a} + \hat{b}^\dagger\hat{b}) + [\kappa\frac{1}{\sqrt{N}}(\hat{a}+\hat{b})\hat{J}_+ + h.c.] \\ &= H_0 + H_I, \end{aligned} \tag{3.10}$$

where $H_0 = \omega_0(\hat{J}_z + \hat{a}^\dagger\hat{a} + \hat{b}^\dagger\hat{b})$ and $H_I = (\kappa/\sqrt{N})(\hat{a}+\hat{b})\hat{J}_+ + h.c.$ are the free and the interaction parts of the Hamiltonian respectively, and J_z is the z component of the collective angular momentum of the ultra-cold atoms. In the Dicke model, the collective spin of the ultra-cold atoms is $J = N/2$, and the eigenstates denoted by $|J, m_J\rangle$, with $|m_J| \leq J$ where N is the number of two-level atoms in the ultra-cold atoms. After these initial considerations, we now proceed to study the unitary evolution of the coupled system of two nanocantilevers and ultra-cold atoms followed by an investigation of the dissipative dynamics of the two indirectly coupled nanocantilevers.

3.3 Unitary evolution

We shall now consider the unitary evolution of a system of two nanocantilevers interacting indirectly via an atomic cloud of N two-level atoms. As mentioned before, we assume that the nanocantilevers have been cooled near to their quantum ground states and thus only the lowest-energy vibrational states of the two oscillators are appreciably populated. In the Schrödinger picture, we restrict the excitation subspace of the two nanocantilevers to one, two and three quanta of vibrational excitations. To a first approximation we neglect any dissipation channel in the system and only study the unitary dynamics. We shall study the coherent dynamics of the system first in the Schrödinger picture followed by an equivalent investigation in the Heisenberg picture.

3.3.1 Schrödinger picture

In the interaction picture a very general initial state representing the interaction between two nanocantilevers and an atomic cloud in a one-excitation manifold takes the form

$$|\Psi_1(t)\rangle = e^{-i\frac{H_0 t}{\hbar}}(C_{g,0,1}(t)|g,0,1\rangle + C_{g,1,0}(t)|g,1,0\rangle + C_{e,0,0}(t)|e,0,0\rangle), \qquad (3.11)$$

where $|g,l,m\rangle$ represents a state with all the atoms in their electronic ground state ($|e,l,m\rangle$ represents a state with just one electronic excitation equally shared between all the atoms), cantilever a with l excitations and cantilever b with m excitations. With the ansatz (3.11), the Schrödinger equation reduces to the following set of coupled differential equations

$$\frac{\partial}{\partial t}\mathbf{C}_1(t) \;=\; \beta\mathbf{C}_1(t), \qquad (3.12)$$

where

$$\beta = -i\begin{bmatrix} 0 & 0 & \kappa \\ 0 & 0 & \kappa \\ \kappa & \kappa & 0 \end{bmatrix}; \qquad C_1(t) = \begin{bmatrix} C_{g,1,0}(t) \\ C_{g,0,1}(t) \\ C_{e,0,0}(t) \end{bmatrix}.$$

The coupling matrix β has the eigenvalues $\lambda_0 = 0$, $\lambda_{\pm}{=}{\pm}i\sqrt{2}\kappa$, with the corresponding normalised eigenvectors given by

$$|\lambda_0\rangle = \tfrac{1}{\sqrt{2}}\begin{bmatrix} 1 \\ -1 \\ 0 \end{bmatrix}, \quad |\lambda_-\rangle = \tfrac{1}{2}\begin{bmatrix} -1 \\ -1 \\ \sqrt{2} \end{bmatrix}, \quad |\lambda_+\rangle = \tfrac{1}{2}\begin{bmatrix} 1 \\ 1 \\ \sqrt{2} \end{bmatrix}.$$

It can be readily seen that $|\lambda_0\rangle$ is not affected by dissipation in the internal electronic states of the atoms in the atomic cloud. Such a state is termed a *dark* state or *trapped* state because the population of such a state doesn't decay even in the presence of

dissipation in ultra-cold gas .

Dark states have been extensively studied in the context of decoherence-free subspaces (DFSs) [80] and there have been many proposals to prepare the qubits in these states and hence protect them from decoherence [81]. If one could prepare the system of two nanocantilevers and the atoms in a one-excitation manifold, then different eigenmodes of the system are excited. The population in the states orthogonal to the *dark* state undergo dissipation and ultimately relax into the ground state, while the population of the *dark* state remains intact. If prepared in a *dark* state, the two nanocantilevers remain uncoupled from the rest of the environment and keep exchanging excitation(s) between them. If the two nanocantilevers couple to the ultra-cold atomic gas with different coupling strengths κ_a, κ_b, then the dark state in a one-excitation manifold takes the form

$$|\lambda_0\rangle_1 = \frac{\kappa_a}{\sqrt{(\kappa_a^2+\kappa_b^2)}}|g,0,1\rangle - \frac{\kappa_b}{\sqrt{(\kappa_a^2+\kappa_b^2)}}|g,1,0\rangle, \tag{3.13}$$

which is a maximally entangled state of two nanocantilevers for $\kappa_a = \kappa_b$. We will further discuss the relevance of such *dark* states for our scheme in the next section, where we will study the dissipative dynamics of the system. With a suitable initial condition, one can very easily solve (3.11) to get the time evolved wave function in a one-excitation manifold. Assuming $C_{g,1,0}(0) = 1$, the joint state of the two nanocantilevers and the ultra-cold atoms evolves to

$$|\Psi_1(t)\rangle = \frac{1}{2}\begin{bmatrix} 1+\cos(\sqrt{2}\kappa t) \\ \cos(\sqrt{2}\kappa t)-1 \\ -i\sqrt{2}\sin(\sqrt{2}\kappa t) \end{bmatrix}, \tag{3.14}$$

with the corresponding probability distribution shown in Fig. [3.2]. The excitation is reversibly transferred between the two nanocantilevers and the ultra-cold atomic gas. We shall explicitly evaluate the entanglement between the two nanocantilevers later, but it turns out that the reversible exchange of excitation(s) between the two

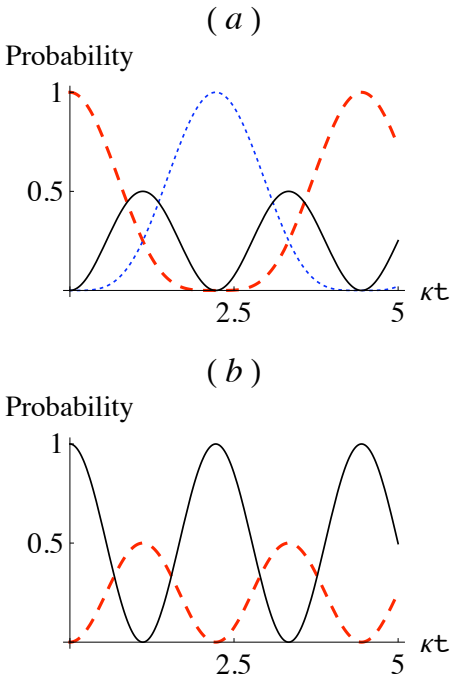

Figure 3.2: Temporal evolution of the occupation probability for (a) the states $|g,1,0\rangle$ (red, dashed), $|g,0,1\rangle$ (blue, dotted) and $|e,0,0\rangle$ (black, solid) with the initial condition $C_{g,1,0}(0)=1$, and (b) for the states $|g,1,0\rangle$ and $|g,0,1\rangle$ (red, dashed, identical) and $|e,0,0\rangle$ (black, solid) with the initial condition $C_{e,0,0}(0)=1$. In both cases time is scaled in units of κ.

oscillators results in a time evolved state, which is inseparable in terms of individual number states of the two oscillators and the ultra-cold atoms.

To study the dynamics of the coupled system of two nanocantilevers and an ensemble of ultra-cold atoms in a subspace with more excitations, equation (3.11) can readily be generalised. In the interaction picture, general state vectors for the system of two indirectly coupled nanocantilevers in the two- and three-excitation manifolds take the form

$$|\Psi_2(t)\rangle = e^{-i\frac{H_0 t}{\hbar}}\Big(\sum_{j=0}^{2} C_{g,j,2-j}(t)|g,j,2-j\rangle + \sum_{j=0}^{1} C_{e,j,1-j}(t)|e,j,1-j\rangle\Big),$$

$$|\Psi_3(t)\rangle = e^{-i\frac{H_0 t}{\hbar}}\Big(\sum_{j=0}^{3} C_{g,j,3-j}(t)|g,j,3-j\rangle + \sum_{j=0}^{2} C_{e,j,2-j}(t)|e,j,2-j\rangle\Big).$$

Using the above ansatz, the Schrödinger equation reduces to following sets of coupled differential equations

$$\frac{\partial}{\partial t}\mathbf{C}_2(t) = -i\mathsf{A}_2\mathbf{C}_2(t); \quad \frac{\partial}{\partial t}\mathbf{C}_3(t) = -i\mathsf{A}_3\mathbf{C}_3(t),$$

where the coupling matrices are of the form

$$\mathsf{A}_2 = \begin{bmatrix} 0 & 0 & 0 & \kappa\sqrt{2} & 0 \\ 0 & 0 & 0 & \kappa & \kappa \\ 0 & 0 & 0 & 0 & \kappa\sqrt{2} \\ \kappa\sqrt{2} & \kappa & 0 & 0 & 0 \\ 0 & \kappa & \kappa\sqrt{2} & 0 & 0 \end{bmatrix};$$

$$\mathsf{A}_3 = \begin{bmatrix} 0 & 0 & 0 & 0 & \kappa\sqrt{3} & 0 & 0 \\ 0 & 0 & 0 & 0 & \kappa & \kappa\sqrt{2} & 0 \\ 0 & 0 & 0 & 0 & 0 & \kappa\sqrt{2} & \kappa \\ 0 & 0 & 0 & 0 & 0 & 0 & \kappa\sqrt{3} \\ \kappa\sqrt{3} & \kappa & 0 & 0 & 0 & 0 & 0 \\ 0 & \kappa\sqrt{2} & \kappa\sqrt{2} & 0 & 0 & 0 & 0 \\ 0 & 0 & \kappa & \kappa\sqrt{3} & 0 & 0 & 0 \end{bmatrix}.$$

Matrix A_2 has following non-degenerate eigenspectrum $\lambda_0 = 0, \lambda_1 = i\sqrt{2}\kappa, \lambda_2 = -i\sqrt{2}\kappa, \lambda_3 = i\sqrt{4}\kappa, \lambda_4 = -i\sqrt{4}\kappa$; and the eigenvector corresponding to λ_0 which is the the *dark* state vector in a two-excitation manifold has the form

$$|\mathbf{X}_0\rangle_2 = \begin{bmatrix} 1/2 \\ -1/\sqrt{2} \\ 1/2 \\ 0 \\ 0 \end{bmatrix} \equiv \begin{bmatrix} C_{g,2,0}(t) \\ C_{g,1,1}(t) \\ C_{g,0,2}(t) \\ C_{e,1,0}(t) \\ C_{e,0,1}(t) \end{bmatrix}, \tag{3.15}$$

while the matrix $\mathsf{A}_3(t)$ has the following eigenvalues $\lambda_0 = 0, \lambda_1 = i\sqrt{2}\kappa, \lambda_2 = -i\sqrt{2}\kappa, \lambda_3 = i\sqrt{4}\kappa, \lambda_4 = -i\sqrt{4}\kappa, \lambda_5 = i\sqrt{6}\kappa, \lambda_6 = -i\sqrt{6}\kappa$; with the corresponding *dark* state vector in a three-excitation manifold given by

$$|\mathbf{X}_0\rangle_3 = \begin{bmatrix} -1/2\sqrt{2} \\ \sqrt{3}/2\sqrt{2} \\ -\sqrt{3}/2\sqrt{2} \\ 1/2\sqrt{2} \\ 0 \\ 0 \\ 0 \end{bmatrix} \equiv \begin{bmatrix} C_{g,3,0}(t) \\ C_{g,2,1}(t) \\ C_{g,1,2}(t) \\ C_{g,0,3}(t) \\ C_{e,2,0}(t) \\ C_{e,1,1}(t) \\ C_{e,0,2}(t) \end{bmatrix}. \tag{3.16}$$

For the initial states $C_{g,2,0}(0) \equiv C_{g,3,0}(0) = 1$, the time evolved wave-function corresponding to the subspaces with two and three excitations takes the form

$$|\Psi_2(t)\rangle = \frac{1}{2\sqrt{2}} \begin{bmatrix} (1+\cos(\sqrt{4}\kappa t) + 2\cos(\sqrt{2}\kappa t))/\sqrt{2} \\ \cos(\sqrt{4}\kappa t) - 1 \\ (1+\cos(\sqrt{4}\kappa t) - 2\cos(\sqrt{2}\kappa t))/\sqrt{2} \\ -i\sqrt{2}\sin(\sqrt{2}\kappa t) - i\sin(\sqrt{4}\kappa t) \\ i\sqrt{2}\sin(\sqrt{2}\kappa t) - i\sin(\sqrt{4}\kappa t) \end{bmatrix}, \tag{3.17}$$

$$|\Psi_3(t)\rangle = \frac{1}{8} \begin{bmatrix} 1+\cos(\sqrt{6}\kappa t) + 3\cos(\sqrt{4}\kappa t) + 3\cos(\sqrt{2}\kappa t) \\ -\sqrt{3} + \sqrt{3}\cos(\sqrt{6}\kappa t) + \sqrt{3}\cos(\sqrt{4}\kappa t) - \sqrt{3}\cos(\sqrt{2}\kappa t) \\ \sqrt{3} + \sqrt{3}\cos(\sqrt{6}\kappa t) - \sqrt{3}\cos(\sqrt{4}\kappa t) - \sqrt{3}\cos(\sqrt{2}\kappa t) \\ -1 + \cos(\sqrt{6}\kappa t) - 3\cos(\sqrt{4}\kappa t) + 3\cos(\sqrt{2}\kappa t) \\ -i\sqrt{2}\sin(\sqrt{6}\kappa t) - i2\sqrt{3}\sin(\sqrt{4}\kappa t) - i\sqrt{6}\sin(\sqrt{2}\kappa t) \\ (-i\sin(\sqrt{6}\kappa t) + i\sqrt{3}\sin(\sqrt{2}\kappa t))2 \\ -i\sqrt{2}\sin(\sqrt{6}\kappa t) + i2\sqrt{3}\sin(\sqrt{4}\kappa t) - i\sqrt{6}\sin(\sqrt{2}\kappa t) \end{bmatrix}. \tag{3.18}$$

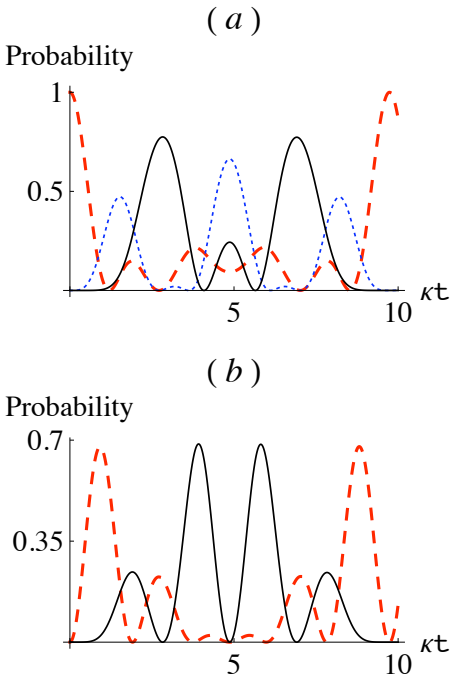

Figure 3.3: Temporal evolution of the occupation probability for (a) the states $|g, 2, 0\rangle$ (red, dashed), $|g, 1, 1\rangle$ (blue, dotted) and $|g, 0, 2\rangle$ (black, solid) and (b) the states $|e, 1, 0\rangle$ (red, dashed) and $|e, 0, 1\rangle$ (black, solid), with the initial condition $C_{g,2,0}(0) = 1$. Time is scaled in units of κ.

Time evolution of the system of two indirectly coupled nanocantilevers initially prepared with two and three excitations quanta is shown in Figs. [3.3] and [3.4] respectively, where occupation probabilities are plotted as a function of time for the different basis states. A coherent coupling between the two nanocantilevers and the ultra-cold gas results in a time varying exchange of excitations between the two nanocantilevers via the ultra-cold atomic gas. The result is a time-varying entanglement between states of each excitation manifold which shall be quantified now. It turns out that a system of two nanocantilevers becomes more entangled in higher excitation subspaces. The entanglement persist even for initial mixed states of the two nanocantilevers, albeit with significantly lower values. Higher initial excitations number of the oscillators correspond to greater non-classical character of the oscillators, which results in a stronger entangled state of the two oscillators.

After arriving at the closed form expressions for the time-evolved wave functions

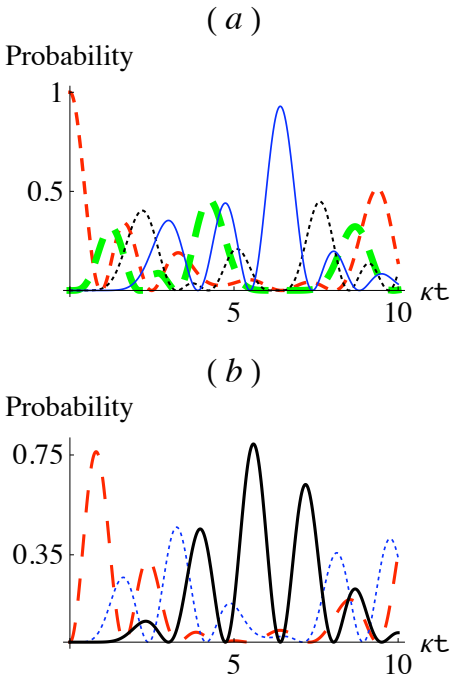

Figure 3.4: Occupation probability, as a function of time, for the states (a) $|g,3,0\rangle$ (red, dashed), $|g,2,1\rangle$ (green, thick dashed), $|g,1,2\rangle$ (black, dotted) and $|g,0,3\rangle$ (blue, solid); (b) $|e,2,0\rangle$ (red, dashed), $|e,1,1\rangle$ (blue, dotted) and $|e,0,2\rangle$ (black, solid), with the initial condition $C_{g,3,0}(0) = 1$. Time is scaled in units of κ.

describing the quantum state of two indirectly coupled nanocantilevers, we shall now quantify the entanglement present between the two nanocantilevers. We use the Peres criterion [82] to quantify entanglement between the two nanocantilevers. To do this, we trace out the ultra-cold atomic gas, and compute the negativity for the reduced density matrix for the two nanocantilevers. The negativity is defined as

$$\mathcal{N} = max(0, -\sum_i \lambda_i), \tag{3.19}$$

where $\sum_i \lambda_i$ is the sum of all the negative eigenvalues of the partially transposed density matrix. It turns out that $\mathcal{N}$ is not only easy to compute but has an added advantage of being an entanglement monotone [58]. For a bipartite system of two qubits, $\mathcal{N}$ lies between 0 and 0.5 for separable and maximally entangled states respectively. For a maximally entangled state of two qudits $\mathcal{N}$ is bounded by $\mathcal{N} \leq (k-1)/2$

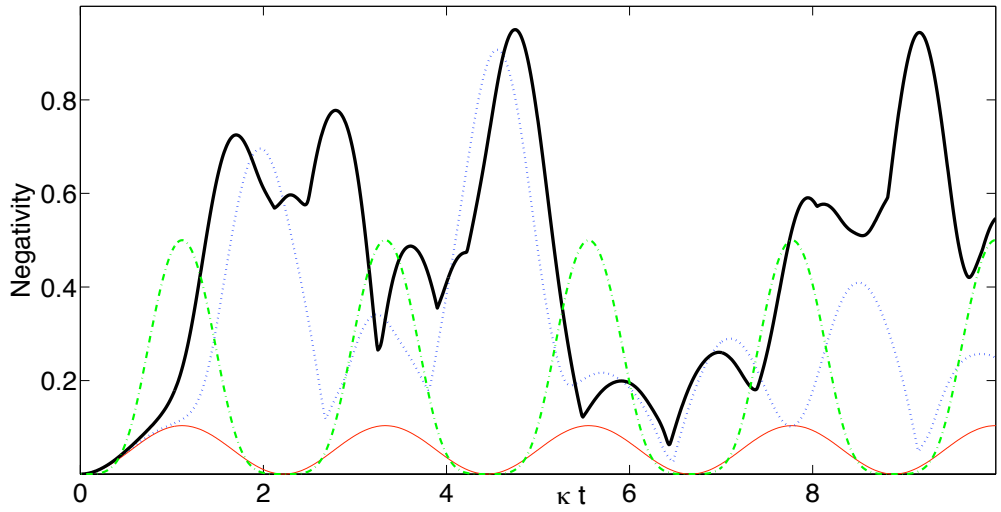

(a)

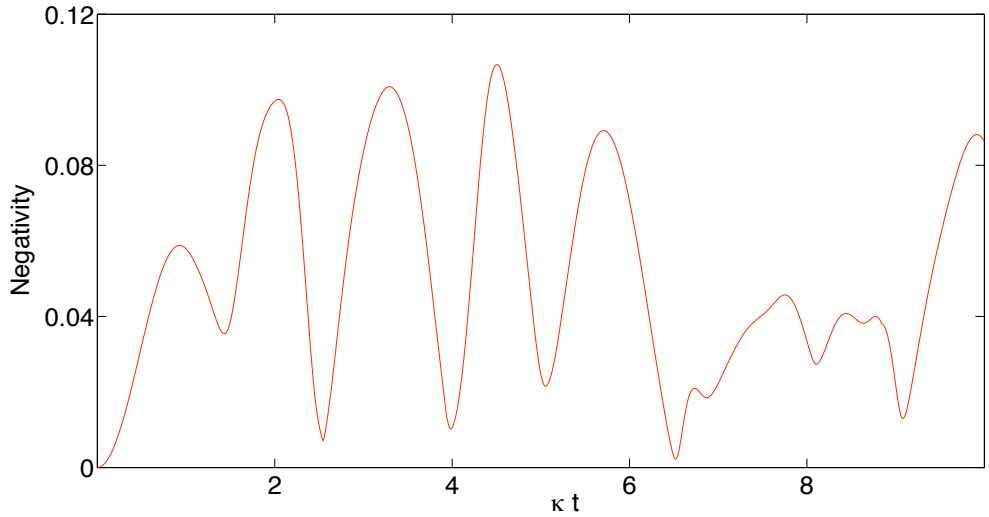

(b)

Figure 3.5: Degree of entanglement, as measured by the negativity defined in equation (3.19), for a system of two nanocantilevers interacting with a dissipation free ultra-cold gas, in (a) the one- (red, thin solid), two- (blue, dotted) and three-excitation (black, thick solid) subspaces, with all the excitations initially present in one of the cantilevers. Also, for comparison, the negativity is presented for the case when the initial excitation is in the gas for the one-excitation subspace (green, broken), (b) For an initial mixed state of the first three excitation subspaces with average occupancy of 0.3. Time is scaled in units of κ.

where k is the number of terms in the *Schmidt* decomposition of an overall pure state of a bipartite system. As shown in Fig. [3.5(a)], in a one-excitation subspace the system of two nanocantilevers remains entangled at all times except at certain instants though the two nanocantilevers never attains the maximal entanglement. In subspaces with higher excitations, the two oscillators become more and more entangled. In Fig. [3.5(a)] we have also compared $\mathcal{N}$ for two different initial conditions in a one-excitation subspace. It is clear from Fig. [3.5(a)] that if the initial excitation lies in the ultra-cold gas then it favours the generation of maximally entangled states of the two nanocantilevers. One of the main feature of our proposed scheme to generate entangled states of spatially separated mechanical oscillators is that entangled states of the two nanocantilevers are generated even for an initial mixed state. As an illustration, we plot in Fig. 3.5(b) the negativity as a measure of entanglement for an initial separable mixture of the first three-excitation subspaces. We have assumed an initial state of the two indirectly coupled nanocantilevers as $\rho(0) = \sum_{n=1}^{3} \frac{\bar{n}^n}{(\bar{n}+1)^{n+1}} |n_a\rangle|0_b\rangle|0_c\rangle\langle n_a|\langle 0_b|\langle 0_c|$, which is a mixture of state vectors corresponding to first three excitation subspaces where the initial excitation lies in one of the cantilever. A non-zero value of negativity in Fig. 3.5(b) again points to a finite entanglement being present between the two nanocantilevers.

As another measure to quantify entanglement present in the system of two indirectly coupled nanocantilevers we shall compute tangle [83]. This entanglement measure gives us the amount of quantum correlations present between two subsystems. Tangle for a bipartite system in an overall pure state with arbitrary subsystems dimensions is defined as

$$\tau_{\Psi_{\rm AB}} = 2\nu_{\rm A}\nu_{\rm B}(1 - {\rm Tr}(\rho_{\rm A}^2)),$$

where A,B are the two subsystems and $\nu_{\rm A}, \nu_{\rm B}$ are the scale factors. In general, $\nu_{\rm A}, \nu_{\rm B}$ depends on the subsystems dimensions $D_{\rm A}$ and $D_{\rm B}$, and are usually taken as one so that the extra unused Hilbert space has no effect on the value of concurrence (square of tangle) [84]. Assuming the ultra-cold atoms constitutes as one subsystem

and the joint state of the two nanocantilevers constituting the other subsystem, the entanglement present between the two subsystems can be computed as

$$\tau_{\Psi_{G(C_1C_2)}} = 2(1 - \mathrm{Tr}(\rho^2_{C_1C_2})), \tag{3.20}$$

where $\rho_{C_1C_2}$ refers to the reduced density matrix representing the joint state of the two nanocantilevers, obtained by tracing over the atomic degrees of freedom. If the overall system starts out in a pure state, then in the subsequent time evolution a non zero value of tangle $\tau_{\Psi_{G(C_1C_2)}}$ points to the quantum correlations built between the two nanocantilevers and the ultra-cold atoms. If a measurement is performed on the ultra-cold atoms, then the quantum back action on the ensemble of two nanocantilevers is given by the above equation [83].

From the time-evolved wave functions of the two indirectly coupled nanocantilevers, the ultra-cold atoms-remainder[4] tangle is evaluated and the result is shown in Fig. [3.6] for all three excitation subspaces. The collapse of entanglement between the two nanocantilevers can be attributed to the fact that there is loss of information of the cantilever dynamics to the ultra-cold atoms, while the resurrection of entanglement can be explained on the grounds that so far we have not considered any losses in our analysis. On the other hand, the entanglement sharing between the two cantilevers and the ultra-cold atoms occurs in a much more complex way in higher excitation manifolds and at no instance of time there is found to be complete disentanglement of the two cantilevers and the ultra-cold atoms. In Fig. [3.7] is shown the evolution of one cantilever-remainder tangle for all three excitation subspaces [5]. The cantilever-remainder tangle is a measure of the quantum back-action on the cantilever-ultra-cold atoms ensemble while making a measurement on the other cantilever.

[4]Remainder here refers to the collective state of two indirectly coupled nanocantilevers.
[5]Remainder here refers to the joint state of the other nanocantilever and ultra-cold atoms.

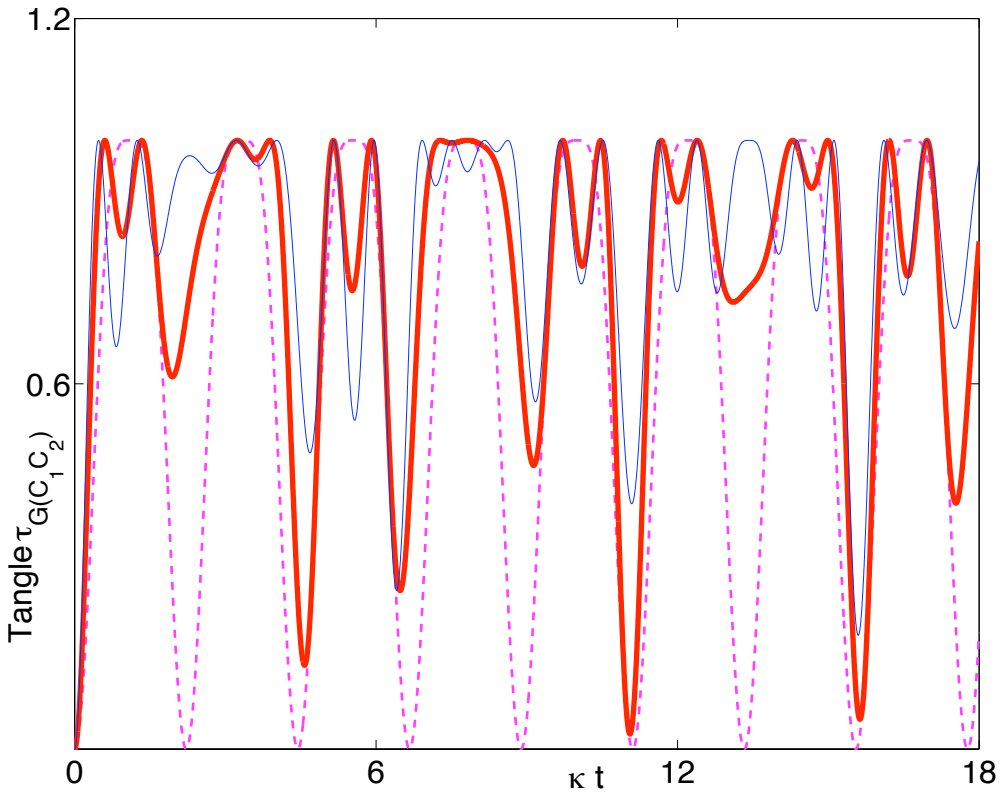

Figure 3.6: Time variation of the ultra-cold atoms-remainder tangle $\tau_{\Psi_{G(C_1C_2)}}$ for the system of two indirectly coupled nanocantilevers in one- (pink, dashed), two-(red, thick solid), three-excitation (blue, thin solid) subspaces. Time is scaled in units of κ.

3.3.2 Heisenberg picture

The unitary evolution of any quantum system can be equivalently described either in the Schrödinger or in the Heisenberg picture. After studying the unitary dynamics of the system of two indirectly coupled oscillators in the Schrödinger picture, we now present a compact way of describing the unitary evolution of the system in the Heisenberg picture. This method allows us to approximately solve for the dynamics of the coupled system of two nanocantilevers and the ultra-cold atoms in an arbitrary excitation subspace.

From the Dicke model introduced previously in the chapter, we have $-J \leq M \leq J$. Since most of the atoms in the ultra-cold atoms are in the electronic ground

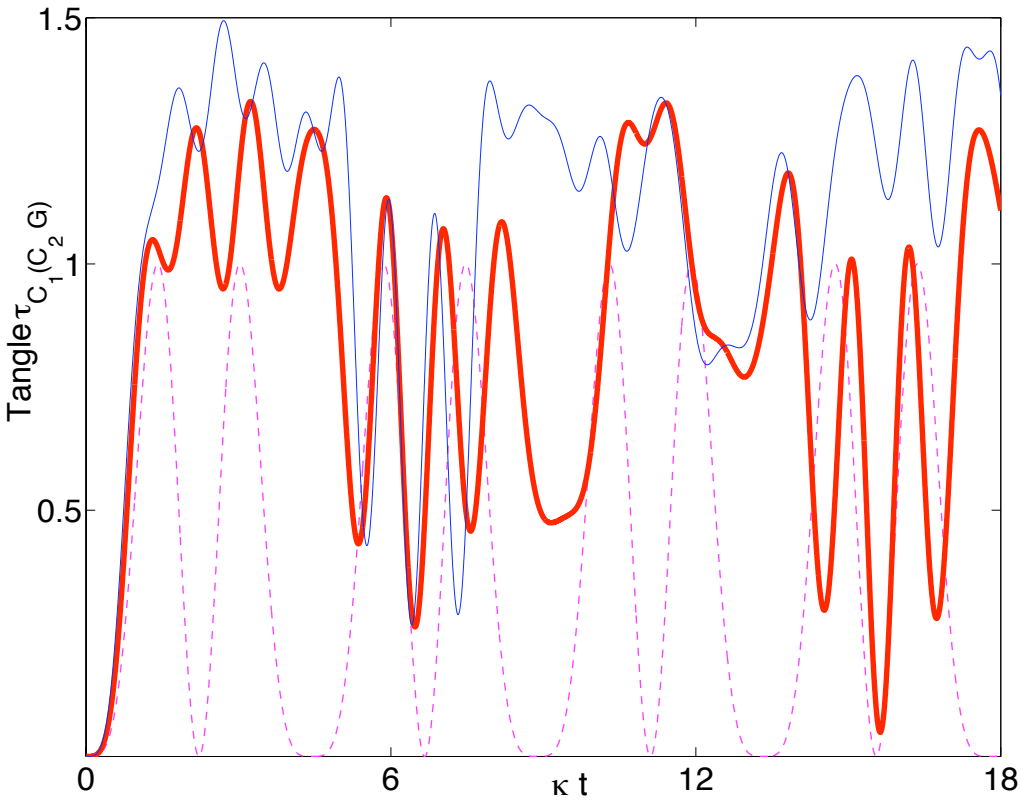

Figure 3.7: Time variation of one cantilever-remainder tangle $\tau_{\Psi_{C_1(C_2G)}}$ for one- (pink, dashed), two- (red, thick solid) and three-excitations (blue, thin solid) subspaces. Time is scaled in units of κ.

state, we can approximate $[J^+, J^-]$=$2J^z$=$-N$. An equivalent way of invoking this approximation is through the Holstein-Primakoff (H.P.) transformation [85]. This transformation is essentially a mapping from angular momentum spin operators to the bosonic operators. With the H.P. mapping, the collective angular momentum spin operators transforms as

$$\begin{aligned} \hat{J}^+ &= \hat{c}^\dagger \sqrt{N - \hat{c}^\dagger \hat{c}}, \\ \hat{J}^- &= \sqrt{N - \hat{c}^\dagger \hat{c}}\hat{c}, \\ \hat{J}^z &= \hat{c}^\dagger \hat{c} - \frac{N}{2}, \end{aligned} \tag{3.21}$$

where $\hat{c}$ and $\hat{c}^\dagger$ are the bosonic lowering and raising operators which satisfy the commutation relation $[\hat{c}, \hat{c}^\dagger] = 1$. In the large N limit, (3.21) reduces to $\hat{J}^+ \approx \hat{c}^\dagger\sqrt{N}$; $\hat{J}^- \approx$

$\hat{c}\sqrt{N}; \hat{J}^z \approx \hat{c^\dagger}\hat{c} - \frac{N}{2}$. Within this approximation, the Hamiltonian (3.10) takes the form

$$\frac{\mathcal{H}}{\hbar} = \omega_0(\hat{c}^\dagger\hat{c} - \frac{N}{2} + \hat{a}^\dagger\hat{a} + \hat{b}^\dagger\hat{b}) + \kappa(\hat{a} + \hat{b})\hat{c}^\dagger + \kappa\hat{c}(\hat{a}^\dagger + \hat{b}^\dagger). \tag{3.22}$$

Under the H.P. mapping, the original problem of nonlinear interaction between N two-level atoms and two bosonic modes has been transformed to a problem of three linearly coupled harmonic oscillators arranged in an open chain. This is a crucial observation as it will turn out to be of great significance in the analysis to follow.

We now introduce $\hat{p}^\dagger(0)$ and $\hat{q}^\dagger(0)$ as two sets of collective excitation creation operators defined as

$$\begin{aligned} \hat{p}^\dagger(0) &= u(\hat{a}^\dagger(0) + \hat{b}^\dagger(0)) + v(\hat{c}^\dagger(0)), \\ \hat{q}^\dagger(0) &= (\hat{a}^\dagger(0) - \hat{b}^\dagger(0))/\sqrt{2}. \end{aligned} \tag{3.23}$$

Requiring $[\hat{p}(0), \hat{p}^\dagger(0)] = 1$ and diagonalising (3.22) in the new basis [86], we find

$$\hat{\mathcal{H}} = \sum_{k=\pm} \hbar\Omega_k \hat{p}_k^\dagger \hat{p}_k, \tag{3.24}$$

where $\Omega_\pm = \omega_0 \pm \sqrt{2}\kappa$ and $\hat{p}_\pm^\dagger(0) = (\hat{a}^\dagger(0) + \hat{b}^\dagger(0))/2 \pm \hat{c}^\dagger(0)/\sqrt{2}$. With (3.24) $\hat{p}^\dagger(0)$ and $\hat{q}^\dagger(0)$ evolves as

$$\hat{p}_\pm^\dagger(t) = e^{i\Omega_\pm t}\hat{p}_\pm^\dagger(0), \tag{3.25}$$

$$\hat{q}^\dagger(t) = e^{i\omega_0 t}\hat{q}^\dagger(0). \tag{3.26}$$

From (3.25) and (3.26) we obtain

$$\hat{a}^\dagger(t) = \frac{\hat{p}_+^\dagger(t) + \hat{p}_-^\dagger(t) + \sqrt{2}\hat{q}^\dagger(t)}{2}, \tag{3.27}$$

$$\hat{b}^\dagger(t) = \frac{\hat{p}_+^\dagger(t) + \hat{p}_-^\dagger(t) - \sqrt{2}\hat{q}^\dagger(t)}{2}. \tag{3.28}$$

The above expressions for the time-evolved creation operators $\hat{a}^\dagger(t)$ and $\hat{b}^\dagger(t)$ along with the equivalent expressions for $\hat{a}(t)$ and $\hat{b}(t)$ can be used to describe the unitary time evolution of the system of two indirectly coupled nanocantilevers for arbitrary initial conditions. For instance, evolution of a state with cantilever a initially prepared in its n:th excited state can easily be determined as

$$|\Psi_n(t)\rangle = e^{-i\mathcal{H}t/\hbar}|g,n,0\rangle = e^{-i\mathcal{H}t/\hbar}\frac{\hat{a}^{\dagger n}}{\sqrt{n!}}|g,0,0\rangle \tag{3.29}$$

$$|\Psi_n(t)\rangle = \frac{\hat{a}^{\dagger n}(t)}{\sqrt{n!}}\exp(-i\mathcal{H}t/\hbar)|g,0,0\rangle \tag{3.30}$$

For instance, for $n = 1$, we obtain

$$|\Psi_1(t)\rangle = \hat{a}^\dagger(t)|g,0,0\rangle = \frac{1}{2}\begin{bmatrix} 1+\cos(\sqrt{2}\kappa t) \\ \cos(\sqrt{2}\kappa t)-1 \\ i\sqrt{2}\sin(\sqrt{2}\kappa t) \end{bmatrix}, \tag{3.31}$$

where the basis vectors are the same as for equation (3.14), obtained in the Schrödinger picture. The results are identical apart from a phase shift on the last component; this is a general feature of the Schrödinger vs. the Heisenberg picture. The dark states of the system are seen to correspond to excitations of the mode labelled q, so that a dark state with n excitations is given by $|\Psi_{q,n}(t)\rangle = (\hat{q}^\dagger(t))^n/(\sqrt{n!})|g,0,0\rangle$. This way, dark states corresponding to different numbers of excitations in the system can be easily computed.

Before concluding this section, we shall briefly point out the similarities and differences in the Schrödinger and Heisenberg approaches. To simplify calculations without compromising with the physical insight, in the Schrödinger picture we restricted the maximum number of excitations in the atomic gas to one. In the Heisenberg picture, this constraint is relaxed, and the system of two nanocantilevers interacting with the ultra-cold atoms is effectively treated as a system of three coupled harmonic oscillators. In reality, however, the number of excitations in the atomic gas is limited by the

total number of atoms N. The Heisenberg solution is therefore valid as long as the total number of excitations is less than the total number of atoms N, so that the gas is effectively equivalent to a harmonic oscillator. The Schrödinger and Heisenberg approaches give identical results if this holds, and if more than one excitation is allowed in the gas in the Schrödinger picture.

Another noteworthy feature is that under the Holstein-Primakoff (H.P.) transformation, an approximate closed form analytical expression describing the evolution of a system of two indirectly coupled nanocantilevers can be derived. This approximate analytical analysis correctly describes the dynamics of two indirectly coupled nanocantilevers in the regime where the number of excitations in the ultra-cold atoms is much smaller as compared to the total number of atoms in the ultra-cold atoms. The H.P. transformation greatly eases the analytical treatment but only at the expense of losing the intrinsic nonlinear interaction between the bosonic fields and a set of two-level atoms. Under the H.P. mapping, the coupled system reduces to a much simpler system of linearly coupled harmonic oscillators. This simplification greatly changes the physical consequences. If the bilinear interactions between the cantilevers are further simplified under the rotating wave approximation (RWA), then an initial classical Gaussian state will *always* evolve to a state with a positive P function [87], the details of which will be provided later. This implies that under the H.P. transformation if the indirect interaction between the oscillators are further simplified under the RWA, then an initial separable classical state of the nanocantilevers will *always* remains classical.

3.4 Dispersive regime

In the previous section we studied a physical scenario where the two nanocantilevers are interacting resonantly with the collective excitations of the ultra-cold atoms. In this section we shall study another interesting regime where the two nanocantilevers

are interacting dispersively with a cloud of ultra-cold atoms [88]. We assume that the two nanocantilevers have the same fundamental resonance frequency ω_0 while the ultra-cold atoms is represented by a single quantised mode of frequency ω_a. If the mean number of excitations in the ultra-cold atomic gas is small compared to the total number of ultra-cold atoms, then under the H.P. transformation the indirect interaction between the two nanocantilevers is modelled by the following Hamiltonian

$$\frac{H}{\hbar} = \omega_a(\hat{c}^\dagger\hat{c} - N/2) + \omega_0(\hat{a}^\dagger\hat{a} + \hat{b}^\dagger\hat{b}) + [\kappa(\hat{a} + \hat{b})\hat{c}^\dagger + h.c.]. \tag{3.32}$$

The dispersive regime is characterised by the criteria $\kappa << |\omega_a - \omega_0| << \omega_a + \omega_0$ [88]. To study the dispersive dynamics of the system we introduce the following unitary transformation, $\hat{\mathcal{U}} = e^{\lambda\alpha}$, where $\hat{\alpha} = \hat{c}(\hat{a}^\dagger + \hat{b}^\dagger) - \hat{c}^\dagger(\hat{a} + \hat{b})$ and $\lambda = \kappa/|\omega_a - \omega_0|$. The transformed Hamiltonian under the above transformation takes the form

$$H_{\text{disp}} = \hat{\mathcal{U}}^\dagger H \hat{\mathcal{U}}. \tag{3.33}$$

Using the Baker-Campbell Hausdorff formula $e^{\hat{A}}\hat{B}e^{-\hat{A}} = \hat{B} + [\hat{A}, \hat{B}] + \frac{[\hat{A},[\hat{A},\hat{B}]]}{2!} + \frac{[\hat{A},[\hat{A},[\hat{A},\hat{B}]]]}{3!} + ...$ and truncating (3.33) to first order in λ we get for the transformed Hamiltonian

$$\begin{aligned} H_{\text{disp}} \;\approx\; & (\omega_0 - 2\lambda\kappa)(\hat{a}^\dagger\hat{a} + \hat{b}^\dagger\hat{b}) + (\omega_a + 4\lambda\kappa)\hat{c}^\dagger\hat{c} - \frac{\omega_a N}{2} \\ & + (\kappa + \lambda(\omega_0 - \omega_a))((\hat{a} + \hat{b})\hat{c}^\dagger + \hat{c}(\hat{a}^\dagger + \hat{b}^\dagger)) - 2\lambda\kappa(\hat{a}^\dagger\hat{b} + \hat{b}^\dagger\hat{a}). \end{aligned} \tag{3.34}$$

Before analysing the dynamics of the system governed by (3.34), it is worth noting that in the dispersive regime the transformed Hamiltonian now contains an effective direct interaction between the two nanocantilevers. To describe the unitary dynamics of the system we now solve for the Heisenberg equations of motion. For a time dependent operator $\hat{A}$, the Heisenberg equation of motion is

$$\frac{d\hat{A}}{dt} = \frac{i}{\hbar}[\hat{H}, \hat{A}]. \tag{3.35}$$

For creation operators $\hat{a}, \hat{b}$ and $\hat{c}$ the Heisenberg equations of motion become

$$\begin{aligned}
\frac{d\hat{a}}{dt} &= -i(\omega_0 - 2\lambda\kappa)\hat{a} - i(\kappa + \lambda(\omega_0 - \omega_a))\hat{c} + 2i\lambda\kappa\hat{b}, && (3.36)\\
\frac{d\hat{b}}{dt} &= -i(\omega_0 - 2\lambda\kappa)\hat{b} - i(\kappa + \lambda(\omega_0 - \omega_a))\hat{c} + 2i\lambda\kappa\hat{a}, && (3.37)\\
\frac{d\hat{c}}{dt} &= -i(\omega_0 + 4\lambda\kappa)\hat{c} - i(\kappa + \lambda(\omega_0 - \omega_a))(\hat{a} + \hat{b}), && (3.38)\\
\frac{d}{dt}(\hat{a} + \hat{b}) &= -i(\omega_0 - 2\lambda\kappa)(\hat{a} + \hat{b}) + 2i\lambda\kappa(\hat{a} + \hat{b}) - 2i(\kappa + \lambda(\omega_0 - \omega_a)\hat{c}. && (3.39)
\end{aligned}$$

These simultaneous set of differential equations can be analytically solved to give

$$\begin{aligned}
\hat{a}(t) &= \frac{\hat{C}_1 e^{m_+ t} + \hat{C}_2 e^{m_- t}}{2} + \frac{(\hat{a}(0) - \hat{b}(0))}{2} e^{-i\omega_0 t}, \qquad (3.40)\\
\hat{b}(t) &= \frac{\hat{C}_1 e^{m_+ t} + \hat{C}_2 e^{m_- t}}{2} - \frac{(\hat{a}(0) - \hat{b}(0))}{2} e^{-i\omega_0 t},
\end{aligned}$$

where

$$\begin{aligned}
\hat{C}_1 &= \frac{-2i(\kappa + \lambda(\omega_0 - \omega_a))\hat{c}(0) + (4i\lambda\kappa - i\omega_0 - m_-)(\hat{a}(0) + \hat{b}(0))}{(m_+ - m_-)};\\
\hat{C}_2 &= \frac{-2i(\kappa + \lambda(\omega_0 - \omega_a))\hat{c}(0) + (4i\lambda\kappa - i\omega_0 - m_+)(\hat{a}(0) + \hat{b}(0))}{(m_- - m_+)};
\end{aligned}$$

$$m_\pm = \frac{-i(\omega_0 + \omega_a) \pm i\sqrt{(\omega_0 - \omega_a)^2 + 4K}}{2};$$

$$K = \kappa^2(2 + 16\lambda^2) + 2\lambda^2(\omega_0 - \omega_a)^2 - \omega_0\omega_a.$$

To first order in λ, the Hamiltonian (3.34) exactly describes the dynamics of two nanocantilevers interacting with an ultra-cold atomic ensemble in the dispersive limit. For instance, in a one-excitation subspace, starting from an initial pure state of one

of the cantilever, the system evolves as,

$$|\Psi_{\rm disp}(t)\rangle_1 = \hat{a}^\dagger(t)|0\rangle_a|0\rangle_b|0\rangle_c, \tag{3.41}$$

where $|0\rangle_a|0\rangle_b|0\rangle_c$ refers to the collective vacuum state of cantilevers a, b and the collective vibrational ground state of the ultra-cold gas. Thus $|\Psi_{\rm disp}(t)\rangle$ in a one-excitation subspace evolves as

$$|\Psi_{\rm disp}(t)\rangle_1 = A_1(t)|0\rangle_a|0\rangle_b|1\rangle_c + B_1(t)|1\rangle_a|0\rangle_b|0\rangle_c + C_1(t)|0\rangle_a|1\rangle_b|0\rangle_c, \tag{3.42}$$

where

$$\begin{aligned}
A_1(t) &= \frac{2i(\kappa\sqrt{N} + \lambda(\omega_0 - \omega_a))(e^{m_+^* t} - e^{m_-^* t})}{2(m_+^* - m_-^*)}, \\
B_1(t) &= (\frac{(4i\kappa\lambda\sqrt{N} - i\omega_0)(e^{m_-^* t} - e^{m_+^* t})}{2(m_+^* - m_-^*)} + \frac{m_+^* e^{m_-^* t} - m_-^* e^{m_+^* t}}{2(m_+^* - m_-^*)} + \frac{e^{i\omega_0 t}}{2}), \\
C_1(t) &= (\frac{(4i\kappa\lambda\sqrt{N} - i\omega_0)(e^{m_-^* t} - e^{m_+^* t})}{2(m_+^* - m_-^*)} + \frac{m_+^* e^{m_-^* t} - m_-^* e^{m_+^* t}}{2(m_+^* - m_-^*)} - \frac{e^{i\omega_0 t}}{2}).
\end{aligned}$$

In a subspace with two excitations, the two indirectly coupled nanocantilevers time evolves as

$$\begin{aligned}
|\Psi_{\rm disp}(t)\rangle_2 &= \frac{(\hat{a}^\dagger(t))^2}{\sqrt{2!}}|0\rangle_a|0\rangle_b|0\rangle_c \\
&= A_2(t)|0\rangle_a|0\rangle_b|2\rangle_c + B_2(t)|0\rangle_a|1\rangle_b|1\rangle_c + C_2(t)|1\rangle_a|0\rangle_b|1\rangle_c \\
&\quad + D_2 t)|1\rangle_a|1\rangle_b|0\rangle_c + E_2(t)|0\rangle_a|2\rangle_b|0\rangle_c + F_2(t)|2\rangle_a|0\rangle_b|0\rangle_c,
\end{aligned} \tag{3.43}$$

where

$$\begin{aligned} A_2(t) &= A_1^2(t)/\sqrt{2}, \\ B_2(t) &= \sqrt{2}A_1(t)C_1(t), \\ C_2(t) &= \sqrt{2}A_1(t)B_1(t), \\ D_2(t) &= \sqrt{2}A_1(t)B_1(t), \\ E_2(t) &= \sqrt{2}C_1^2(t), \\ F_2(t) &= \sqrt{2}B_1^2(t). \end{aligned}$$

With the solution of the time-evolved wave function describing the state of two indirectly coupled nanocantilevers interacting dispersively with the atomic cloud in hand, we can now compute the quantum entanglement between the two nanocantilevers. As a measure of degree of inseparability between indirectly coupled nanocantilevers, we compute the logarithmic negativity. The time evolution of the negativity for a subspace with one and two excitations is shown in Fig. 3.8 and Fig. 3.9 respectively. We find that in the dispersive regime, the excitation(s) is always shared between the two nanocantilevers and the atoms remain completely decoupled from the dynamics. We again find that the time evolved state of the two nanocantilevers interacting dispersively via ultra-cold atoms exhibit time varying entanglement. The entanglement being maximal in one-excitation subspace, while in a subspace with more excitations the value of entanglement is very close to its value for a maximally entangled state.

3.5 Beyond the rotating wave approximation

So far we have modelled the interaction between the collective excitations of the ultra-cold atoms and the vibrational mode of each nanocantilever under the rotating wave approximation (RWA). To illustrate the validity of the RWA, we first start with the

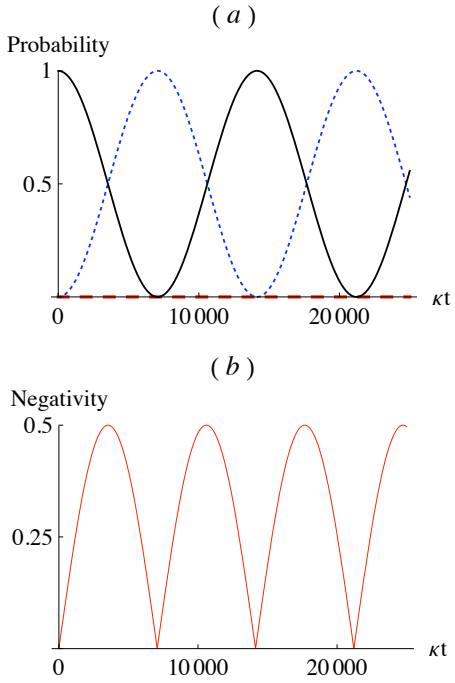

Figure 3.8: (a) Occupation probability, as a function of time, for the states $|e,0,0\rangle$ (red, thick dashed), $|g,0,1\rangle$ (blue, dotted), $|g,1,0\rangle$ (black, solid); (b) Time variation of entanglement between the two nanocantilevers interacting dispersively with an ultra-cold atoms and quantified in terms of the negativity where $|\omega_0 - \omega_a| = 9000$. Time is scaled in units of κ.

following Hamiltonian

$$H = \hbar\omega_a \hat{J}_z + \hbar\omega_0(\hat{a}^\dagger\hat{a} + \hat{b}^\dagger\hat{b}) + \frac{\kappa}{\sqrt{N}}(\hat{a} + \hat{a}^\dagger)\hat{J}_x + \frac{\kappa}{\sqrt{N}}(\hat{b} + \hat{b}^\dagger)\hat{J}_x, \tag{3.44}$$

which describes the interaction between the quantised motion of each nanocantilever and the collective magnetic moment of the ultra-cold atoms under the dipole approximation.

Despite its simplicity, finding an exact analytical solution of the Hamiltonian (3.44) is difficult in general (see also [89] for some recent breakthrough regarding this). The Hamiltonian (3.44) is thus often simplified under the rotating-wave approximation (RWA). Expressing $\hat{J}_x$ in terms of collective raising and lowering operators, the

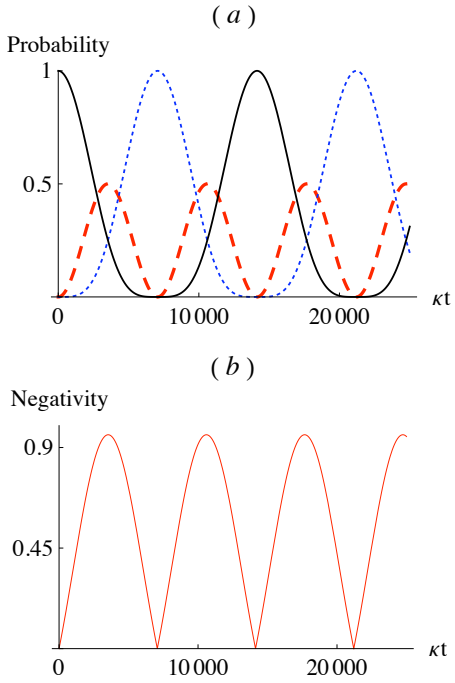

Figure 3.9: (a) Occupation probability, as a function of time, for the states $|g,2,0\rangle$ (black, solid), $|g,1,1\rangle$ (red, thick dashed), $|g,0,2\rangle$ (blue, dotted); (b) Time variation of entanglement between the two nanocantilevers interacting dispersively with an ultra-cold atoms and quantified in terms of the negativity where $|\omega_0 - \omega_a| = 9000$. Time is scaled in units of κ.

Hamiltonian (3.44) can be re-expressed as

$$H = \hbar\omega_a \hat{J}_z + \hbar\omega_0(\hat{a}^\dagger\hat{a} + \hat{b}^\dagger\hat{b}) + \frac{\kappa}{\sqrt{N}}(\hat{a} + \hat{a}^\dagger)(\hat{J}_+ + \hat{J}_-) + \frac{\kappa}{\sqrt{N}}(\hat{b} + \hat{b}^\dagger)(\hat{J}_+ + \hat{J}_-). \quad (3.45)$$

In the interaction picture of the free evolution of the two nanocantilevers and the ultra-cold atoms, the Hamiltonian (3.45) takes the form

$$\begin{aligned} H = &\frac{\kappa}{\sqrt{N}}(\hat{a}e^{-i\omega_0 t} + \hat{a}^\dagger e^{i\omega_0 t})(\hat{J}_+ e^{i\omega_a t} + \hat{J}_- e^{-i\omega_a t}) \\ &+ \frac{\kappa}{\sqrt{N}}(\hat{b}e^{-i\omega_0 t} + \hat{b}^\dagger e^{i\omega_0 t})(\hat{J}_+ e^{i\omega_a t} + \hat{J}_- e^{-i\omega_a t}). \end{aligned}$$

Now it is easy to see that the operators $\hat{a}\hat{J}_+$ $(\hat{a}^\dagger\hat{J}_-)$ and $\hat{a}\hat{J}_-$ $(\hat{a}^\dagger\hat{J}_+)$ oscillate with the phase factors $\mathrm{e}^{+i(\omega_a-\omega_0)t}$ $(\mathrm{e}^{-i(\omega_a-\omega_0)t})$ and $\mathrm{e}^{-i(\omega_a+\omega_0)t}$ $(\mathrm{e}^{+i(\omega_a+\omega_0)t})$ respectively. Under near resonant interactions $|\omega_a - \omega_0| \ll \omega_a + \omega_0$, the operators $\hat{a}\hat{J}_+$ and its hermitian con-

jugate oscillate slowly, whereas the operators $\hat{a}\hat{J}_-$ and its hermitian conjugate exhibit fast oscillations. If in addition, the coupling is sufficiently weak, $\kappa \ll \min(\omega_0, \omega_a)$, one can separate the time scales for the slow and the fast oscillations and replace the counter-rotating terms by their vanishing time averages. This approximation under which the fast oscillating terms are dropped from the Hamiltonian is what is known as the rotating-wave approximation (RWA) in quantum optics [79].

The RWA works very well for the commonly encountered quantum optical systems operating in the 'weak coupling' regime, such as atoms interacting with a quantised mode of radiation in a cavity. But the RWA fails to correctly describe the dynamics of coupled quantum systems operating in the 'strong coupling' regime, such as the ones encountered in solid state systems [90]. In this section, we shall model the indirect interaction between the cantilevers beyond the RWA, but for the sake of simplifying the calculations we shall still work in the resonant case *i.e.* $\omega_0 = \omega_a = \omega$.

Under the Holstein-Primakoff transformation, the Hamiltonian (3.45) takes the form,

$$\frac{H}{\hbar} = \omega(\hat{a}^\dagger\hat{a} + \hat{b}^\dagger\hat{b} + \hat{c}^\dagger\hat{c} - N/2) + \kappa(\hat{a} + \hat{b})(\hat{c}^\dagger + \hat{c}) + h.c.. \tag{3.46}$$

We introduce the following operators,

$$\hat{f} = \frac{(\hat{a} + \hat{b})}{2} + \frac{\hat{c}}{\sqrt{2}}; \tag{3.47}$$

$$\hat{g} = \frac{(\hat{a} + \hat{b})}{2} - \frac{\hat{c}}{\sqrt{2}}; \tag{3.48}$$

$$\hat{s} = \frac{(\hat{a} - \hat{b})}{\sqrt{2}}, \tag{3.49}$$

where $[\hat{f}, \hat{f}^\dagger] \equiv [\hat{g}, \hat{g}^\dagger] \equiv [\hat{s}, \hat{s}^\dagger] = 1$ and $[\hat{f}, \hat{g}^\dagger] \equiv [\hat{g}, \hat{s}^\dagger] \equiv [\hat{s}, \hat{f}^\dagger] = 0$. Rewriting (3.46) in terms of these collective operators we get

$$\begin{aligned} H &= \omega(\hat{f}^\dagger\hat{f} + \hat{g}^\dagger\hat{g} + \hat{s}^\dagger\hat{s}) + \frac{\kappa}{\sqrt{2}}(\hat{f}^\dagger\hat{f} + \hat{f}\hat{f}^\dagger + \hat{f}\hat{f} + \hat{f}^\dagger\hat{f}^\dagger) \\ &\quad -\frac{\kappa}{\sqrt{2}}(\hat{g}^\dagger\hat{g} + \hat{g}\hat{g}^\dagger + \hat{g}\hat{g} + \hat{g}^\dagger\hat{g}^\dagger). \end{aligned} \tag{3.50}$$

The Hamiltonian (3.50) can be diagonalised by a Bogoliubov transformation, details of which has been provided in Appendix A. To study the dynamics of the system beyond the rotating wave approximation, we define the Hermitian operators $\hat{Q}$ and $\hat{P}$ corresponding to the two-mode quadratures of cantilevers a and b as follows

$$\hat{Q}(t) = \frac{(\hat{a}(t) + \hat{a}^\dagger(t) + \hat{b}(t) + \hat{b}^\dagger(t))}{4}, \tag{3.51}$$

$$\hat{P}(t) = \frac{i(\hat{a}^\dagger(t) + \hat{b}^\dagger(t) - \hat{a}(t) - \hat{b}(t))}{4}. \tag{3.52}$$

The quantum fluctuations of these quadratures is well characterised by the variances of these operators defined as

$$\Delta O^2(t) = \langle \hat{O}^2(t) \rangle - \langle \hat{O}(t) \rangle^2. \tag{3.53}$$

We compute $\Delta P^2(t)$ and $\Delta Q^2(t)$ for an initial state $|\alpha\rangle_a|\alpha\rangle_b|0\rangle_c$. The result is shown in Fig. 3.10. As can be seen from Fig. 3.10, the quadrature operator $\hat{Q}$ exhibits a time dependent squeezing beyond its respective value for a coherent state for which $\Delta Q^2(0) = \Delta P^2(0) = 1/8$.

If the two nanocantilevers are initially prepared in coherent states and the time evolution is described under the Hamiltonian (3.22), we find no squeezing of the quadratures $\hat{P}$ and $\hat{Q}$. This confirms the assertion that inclusion of counter-rotating terms in the Hamiltonian is responsible for squeezing one of the two-mode quadratures of the two nanocantilevers.

3.6 Dissipative dynamics

So far we have only considered the closed system dynamics of two nanocantilevers interacting indirectly via an atomic ensemble. But in practise almost all physical systems of interest belong to the class of open systems. The coupling of the system

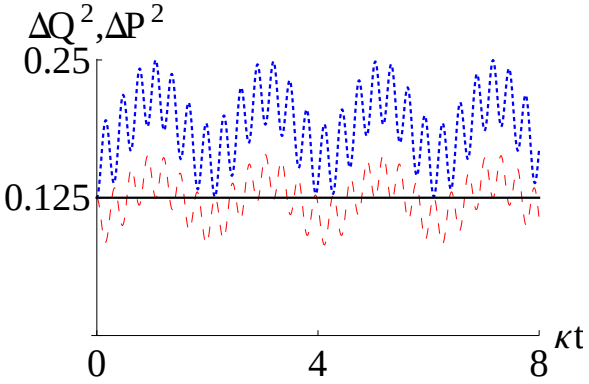

Figure 3.10: Variances in the quadratures $\hat{Q}$ (red, thin dashed) and $\hat{P}$ (blue, thick dashed) as a function of time. Quadrature $\hat{Q}$ exhibits a time-dependent squeezing beyond an initial coherent state (black, thin solid) with $|\psi(0)\rangle = |\alpha\rangle_a|\alpha\rangle_b|0\rangle_c$, where ω=10κ and $|\alpha|^2$=1. As a result of counter rotating terms present in the Hamiltonian (3.46), coupled oscillators exhibit time dependent squeezing in one of their collective quadratures beyond a minimum uncertainty coherent state. Time is scaled in units of κ.

of interest to numerous degrees of freedom of the environment is inevitable and this will be the concern of the present section.

Dissipation can occur in the atomic gas with a decay rate Γ, or by thermal decay of the nanocantilevers with a decay rate γ. For a nanocantilever with resonant frequency $\omega_0/2\pi = 1$ MHz and quality factor $Q = 10^6$ [6] one obtains $\gamma \sim 1$ Hz [10], whereas Γ is largely governed by spin flips due to collisions or stray currents in the magnet or the cantilever [91, 92]. We thus neglect the direct thermal decay of the two nanocantilevers and only consider the much more rapid decay of the internal electronic states of the atomic ensemble as the only dissipation channel.

The dissipative evolution of the system, under the Born-Markov approximation [93], is well described by a Lindblad type master equation of the following form

$$\frac{\partial}{\partial t}\hat{\rho} = \frac{-i}{\hbar}[\mathcal{H}, \hat{\rho}] + \mathcal{L}\hat{\rho}, \tag{3.54}$$

[6]Such high Q-values have so far only been achieved with doubly clamped prestressed resonators [10]. We note that our analysis could equally well be applied to a geometry where two such resonators interact via the atomic ensemble.

where $\hat{\rho}$ is the density matrix of the system and $\mathcal{L}\hat{\rho} \equiv \Gamma(2\hat{J}_-\hat{\rho}\hat{J}_+ - \hat{J}_+\hat{J}_-\hat{\rho} - \hat{\rho}\hat{J}_+\hat{J}_-)/2$ is the Lindblad operator and $\hat{J}_+$ and $\hat{J}_-$ are the collective atomic raising and lowering operators [7].

In a one-excitation manifold (3.54) can be solved by evaluating

$$(\mathcal{L}\rho)_{i,j} = \langle i| \left(\sum_{k=0,l=0}^{3} \mathcal{L}\rho_{kl}|k\rangle\langle l| \right) |j\rangle, \tag{3.55}$$

where $|0\rangle = |g,0,0\rangle$, $|1\rangle = |e,0,0\rangle$, $|2\rangle = |g,1,0\rangle$ and $|3\rangle = |g,0,1\rangle$. In this basis (3.54) transforms to a set of coupled differential equations

$$\frac{\partial}{\partial t}\hat{\rho} + \frac{i}{\hbar}[\mathcal{H}, \hat{\rho}] = \mathcal{L}\hat{\rho(t)}, \tag{3.56}$$

where

$$\mathcal{L}\hat{\rho(t)} = -\frac{N\Gamma}{2} \begin{bmatrix} -2\rho_{1,1} & \rho_{0,1} & 0 & 0 \\ \rho_{1,0} & 2\rho_{1,1} & \rho_{1,2} & \rho_{1,3} \\ 0 & \rho_{2,1} & 0 & 0 \\ 0 & \rho_{3,1} & 0 & 0 \end{bmatrix}. \tag{3.57}$$

A numerical solution of equation (3.56), for the initial condition $C_{g,1,0}(0) = 1$, is shown in Fig. 3.11. In the steady state the system relaxes to a statistical mixture of ground state and the *dark* state corresponding to the one-excitation subspace with equal probability. Hence we are able to show that dissipation assisted time evolution leads to a long-lived maximally entangled state of two nanocantilevers.

Following a similar series of steps as outlined above, we solve for the dissipative dynamics of our system in two- and three-excitation manifolds and find a similar behaviour. Numerical solutions of (3.54) in a two-excitation subspace is shown in Fig. [3.12]. We

[7] This way of modelling dissipation in terms of collective atomic raising and lowering operators may not be the most appropriate way to model dissipation in excitation subspaces with more than one excitation. However this analysis holds good when the collective excitations in the atomic ensemble are approximated under the H.P. mapping.

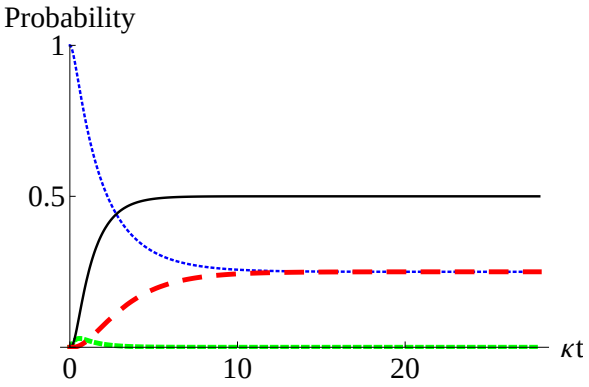

Figure 3.11: Evolution with time of the occupation probability for the states $|g,0,0\rangle$ (black, solid), $|g,1,0\rangle$ (blue, dotted), $|g,0,1\rangle$ (red, thick dashed) and $|e,0,0\rangle$ (green, thin dashed). Initially $C_{g,1,0}(0) = 1$, and $\Gamma = 10$. Time is scaled in units of κ.

found that in a two-excitation manifold the system relaxes to a statistical mixture of *dark* states of zero, one and two-excitation subspace with probabilities $0.25, 0.5$ and 0.25 respectively, while in a three-excitation subspace (not shown here) the steady state is a mixture of *dark* states of zero, one, two- and three-excitation manifolds with respective statistical weights being $0.125, 0.375, 0.375$ and 0.125. The robustness of our scheme lies in the fact that it is capable of generating long lived entangled states of nanomechanical systems even if the nanocantilevers were initially prepared in mixed states. We solve for the dynamics of the system with one of the cantilevers and the ultra-cold gas prepared in their respective ground states while the other cantilever is in a mixed state of zero, one, two and three excitations. The numerical solution of the master equation is shown in Fig. [3.13] , which clearly ascertains our claim. To summarise this section, we have shown that independent interactions of the two nanocantilevers with the common cloud of an atomic ensemble with dissipation in internal electronic states leads to generation of entangled states of the two nanocantilevers. This opens up the possibility of achieving long-lived entangled states of nanomechanical systems.

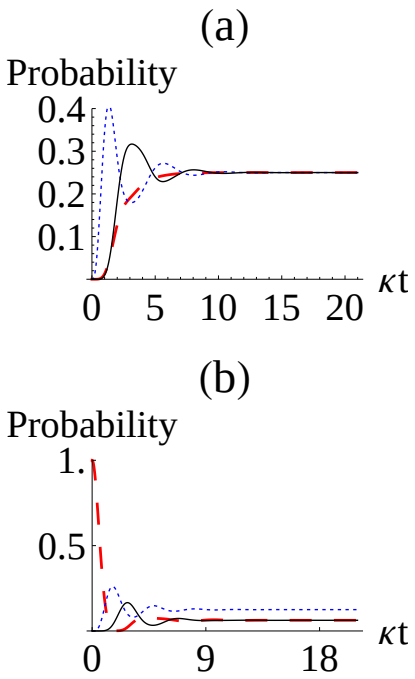

Figure 3.12: Occupation probability, as a function of time, for the states (a) $|g,0,0\rangle$ (black, solid), $|g,1,0\rangle$ (blue, dotted), and $|g,0,1\rangle$ (red, dashed); (b) $|g,0,2\rangle$ (black, solid), $|g,1,1\rangle$ (blue, dotted), and $|g,2,0\rangle$ (red, dashed). Initially $C_{g,2,0}(0) = 1$ and $\Gamma = 2$. Excitations in the ultra-cold gas decay so quickly that the probability for states containing such excitations to be occupied are much smaller than the probabilities shown here. Time is scaled in units of κ.

3.7 Conclusions

In the present chapter we have discussed a scheme to entangle the vibrational modes of two spatially separated nanocantilevers. The interactions between the nanocantilevers are mediated via a cloud of ultra-cold atoms. We have discussed in detail the dynamical evolution of the system of two indirectly coupled nanocantilevers both under the unitary and dissipative evolution. The theoretical framework builds on treating the quantised motion of the two nanocantilevers by approximating them as harmonic oscillators. The collection of ultra-cold atoms are also treated quantum mechanically. Due to the identical quantum state of the ultra0cold atoms, the collective excitations in the atomic ensemble are approximated as Dicke states, which are the simultaneous eigenstates of the collective angular momentum operators $\hat{J}_z$ and $\hat{J}^2$. The interaction

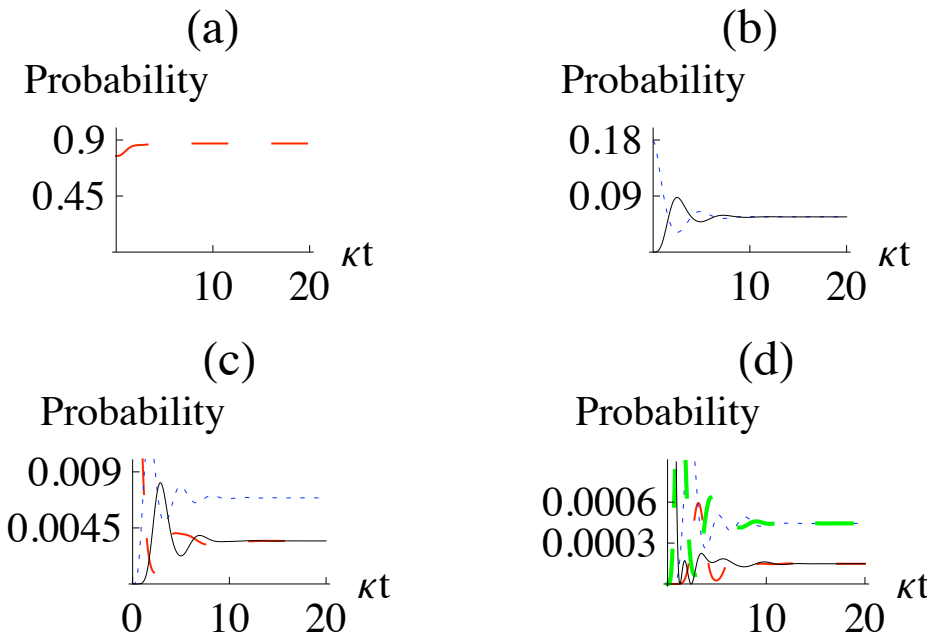

Figure 3.13: Occupation probability, as a function of time, for the states (a) $|g,0,0\rangle$ (red, dashed); (b) $|g,1,0\rangle$ (blue, dotted), $|g,0,1\rangle$ (black, solid); (c) $|g,2,0\rangle$ (red, dashed), $|g,1,1\rangle$ (blue, dotted), $|g,0,2\rangle$ (black, solid); (d) $|g,3,0\rangle$ (black, solid), $|g,2,1\rangle$ (green, thick dashed), $|g,1,2\rangle$ (blue, dotted) and $|g,0,3\rangle$ (red, thin dashed). Cantilever a is initially in a mixed state of zero, one, two and three excitations, with average occupancy $\langle n_{\rm average}\rangle = 0.3$ and $\Gamma = 2$. Excitations in the ultra-cold gas decay so quickly that the probability for states containing such excitations to be occupied are much smaller than for the other states considered here. Time is scaled in units of κ.

between collective excitations of the atomic ensemble and the quantised motion of each nanocantilever arises as a result of interaction between the collective magnetic moment of the ultra-cold atoms and spatially varying magnetic field generated by the motion of a strong ferromagnet at the tip of each nanocantilever. These interactions are modelled with the Dicke Hamiltonian.

We find that a reversible exchange of excitations between the two nanocantilevers, mediated via the atomic cloud, results in a time varying entangled state of the two nanocantilevers. The entangled state is generated both for initial pure and mixed states. As expected, the degree of entanglement between the two nanocantilevers is substantially higher for initial pure states compared to initial mixed states.

While studying the dissipative evolution of the system we illustrated a possibility to generate *long-lived* entangled states of two nanocantilevers. The main idea behind our scheme is to avoid the direct thermal decay of the two nanocantilevers and only allow them to undergo dissipation through the internal electronic states of the atomic ensemble. It turns out that the eigenspectrum of the system is such that there is one (*dark*) mode which remains decoupled from the dynamical evolution of the ultra-cold atoms. If the direct mechanical damping can be avoided, then the population of the dark modes remain intact.

Under the assumption that most of the atoms are in their ground states, a nonlinear problem describing the interaction between two electromagnetic fields and a set of two-level atoms can be mapped on to a simpler problem of three linearly coupled harmonic oscillators. This is the essence of the Holstein Primakoff (H. P.) transformation used in this chapter. The H.P. mapping and the theoretical framework provided in this chapter will be relevant throughout the thesis.

CHAPTER 4

ANHARMONIC MECHANICAL OSCILLATORS

4.1 Introduction

In the previous chapter we studied in detail a physical scenario where two nanocantilevers were interacting indirectly via collective excitations of an ultra-cold atomic ensemble. In the preceding chapter it was assumed that if both nanocantilevers had been cooled to near their ground states, then only their low lying vibrational states were occupied. It was further assumed that at such low ambient temperature and in absence of any external driving, each nanocantilever was performing simple harmonic motion. It was shown that a coherent exchange of excitation(s) between the two nanocantilevers resulted in an entangled state of the two oscillators. In the present chapter we shall discuss the quantum features of two such nanocantilevers when their potential is further modulated with an anharmonic component.

Most of vibrating physical systems, including the nano- and micromechanical systems are normally endowed with a degree of anharmonicity, although with proportionately much weaker strength as compared to the leading order harmonic component. In the present chapter, however, we shall concentrate on the influence of an externally induced nonlinearity on the entangled states of two indirectly coupled oscillators and

shall also outline a proposal to induce a particular nonlinear contribution to the potential landscape of a vibrating mechanical system [54].

Quantum dynamics of an anharmonic oscillator has already been studied in great detail in the literature [47, 48, 49, 50]. In the present chapter we therefore address another situation where an anharmonic oscillator is coupled to a second quantum system. Firstly, we investigate the quantum dynamics of two anharmonic oscillators interacting with a linear oscillator. We show that as a result of indirect interaction mediated by the linear oscillator, the two nonlinear oscillators exhibit time-varying entanglement. Interestingly, we find that the effect of a nonlinearity is much more pronounced for certain initial states. When dissipation is included, the effect of nonlinearity strongly governs the steady state evolution of the two indirectly coupled nonlinear oscillators.

As a second illustration to demonstrate the effect of external nonlinearity, we investigate the unitary evolution of a cavity mode interacting with a movable mirror which is modelled as an anharmonic oscillator. We provide a full analytical treatment of a physical model describing this interaction in a regime where both the nonlinearity and the coupling due to the radiation pressure is weak. We show that unitary evolution results in time-dependent entanglement between the oscillator and the cavity mode. Moreover, under the joint action of radiation pressure coupling and intrinsic nonlinearity, the movable mirror will also exhibit non-classical dynamics [54, 94].

Nonlinear effects are typically small in nanocantilevers, since the amplitude of their oscillations are inevitably small compared to their length. Moreover, it is difficult to control the nonlinearities externally. In this chapter we propose to use an electromagnetic setup based on a Helmholtz coil configuration, where the nonlinearity stems from the fact that the energy due to the interaction between the magnetic field produced by the coils and permanent magnets at the tips of the cantilevers has a term that depends on the fourth power of the deflection of a tip from its equilibrium position [54]. This allows us to externally tune the strength of the nonlinearity, which

may be difficult in other realisations [12, 52].

4.2 Indirectly coupled anharmonic oscillators

In this section we shall explore the quantum dynamics of two anharmonic oscillators, both of which interact with the same linear oscillator. We will keep the theoretical treatment general at this point, but in Section 4.4 we will discuss a potential realisation of the required nonlinearites.

4.2.1 Unitary dynamics

Consider two identical nano- or micromechanical oscillators each of mass m and operating in the quantum regime with fundamental vibrational frequency ω_m. Denoting the position and momentum operators of each oscillator by $\hat{q}_i$ and $\hat{p}_i$, where $i = 1, 2$, the free evolution of the two oscillators is governed by the Hamiltonian

$$\hat{H} = \sum_{i=1}^{2} \left[\frac{\hat{p_i}^2}{2m} + \frac{m\omega_m^2 \hat{q_i}^2}{2} \right]. \tag{4.1}$$

If we can modulate the potential seen by the oscillator such that there is an additional term proportional to $\hat{q}_i^4$, then this will introduce an effective nonlinearity for the mechanical oscillator. The Hamiltonian of two such independent anharmonic oscillators then takes the form

$$\hat{H}_1 = \sum_{i=1}^{2} \left[\frac{\hat{p_i}^2}{2m} + \frac{m\omega_m^2 \hat{q_i}^2}{2} + \tilde{\beta}\hat{q}_i^4 \right], \tag{4.2}$$

where $\tilde{\beta}\hat{q}_i^4$ is the nonlinear interaction energy. Expressing the position and momentum operators of each oscillator as

$$\hat{q}_1 = \sqrt{\frac{\hbar}{2m\omega_m}}(\hat{a}^\dagger + \hat{a}); \qquad \hat{p}_1 = i\sqrt{\frac{\hbar m\omega_m}{2}}(\hat{a}^\dagger - \hat{a})$$
$$\hat{q}_2 = \sqrt{\frac{\hbar}{2m\omega_m}}(\hat{b}^\dagger + \hat{b}); \qquad \hat{p}_2 = i\sqrt{\frac{\hbar m\omega_m}{2}}(\hat{b}^\dagger - \hat{b}),$$

where $\hat{a}^\dagger(\hat{a})$ and $\hat{b}^\dagger(\hat{b})$ are the creation (annihilation) operators for the vibron excitations of the two anharmonic oscillators, and further neglecting all the counter-rotating terms, (4.2) takes the form

$$\widetilde{\hat{H}}_1/\hbar \approx \omega_m(\hat{a}^\dagger\hat{a} + \hat{b}^\dagger\hat{b}) + \beta(\hat{n}_a^2 + \hat{n}_a) + \beta(\hat{n}_b^2 + \hat{n}_b), \tag{4.3}$$

where $\hat{n}_a$ and $\hat{n}_b$ are the number operators of the two anharmonic oscillators and $\beta{=}\tilde{\beta}$ $(\hbar/2m\omega_m)^2/\hbar$ is the nonlinearity strength in units of Hz. It is worth stressing that in general, for a driven nonlinear oscillator, the oscillation frequency depends on the driving amplitude [1], although a single resonance frequency can still be a valid approximation in the case of a very weak driving force. Moreover, in the present work we are considering a system of two undriven nonlinear oscillators, for which assigning a single resonance frequency seems to be a reasonable assumption. Nonetheless, depending on the initial excitation amplitude, the nonlinear oscillator might exhibit multistable behaviour. But as long as the initial average number of excitations $\langle\hat{n}\rangle$ of each oscillator is such that $\omega_m + \langle n\rangle\beta \approx \omega_m$, the assumption of a single resonant frequency for each oscillator is still a reasonable approximation. Keeping this is mind in the discussion to follow, we shall restrict ourselves to subspaces with a low number of excitation quanta of each oscillator.

We are interested in the indirect interaction between the two nonlinear oscillators mediated by a linear oscillator with quantised energy levels equispaced by energy $\hbar\omega$. The indirect coupling is advantageous because it allows for accurate control of the interaction strength by manipulating the mediating oscillator, and consequently gives a handle on the quantum dynamics of two nonlinear oscillators. The importance of the indirect interactions can be further appreciated in the dissipative regime. There, if the dissipation rate of the mediating oscillator is much faster than the thermal relaxation rates of the individual oscillators, steady state entangled states of the two nonlinear

[1] A nonlinear oscillator may have an amplitude-dependent oscillation frequency and exhibit for instance quantum chaotic features. See, e.g., [95] and [96]

oscillators can be achieved. The linear oscillator is here assumed to be addressable by electromagnetic radiation created by excess charge or by nano-magnets at the tip of the oscillators, which produces an oscillating electromagnetic field [24]. Making the rotating wave and dipole approximations, the unitary evolution of the system of two indirectly coupled nonlinear oscillators is given by the Hamiltonian

$$\begin{aligned}\widetilde{\hat{H}}_1/\hbar &= \omega_m(\hat{a}^\dagger\hat{a}+\hat{b}^\dagger\hat{b})+\omega\hat{c}^\dagger\hat{c}+\beta(\hat{n}_a^2+\hat{n}_a+\hat{n}_b^2+\hat{n}_b)\\ &\quad +\kappa(\hat{a}^\dagger\hat{c}+\hat{b}^\dagger\hat{c})+\kappa(\hat{c}^\dagger\hat{a}+\hat{c}^\dagger\hat{b}),\end{aligned} \tag{4.4}$$

where $\hat{c}^\dagger, \hat{c}$ are the creation and annihilation operators for the single quantised mode of the linear oscillator, which couples symmetrically — with coupling strength κ — to each of the nonlinear oscillators. The Hamiltonian (4.4) may, for instance, describe the coherent interaction of two anharmonic oscillators with an ultra-cold atomic ensemble [40], in which case in the limit of low atomic excitations, the creation and annihilation operators $\hat{c}^\dagger$ and $\hat{c}$ will be analogous to the collective atomic raising and lowering operators $\hat{J}^+$, $\hat{J}^-$ [40, 75]. As shown in [40], the indirect coupling strength κ between the two nonlinear oscillators can be made to exceed the direct coupling κ_{direct} between them. Moreover, the nonlinearity strength β can also be made stronger than the direct coupling strength κ_{direct} such that $\kappa_{\text{direct}} < \beta < \kappa$. For instance, a nanocantilever with a zero-point oscillation amplitude of 50 pm and a ferromagnet with 10^6 atoms on each cantilever tip, together with the atomic cloud trapped at a distance $d = 1$ μm above the nanocantilevers and $N = 10^4$ atoms in the trap, then $\kappa/\kappa_{\text{direct}} = 8$ and $\beta/\kappa_{\text{direct}} = 5$ (see Section 4.4).

A general solution of (4.4) may be found, where the conservation of the total number of excitations significantly simplifies the treatment. If the oscillators can be cooled near to their ground states we can restrict ourselves to subspaces with few excitations. Furthermore, in order to simplify the analytical and numerical treatment we will truncate the Hilbert space of the middle linear oscillator to its first two lowest excitation subspaces. This assumption results in a rescaling of the Rabi oscillations

without altering the qualitative picture [40].

In the one-excitation subspace, the relevant basis states for the unitary dynamics governed by the Hamiltonian (4.4) are $|1\rangle_a|0\rangle_b|0\rangle_c$, $|0\rangle_a|1\rangle_b|0\rangle_c$ and $|0\rangle_a|0\rangle_b|1\rangle_c$. Here $|1\rangle_a|0\rangle_b|0\rangle_c$ denotes a state where one of the anharmonic oscillators is in its first excited state while the other nonlinear oscillator and the linear oscillator are in their ground states, and similarly for the other combinations. If we assume that the energy splitting of the linear oscillator can be brought in resonance with the oscillation frequency of the anharmonic oscillator, then the Hamiltonian (4.4) in the interaction picture takes the form

$$\hat{H}_{\rm int} = \hbar\beta(\hat{n}_a^2 + \hat{n}_a + \hat{n}_b^2 + \hat{n}_b) + \hbar\kappa(\hat{a}^\dagger\hat{c} + \hat{b}^\dagger\hat{c}) + h.c.. \tag{4.5}$$

A general initial state of the nonlinear-linear coupled oscillator system in the subspace of one-excitation can be written as,

$$|\Psi_1(t)\rangle = \sum_{j=0}^{1} C_{j,1-j,0}(t)|j\rangle_a|1-j\rangle_b|0\rangle_c + C_{0,0,1}(t)|0\rangle_a|0\rangle_b|1\rangle_c. \tag{4.6}$$

With the initial condition $|\Psi(0)\rangle = |1\rangle_a|0\rangle_b|0\rangle_c$, the time-dependent wave function becomes

$$|\Psi_1(t)\rangle = \alpha_1(t)|1\rangle_a|0\rangle_b|0\rangle_c + \alpha_2(t)|0\rangle_a|1\rangle_b|0\rangle_c + \alpha_3(t)|0\rangle_a|0\rangle_b|1\rangle_c,$$

where,

$$\begin{aligned}
\alpha_1(t) &= \left(\frac{1}{2} + \frac{e^{-i\beta t/2}}{2}\cos(K_1 t/2) - i\beta\frac{e^{-i\beta t/2}}{2K_1}\sin(K_1 t/2)\right) \\
\alpha_2(t) &= \left(-\frac{1}{2} + \frac{e^{-i\beta t/2}}{2}\cos(K_1 t/2) - i\beta\frac{e^{-i\beta t/2}}{2K_1}\sin(K_1 t/2)\right) \\
\alpha_3(t) &= -2i\frac{\kappa}{K_1}e^{-i\beta t/2}\sin(K_1 t/2)|0\rangle_a|0\rangle_b|1\rangle_c,
\end{aligned}$$

with $K_1 = \sqrt{\beta^2 + 8\kappa^2}$. In the limit $\beta \to 0$ we obtain

$$\begin{aligned} |\Psi_1(t)\rangle &= \frac{(1+\cos\sqrt{2}\kappa t)}{2}|1\rangle_a|0\rangle_b|0\rangle_c + \frac{(-1+\cos(\sqrt{2}\kappa t))}{2}|0\rangle_a|1\rangle_b|0\rangle_c \\ &\quad -\frac{i}{\sqrt{2}}(\sin(\sqrt{2}\kappa t))|0\rangle_a|0\rangle_b|1\rangle_c, \end{aligned} \tag{4.7}$$

which coincides with the wavefunction that describes the dynamics of two indirectly coupled linear oscillators as obtained in (3.14). It should be noted that the effect of the nonlinearity cannot be fully appreciated only in a one-excitation subspace. In this case the effect of the nonlinearity can be mimicked by making the two oscillators non-resonant with the mediating linear oscillator. Hence to better understand the effect of the intrinsic nonlinearity on the quantum dynamics of each oscillator, we have to study subspaces with more excitations. We illustrate this by solving the case with two and three excitations.

With the result of the unitary evolution for all three-excitation subspaces in hand, we can now attempt to characterise the entanglement between the two anharmonic oscillators, and by doing so we shall try to understand the influence of the inherent nonlinearities on the emergence of quantum correlations. The time-dependent state of the two anharmonic oscillators is a mixed state found by tracing over the degrees of freedom of the linear oscillator. To quantify the entanglement in a bipartite system in an overall mixed state, we again use the Peres criterion [82] and following the same steps as outlined in the previous chapter we compute the negativity as a measure of the bipartite entanglement.

A coherent exchange of excitation(s) between the two anharmonic oscillators mediated indirectly via the linear oscillator, results in an entangled state of the two nonlinear oscillators. As shown in Fig. 4.1, the oscillators exhibit a time-dependent entanglement, and at certain instants the entanglement is found to be maximal or nearly maximal in both excitation subspaces.

For the sake of comparison we also plot the negativity for two indirectly coupled linear

oscillators. As can be seen from Fig. 4.1, for an initial state given by $|1\rangle_a|0\rangle_b|0\rangle_c$, the nonlinear oscillators exhibit stronger entanglement compared to their linear counterparts. On the other hand, we find that for a symmetric initial state $|0\rangle_a|0\rangle_b|1\rangle_c$, a stronger nonlinearity strength β leads to a more weakly entangled state of the two oscillators.

The time evolution of entanglement for the indirectly coupled nonlinear oscillators in subspaces of higher excitations are shown in Fig. 4.2 and Fig. 4.3. As can be seen in subspaces of two and three excitations the effect of nonlinearity is clearly imprinted on the entangled state of the two oscillators. All these results indicate that the effect of nonlinearity is much more pronounced for certain initial states. The dynamics becoming more complex in subspaces with higher excitations. As mentioned before, the particular form of nonlinearity that we are interested in is clearly manifested in subspaces with higher excitations. A more realistic scenario is when the oscillators start in a mixed state. As an illustration of this case, we plot the logarithmic negativity for an initial mixed state of two indirectly coupled nonlinear oscillators in Fig. 4.4. As expected, the degree of entanglement is reduced considerably compared to the case of initial pure states. Furthermore, and crucially depending on the initial state, a non zero value of β may or may not enhance quantum entanglement between the oscillators.

4.2.2 Dissipation of the oscillator

Every physical system is susceptible to dissipation. A more realistic approach will therefore take decoherence induced by an environment into account. Dissipation can either occur through the thermalisation of the two anharmonic oscillators or through the mediating linear oscillator. As a first approximation we assume that the two nonlinear oscillators and the linear oscillator are coupled to independent zero-temperature heat baths with coupling rates $\gamma_{a,b}$ and γ_c, respectively. The effect of dissipation on

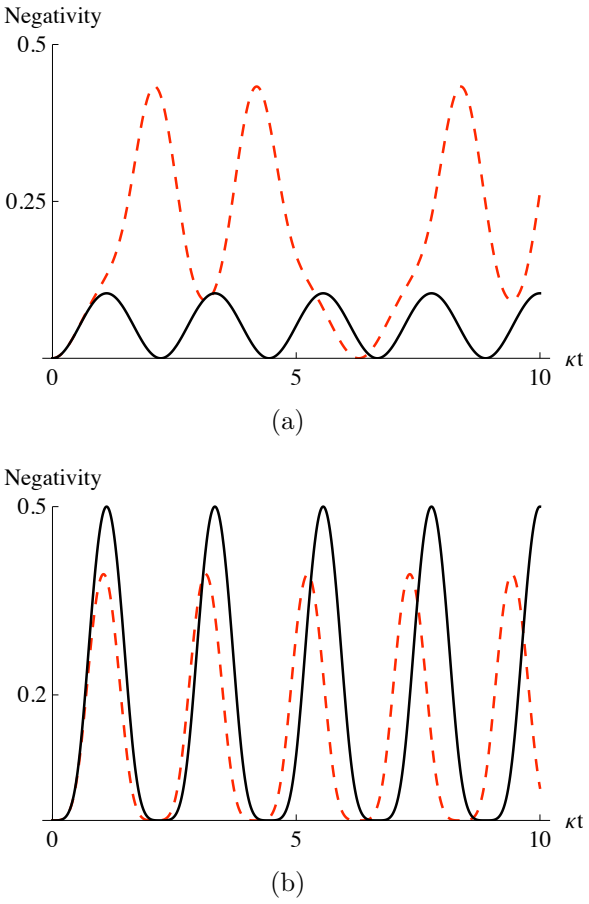

Figure 4.1: Degree of entanglement, as measured by the negativity for $\beta/\kappa = 0$ (solid) and $\beta/\kappa = 0.5$ (dashed). The initial states are (a) $C_{1,0,0}(0) = 1$ (b) $C_{0,0,1}(0) = 1$. Time is scaled in units of κ.

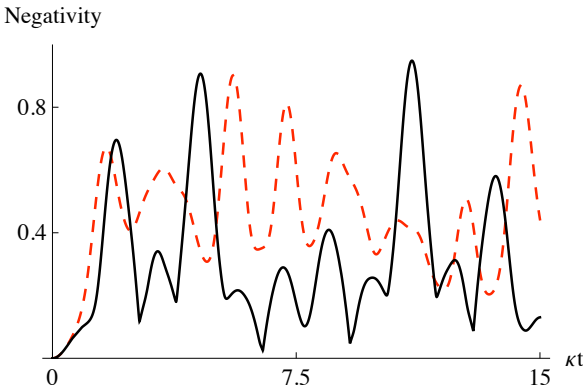

(a)

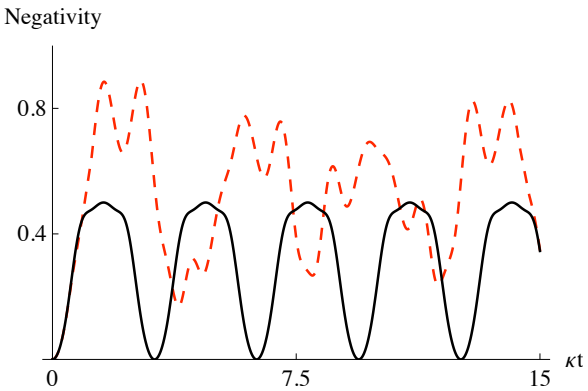

(b)

Figure 4.2: Degree of entanglement, as measured by the negativity for $\beta/\kappa = 0$ (solid) and $\beta/\kappa = 0.5$ (dashed). The initial states are (a) $C_{2,0,0}(0) = 1$ (b) $C_{1,1,0}(0) = 1$. Time is scaled in units of κ.

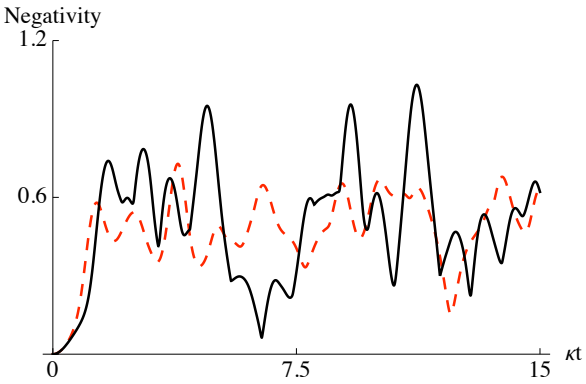

(a)

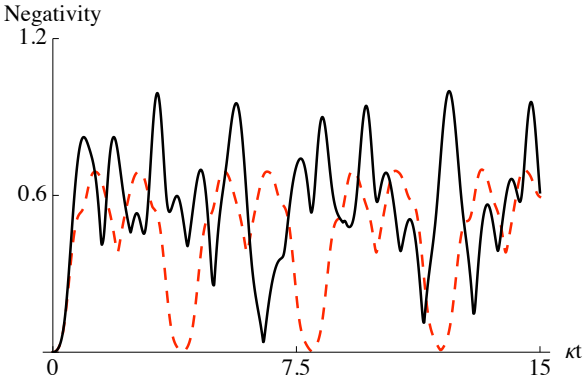

(b)

Figure 4.3: Degree of entanglement, as measured by the negativity for $\beta/\kappa = 0$ (solid) and $\beta/\kappa = 0.5$ (dashed). The initial states are (a) $C_{3,0,0}(0) = 1$ (b) $C_{1,1,1}(0) = 1$. Time is scaled in units of κ.

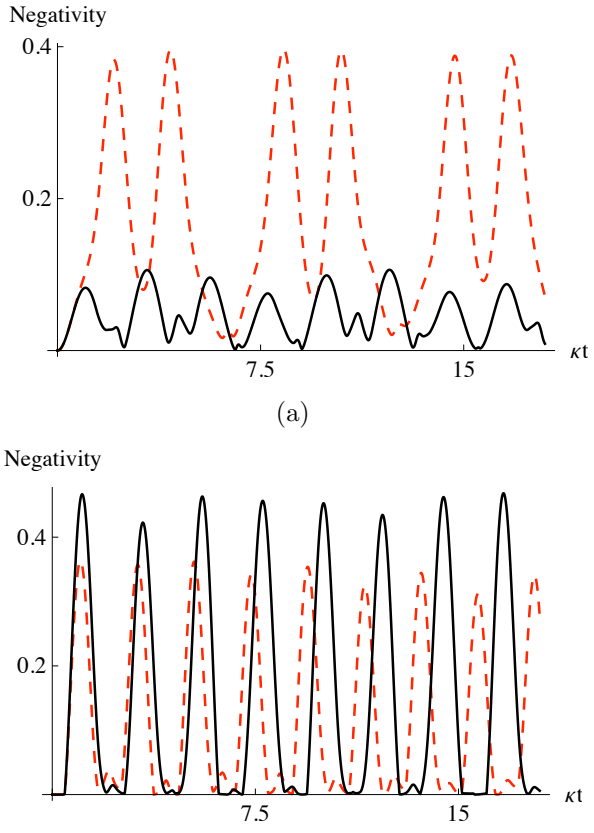

Figure 4.4: Degree of entanglement as measured by the negativity for $\beta/\kappa = 0$ (solid) and $\beta/\kappa = 0.5$ (dashed). The initial states are: in (a) a mixture of initial asymmetric states of the three lowest lying excitation subspaces, in (b) a mixture of initial symmetric states of the three lowest lying excitation subspaces with average occupancy 0.1. Time is scaled in units of κ.

their evolution — under the Born-Markov approximation — is well described by a Lindblad-type master equation of the form

$$\frac{\partial}{\partial t}\hat{\rho} = \frac{-i}{\hbar}[\hat{H}_{\rm int}, \hat{\rho}] + \mathcal{L}_a\hat{\rho} + \mathcal{L}_b\hat{\rho} + \mathcal{L}_c\hat{\rho}. \tag{4.8}$$

Here $\hat{\rho}$ is the density matrix of the system, and $\mathcal{L}_x\hat{\rho} \equiv \gamma_x(2\hat{x}\hat{\rho}\hat{x}^\dagger - \hat{x}^\dagger\hat{x}\hat{\rho} - \hat{\rho}\hat{x}^\dagger\hat{x})/2$ is the Lindblad operator representing the coupling of the oscillators to their independent zero-temperature heat baths. Here too, we have assumed that the coupling strength between the indirectly coupled anharmonic oscillators is weak enough so that the dissipative evolution is safely described by *adding* local Lindblad operators.

A typical numerical solution of (4.8) in the one-excitation subspace is shown in Fig. 4.5. As can be seen from the figure, the effect of external nonlinearity is clearly imprinted on the entangled state of the two oscillators even when they undergo dissipation. As for the case of unitary evolution, the effect of an inherent nonlinearity of the oscillator is much more pronounced for certain initial states.

The intrinsic nonlinearity of the two oscillators has another dramatic effect in the sense that it determines the dissipative dynamics of the coupled oscillators in higher excitation subspaces. To see this we solve (4.8) in the two-excitation subspace. This time we only allow the mediating linear oscillator to undergo dissipation on the time scale of interest. An equivalent problem has been studied in [40], where under similar conditions long-lived entangled states of two linear oscillators were achieved.

If $\beta = 0$ then $\hat{a} - \hat{b}$ is a constant of motion of the Hamiltonian (4.5). Exploiting this fact one can obtain steady states of the two linear oscillators which are entangled [40]. On the other hand, for nonlinear oscillators this does not hold true. Here, depending on the initial state, one may or may not see a steady-state entangled state of the two nonlinear oscillators develop [54].

To prove this statement a numerical solution of (4.8) is shown in Fig. 4.6. For an initial asymmetric state the steady state is an entangled state of the two nonlinear

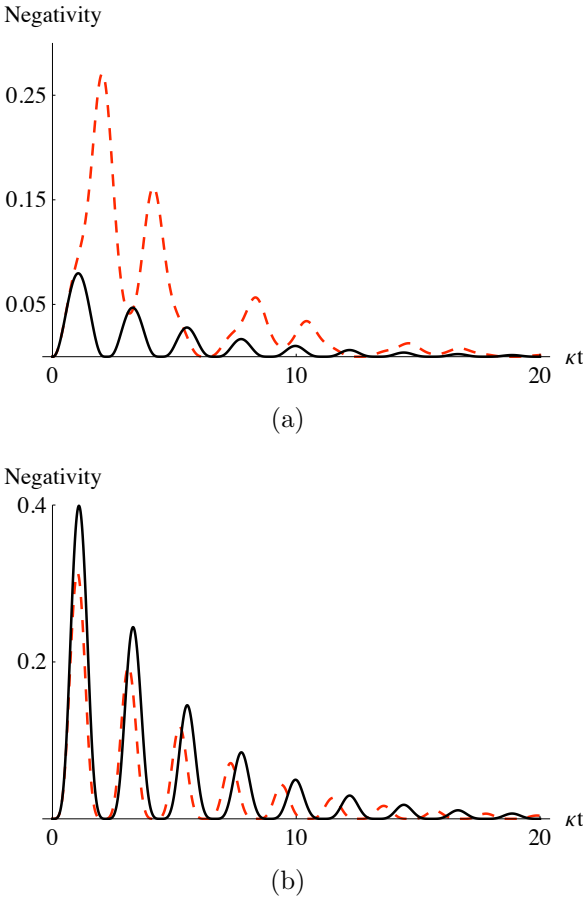

Figure 4.5: Degree of entanglement, as measured by the negativity for $\beta/\kappa = 0$ (solid) and $\beta/\kappa = 0.5$ (dashed) and $\gamma_{a,b}/\kappa = \gamma_c/\kappa = 0.1$. The initial states are (a) $C_{1,0,0}(0) = 1$ and (b) $C_{0,0,1}(0) = 1$. Time is scaled in units of κ.

oscillators while for an initial symmetric state the steady state is separable. These observations can thus also be used as an indirect signature of the state of the nonlinear oscillator.

The degree of inseparability of the two indirectly coupled oscillators has a non trivial dependence on both the nonlinearity parameter β and the initial state. Depending on the initial state a non zero value of nonlinearity strength β can enhance or suppress the degree of entanglement. This behaviour holds true both when the system undergoes unitary evolution and in the dissipative regime.

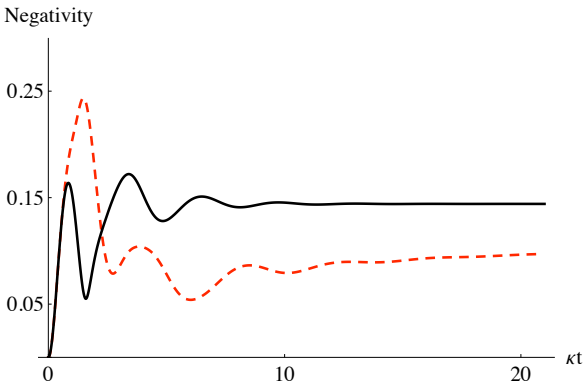

(a)

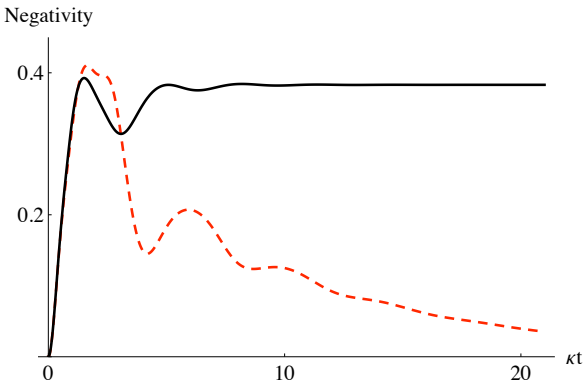

(b)

Figure 4.6: (a) Degree of entanglement, as measured by the negativity for $\beta/\kappa = 0$ (solid) and $\beta/\kappa = 0.5$ (dashed), $\gamma_c/\kappa = 2$ and $\gamma_{a,b}/\kappa = 0$. The initial states are (a) $C_{2,0,0}(0) = 1$ and (b) $C_{1,1,0}(0) = 1$. Time is scaled in units of κ.

4.3 Interaction with a quantised cavity mode

In the previous section we saw how an intrinsic nonlinearity can strongly affect the entanglement between the oscillators. Here we will discuss a second physical scenario where an external nonlinearity plays a key role in governing the quantum dynamics of an anharmonic oscillator. The physical system we have in mind is an anharmonic oscillator coupled to a mode of a Fabry-Pérot cavity with one fixed and one movable mirror.

In [97, 98] the problem of a cavity with a movable mirror has been discussed in great detail. In these studies the movable mirror was treated as a simple harmonic oscillator. This work was purely analytical, and showed that the coherent interaction of a movable mirror with the cavity mode generates various non-classical states of the cavity mode and the mirror. Here we are interested in probing the quantum features of an anharmonic oscillator. We shall model the movable mirror as a nonlinear oscillator with a nonlinearity proportional to x^4, where x is the displacement of the mirror from its equilibrium position. In what follows we study the coherent interaction between a single quantised cavity mode and a nonlinear mirror coupled by the radiation pressure [99]. We derive a closed analytical expression for the time-dependent state of the cavity field and the movable anharmonic mirror, which is valid in the limit of weak nonlinearity and low radiation pressure coupling.

If we assume that leakage of photons through the cavity can be neglected, then the main source of decoherence is the coupling of the mirror to its surroundings, which to some extent can also be avoided [100]. In what follows we therefore neglect any dissipation channel in our physical model and only consider unitary evolution of the system of the coupled cavity- and nonlinear-mirror system.

To construct the theoretical model we consider a single quantised cavity mode with creation and annihilation operators $\hat{k}^\dagger$ and $\hat{k}$, and resonance frequency $\omega_k = 2\pi c/L$, where L is the length of the cavity. We assume that the movable mirror has been

cooled near to its ground state and thus is operating in its quantum regime. Under the action of cavity photon induced radiation pressure, the movable mirror will oscillate about its equilibrium position. If we assume that the mirror moves a distance x along the cavity axis such that the displacement is much smaller than the wavelength of the cavity mode in one cavity round-trip time, then the scattering of photons to other cavity modes can be safely neglected [99]. The length of the cavity then becomes $L + x$ so that the resonance frequency of the cavity is of the form $\omega_k' = 2\pi c/(L + x)$. The Hamiltonian of the cavity can then be rewritten as

$$\hat{H}_{cav} = \hbar\omega_k'\hat{k}^\dagger\hat{k} = 2\pi\hbar\,\frac{c}{L+x}\,\hat{k}^\dagger\hat{k}, \tag{4.9}$$

which, in a quantum description of the mirror motion, becomes

$$\hat{H}_{cav} = \hbar\omega_k\hat{k}^\dagger\hat{k} - \hbar g_k\hat{k}^\dagger\hat{k}(\hat{a}^\dagger + \hat{a}), \tag{4.10}$$

where it is assumed that $x/L \ll 1$, $g_k = (\omega_k/L)\sqrt{\hbar/2m\omega_m}$ is the radiation pressure coupling constant between the nonlinear mirror and the cavity field and $\hat{a}^\dagger(\hat{a})$ are the creation (annihilation) operators for the vibron excitations of the anharmonic mirror. Thus the unitary dynamics of the above physical system is governed by the Hamiltonian

$$\hat{H}_2/\hbar = \omega_k\hat{k}^\dagger\hat{k} + (\omega_m + \beta)\hat{a}^\dagger\hat{a} + \beta(\hat{a}^\dagger\hat{a})^2 - g_k\hat{k}^\dagger\hat{k}(\hat{a}^\dagger + \hat{a}), \tag{4.11}$$

where the nonlinear mirror has been approximated by a quartic anharmonicity as in (4.3). The Hamiltonian in (4.11) can be rewritten using the transformation

$$\hat{H}_{\text{trans}} = e^{\hat{S}}\hat{H}_2 e^{-\hat{S}}, \tag{4.12}$$

where the unitary operator $\hat{S}$ is given by

$$\hat{S} = -\frac{g_k}{\omega_m + \beta}\hat{k}^\dagger\hat{k}(\hat{a}^\dagger - \hat{a}). \tag{4.13}$$

Consequently the operators $\hat{a}$ and $\hat{k}$ transform as

$$\hat{a} \rightarrow \hat{a} + \frac{g_k}{\omega_m + \beta}\hat{k}^\dagger\hat{k}, \tag{4.14}$$

$$\hat{k} \rightarrow \hat{k}\exp\left[\frac{g_k}{\omega_m + \beta}(\hat{a}^\dagger - \hat{a})\right]. \tag{4.15}$$

Neglecting the counter-rotating terms, the transformed Hamiltonian in (4.12) becomes

$$\begin{aligned}\frac{\hat{H}_{\rm trans}}{\hbar} &= \omega_k\hat{k}^\dagger\hat{k} + (\omega_m + \beta)\hat{a}^\dagger\hat{a} - \frac{g_k^2\omega_m}{(\omega_m + \beta)^2}(\hat{k}^\dagger\hat{k})^2 + \beta(\hat{a}^\dagger\hat{a})^2 \\ &+ \frac{4g_k^2\beta}{(\omega_m + \beta)^2}(\hat{a}^\dagger\hat{a})(\hat{k}^\dagger\hat{k})^2 + 2\beta\left(\frac{g_k}{\omega_m + \beta}\right)^3(\hat{k}^\dagger\hat{k})^3(\hat{a} + \hat{a}^\dagger) + \frac{g_k^4\beta(\hat{k}^\dagger\hat{k})^4}{(\omega_m + \beta)^4}.\end{aligned} \tag{4.16}$$

To further simplify the analysis we assume that both the nonlinearity and the radiation-pressure coupling are weak, so that quadratic and higher orders terms in $g_k/(\omega_m + \beta)$ can be neglected. This can be justified since a cavity of length $L \sim 10^{-3}$ m and a movable mirror with oscillation frequency $\omega_m \sim 10^6$ Hz and zero-point oscillation amplitude 50 pm gives $g_k/\omega_m \sim 0.01$. Thus (4.16) reduces to

$$\frac{\hat{H}_{\rm trans}}{\hbar} = \omega_k\hat{k}^\dagger\hat{k} + (\omega_m + \beta)\hat{a}^\dagger\hat{a} - \frac{g_k^2\omega_m}{(\omega_m + \beta)^2}(\hat{k}^\dagger\hat{k})^2 + \beta(\hat{a}^\dagger\hat{a})^2. \tag{4.17}$$

It should be noted that $\hat{n}_k = \hat{k}^\dagger\hat{k}$ and $\hat{n}_a = \hat{a}^\dagger\hat{a}$ are constants of motion since $[\hat{H}_{\rm trans}, \hat{n}_k] = [\hat{H}_{\rm trans}, \hat{n}_a] = 0$. The transformed unitary time-evolution operator corresponding to $\hat{H}_{\rm trans}$ takes the form

$$\begin{aligned}\hat{U}_{\rm trans}(t) &= \exp[-i\omega_k t\hat{k}^\dagger\hat{k} + i\frac{g_k^2\omega_m}{(\omega_m + \beta)^2}t(\hat{k}^\dagger\hat{k})^2] \\ &\times \exp[-i(\omega_m + \beta)t\hat{a}^\dagger\hat{a} - i\beta t(\hat{a}^\dagger\hat{a})^2].\end{aligned} \tag{4.18}$$

The corresponding untransformed time evolution operator is $\hat{U}(t) = e^{-\hat{S}}\hat{U}_{\rm trans}(t)e^{\hat{S}}$. See Appendix B for technical details regarding the exact form of $\hat{U}(t)$.

Under the assumption of weak nonlinearity and low radiation pressure coupling, $\hat{U}(t)$ describes the undamped motion of an anharmonic oscillator interacting with a cavity

mode. If we assume that both the cavity mode and the nonlinear movable mirror are prepared in coherent states with amplitudes α and η respectively, then the state of the combined system evolves as

$$\begin{aligned} |\Psi(t)\rangle &= \hat{U}(t)|\Psi(0)\rangle \\ &= \sum_{n=0}^{\infty} e^{-|\alpha|^2/2}\frac{\alpha^n}{\sqrt{n!}} e^{i\left[(\frac{g_k}{\omega_m+\beta})^2 n^2(\omega_m t-\sin(\omega_m+\beta)t\right]} e^{-in\omega_k t}|n\rangle_c|\tilde{\eta}(t)\rangle_a, \end{aligned} \quad (4.19)$$

where the state of the mirror is a mixture of Fock states given by

$$|\tilde{\eta}(t)\rangle_a = \sum_{m=0}^{\infty}[\tilde{\eta}(t)]^m e^{-|\tilde{\eta}(t)|^2/2} e^{-i\beta t m^2}\frac{1}{\sqrt{m!}}|m\rangle_a, \quad (4.20)$$

with

$$\tilde{\eta}(t) = \eta e^{-i(\omega_m+\beta)t} + \frac{g_k}{\omega_m+\beta} n[1-e^{-i(\omega_m+\beta)t}]. \quad (4.21)$$

In the limit $\beta \to 0$ we retrieve the result obtained in [97, 98] where the mirror state reduces to a mixture of coherent states. It is worth noting that even in the weakly nonlinear regime the effect of the nonlinearity is clearly imprinted on the state of the movable mirror which is now in a mixture of Fock states. Also evident from (4.20) is the inseparable state of the nonlinear oscillator and the cavity mode. As can be seen from (4.19), the anharmonic oscillator exhibits periodic entanglement with the cavity mode, except at certain instants where the state of the oscillator is completely separable from the cavity mode. This happens when $(\omega_m+\beta)t = 2q\pi$ for $q \in \mathbb{N}$. The reduced density matrix of the state of the mirror is thus given by,

$$\begin{aligned} \hat{\rho}_{\text{mirror}}(\text{t}) &= \text{Tr}_k(|\Psi(\text{t})\rangle\langle\Psi(\text{t})|) \\ \hat{\rho}_{\text{mirror}}(\text{t}) &= \sum_{m,q,n=0}^{\infty} e^{-|\alpha|^2}|\alpha|^{2n}\frac{1}{\sqrt{n!}}(\tilde{\eta}(t))^m(\tilde{\eta^*}(t))^q \\ &\quad e^{-|\tilde{\eta}(t)|^2} e^{i\beta t(q^2-m^2)}\frac{1}{\sqrt{m!}}\frac{1}{\sqrt{q!}}|m\rangle_a\langle q| \end{aligned} \quad (4.22)$$

It is now a straightforward exercise to compute the Wigner function $W(\lambda,\lambda^*)$ [79] of the mirror, which we plot in Fig. 4.7. As can be seen from this figure the negativity of

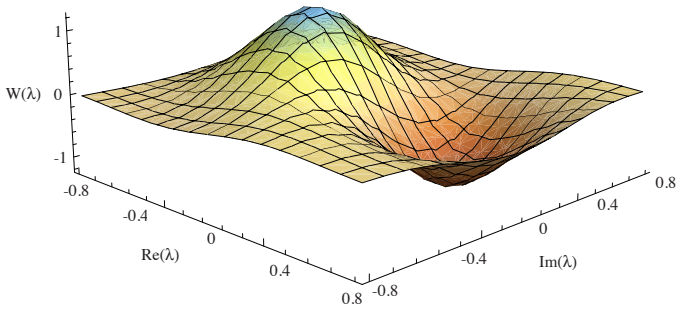

(a)

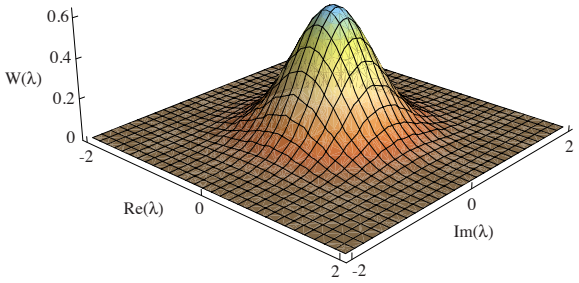

(b)

Figure 4.7: (a) Wigner function of the movable mirror initially prepared in its ground state and interacting with a cavity mode with(a) $\beta/(\omega_m+\beta) = 10^{-4}$ (b) $\beta/(\omega_m+\beta) = 0$. Initially $|\alpha|^2 = 1$; $g_k/(\omega_m + \beta) = 10^{-2}$ and $(\omega_m + \beta)t = \pi/4$.

the Wigner function $W(\lambda, \lambda^*)$ clearly identifies the non-classical state of the mirror. It should be contrasted with the case of a linear oscillator interacting with a cavity mode. There the state of the mirror is a mixture of coherent states and thus is always characterised by a positive Wigner function. The evolution of the mirror into a non-classical state is an effect of the combination of an intrinsic nonlinearity of the mirror and the radiation pressure coupling with the cavity mode. This feature should be compared with the results obtained in [98] where it has been shown that only a conditional measurement on the cavity mode can project the linear mirror into a non-classical state.

One would also expect the amplitude and the phase quadratures of the movable mirror to be influenced by the intrinsic nonlinearity in the mirror. In order to quantify this we define two Hermitian operators $\hat{Q}$ and $\hat{P}$, which correspond to the amplitude and

phase quadratures of the movable mirror and are given by

$$\hat{Q}(t) = (\hat{a}^{\dagger}(t) + \hat{a}(t)), \tag{4.23}$$

$$\hat{P}(t) = i(\hat{a}^{\dagger}(t) - \hat{a}(t)). \tag{4.24}$$

The coherent interaction of the cavity with the anharmonic oscillator should be reflected in the variance of the quadratures $\hat{P}$ and $\hat{Q}$ defined by

$$\Delta\hat{P}^2(t) = \langle\hat{P}^2(t)\rangle - \langle\hat{P}(t)\rangle^2, \tag{4.25}$$

$$\Delta\hat{Q}^2(t) = \langle\hat{Q}^2(t)\rangle - \langle\hat{Q}(t)\rangle^2. \tag{4.26}$$

We analytically solve for $\Delta\hat{P}^2(t)$ and $\Delta\hat{Q}^2(t)$ and plot the variance of the quadratures $\hat{P}$ and $\hat{Q}$ in Fig. 4.8. As can be seen there, the coherent interaction between a quantised cavity mode and an anharmonic oscillator induces a time-dependent squeezing in one of the mirror quadratures beyond the minimum uncertainty limit.

It is worth pointing out that the squeezing in the variance of the mirror quadratures beyond the minimum uncertainty limit is the result of a combined effect of the intrinsic nonlinearity and the radiation pressure coupling. This can be understood from the fact that if the mirror is initially prepared in its vacuum state then it is known that a nonlinearity of the form (4.3) alone cannot induce squeezing in the mirror quadratures [12]. As a result of joint coherent interaction with the cavity mode and intrinsic nonlinearity an initial vacuum state of the nonlinear mirror exhibit time dependent squeezing beyond the minimum uncertainty limit.

4.4 Origin of the nonlinearities

The harmonic oscillator is often the result of an approximation of a more complicated potential landscape. Nonlinear force terms are often naturally present in many physical systems, but they are of higher order, hence small. Here we shall outline one

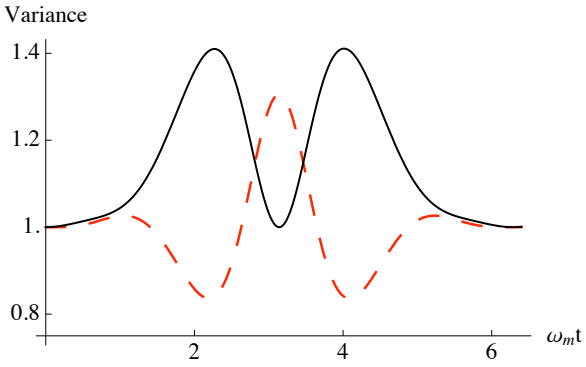

(a)

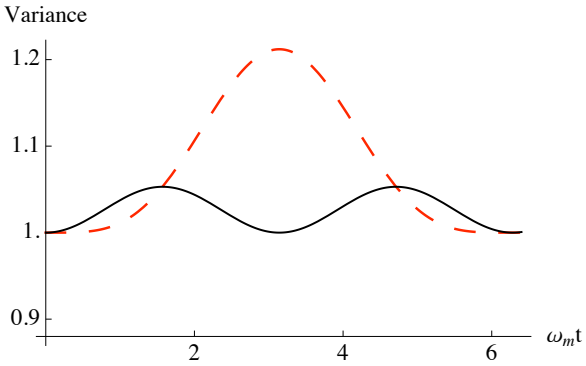

(b)

Figure 4.8: Time variation of the variance of the mirror quadratures $\hat{P}$ (solid) and $\hat{Q}$ (dashed) with the mirror initially prepared in its vacuum state, where $g_k/(\omega_m + \beta) = 0.06$ and $|\alpha|^2 = 5$. (a) $\beta/(\omega_m + \beta) = 10^{-4}$ and (b) $\beta/(\omega_m + \beta) = 0$. As a result of coherent interactions with a cavity mode an anharmonic oscillator exhibits time dependent squeezing beyond the minimum uncertainty limit in one of its quadratures. Time is scaled in units of ω_m.

possible physical scheme for inducing a nonlinearity, where the nonlinear quartic term appears as a lowest order approximation. We propose to use a hybrid system which relies on the electromagnetic coupling between nano-magnets located at the tip of the cantilever [2] and external magnetic fields.

Consider a setup consisting of two identical circular magnetic coils of radii R placed a distance of $R/2$ apart, with their common axis along the x direction. This Helmholtz coil configuration is known to produce a very uniform magnetic field near the centre. A nanocantilever with a strong ferromagnet of magnetic moment $\vec{\mu}$ attached to its tip is placed at the centre of the Helmholtz coil setup.

The magnetic field experienced by the ferromagnet at the tip of the nanocantilever, is given by

$$B(x) = \frac{\mu_0 n_{\text{turns}} I}{2R} \left\{ \left[1 + \frac{(\frac{R}{2} - x)^2}{R^2} \right]^{-\frac{3}{2}} + \left[1 + \frac{(\frac{R}{2} + x)^2}{R^2} \right]^{-\frac{3}{2}} \right\}, \tag{4.27}$$

where x is the displacement of the tip of the oscillator from the centre and I is the current in the pair of coils. Simplifying (4.27) for $x/R \ll 1$ we get

$$B(x) = \frac{8\mu_0 I}{5R\sqrt{5}} \left[1 - \frac{144}{125} \left(\frac{x}{R} \right)^4 \right]. \tag{4.28}$$

Thus the interaction energy of the ferromagnet is given by

$$H_{\text{int}} = -\mu \cdot B(x) \approx \frac{0.8\mu_0 \mu I}{R} \left(\frac{x}{R} \right)^4. \tag{4.29}$$

Representing the quantised motion of the oscillator in terms of creation and annihilation operators $\hat{a}^\dagger$ and $\hat{a}$, the interaction Hamiltonian takes the form

$$H_{\text{int}} = \hbar\beta(\hat{a} + \hat{a}^\dagger)^4, \tag{4.30}$$

[2] We note that our analysis could equally well be applied to a doubly clamped resonator or a membrane.

where $\beta = 1.28\mu_0\mu_B N_{\rm mag} I {a_0}^4/\hbar R^5$, $N_{\rm mag}$ is the number of atoms in the ferromagnet, and a_0 is the zero point amplitude of the nanomechanical cantilever.

Using the physical setup described above, a nonlinearity of strength β can be induced in the nanomechanical oscillator provided the zero point motion of the cantilever can be made large (see [73] for a review of the present state of the art manufacturing of nanomechanical oscillators). For a set of parameters where $R \sim 80$ nm, $I \sim 1$ mA, $N_{\rm mag} \sim 10^6$, and $a_0 \sim 50$ pm, one obtains a nonlinearity strength of the order of $\beta \sim 250$ Hz, where we have neglected any finite size effects stemming form the nanomagnet and coils.

4.5 Conclusions

In this chapter we have studied the dynamics of a harmonic oscillator when its potential is modulated with a quartic nonlinearity. We have described, in detail, the quantum evolution of two such anharmonic oscillators interacting indirectly via a linear oscillator. The mediating linear oscillator could also, for example, be represented by some chosen collective excitations of an atomic ensemble. We have shown that the indirect coherent interaction causes the two anharmonic oscillators to exhibit time-dependent entanglement. Inherent nonlinearities in the nano-mechanical systems are found to strongly influence the entangled state of the two oscillators. Interestingly, the effect of nonlinearity is much more pronounced for certain initial states. The signature of nonlinearity is clearly imprinted on the entangled state of the two anharmonic oscillators even when these oscillators are subject to decoherence. Nonlinearity also plays a crucial role in determining the steady state evolution of the indirectly coupled harmonic oscillators.

The coupling strength between the two oscillators can be characterised by the connectivity [50]. Connectivity as defined in [50] is the ratio of the coupling strength between the oscillators and the frequency difference between them, and diverges in the limit

of identical oscillators. A high value of the connectivity corresponds to coherent exchange of excitations between the oscillators, which is desirable in order to operate in the strong coupling regime where coherent interactions supersede all the losses in the system. In the particular physical model studied here, however, we have found that a larger value of the coupling strength does not always guarantee a strongly entangled state of the two oscillators. The strength of the quantum correlations also depends on the nonlinearity parameter and the initial state distribution. In addition, a very large coupling strength also makes the rotating wave approximation used in modelling the interaction between the oscillators questionable.

As a second illustration of the effect of nonlinearity, we have studied the coherent interaction between a single quantised cavity mode and a movable mirror modelled as a weakly nonlinear oscillator. In this case we have been able to find an analytical solution for the unitary evolution of the oscillator state. In particular, we have shown that non-classical states of the mirror arise as a result of the combination of the radiation pressure coupling and the intrinsic nonlinearity in the mirror. A non-classical state of the mirror can be generated both for initial ground and coherent states. Unlike in previously studied cases, non-classical states of the mirror can be generated without the need of conditional measurements on the cavity mode [97, 98]. In addition we have shown how squeezing appears in the variance of the quadratures beyond the minimum uncertainty state. It should be stressed that for an initial ground state of a single nonlinear mirror no squeezing will be generated. Squeezing only occurs due to the interaction between the nonlinear mirror and the cavity field.

CHAPTER 5

OPTOMECHANICS: A NEW PARADIGM

5.1 Introduction

It is not yet completely clear to what extent quantum mechanics applies to macroscopic objects [14]. Quantum phenomena such as entanglement generally do not appear in the macroscopic world. The difficulty of seeing quantum superpositions of macroscopic systems is often attributed to environment-induced decoherence. Such decoherence is thought to be the main cause reducing any quantum superposition to a classical statistical mixture [2]. Thus, an obvious but impractical choice would be to minimise the detrimental effect of the environment through perfect isolation of the system of interest. Nonetheless, with the spectacular level of experimental advancements, the possibility of seeing macroscopic quantum superpositions appears to be within current experimental reach [101].

Related to this, quantum engineering [102] in the field of optomechanics has made rapid advancement [55]. In a typical optomechanical setup, a mechanical system can be manipulated by radiation forces. Such systems have recently attracted much theoretical and experimental attention [103, 104]. This is partly because of their potential usefulness in extremely sensitive sensor technology and in quantum information pro-

cessing [103]. Also, they are potentially one of the best tools to test the foundations of quantum mechanics. Seminal progress has been made both theoretically and experimentally in this novel emerging field [55, 104].

In a typical physical system exploiting optomechanical interaction, the main component is a cavity with a movable mirror. Light in the cavity and the movable mirror interact due to a coupling induced by the radiation pressure. As a result, the movable mirror executes simple harmonic motion around its equilibrium value [105], which thus alters the cavity resonance frequency. This, in turn, changes the circulating power in the cavity and hence the radiation pressure force acting on the movable mirror, leading to intrinsic nonlinearities [106]. Strong light-matter coupling, both for opto- and for electromechanical systems, is a main ingredient in this emerging research field [107, 108]. Within the strong coupling regime, radiation-pressure interaction has been successfully utilised for ground state cooling of mechanical oscillators [18, 19, 21]. Some of the fascinating schemes include preparing the cavity mode and the movable mirror in a non-classical state [97, 98], preparing optomechanical or fully mechanical Schrödinger cat states [64, 109, 110], and even inducing quantum correlations between the subsystems [65, 111, 112, 113]. Apart from the mostly studied cavity-movable mirror geometry, there have been some recent breakthroughs in exploring quantum features of a membrane in a cavity [39, 114]. There is also a recent proposal exploring the possibility of observing photonic analogs of the Josephson effect in an optomechanical setting [115].

A common feature of most of these studies involve enhancement of the radiation pressure coupling through intense laser driving of the cavity field. This is required to achieve strong radiation pressure coupling which otherwise is too weak to observe any non-classical phenomenon. Although most of these studies are restricted to Gaussian state preparation involving optomechanical interaction, there have also been some recent proposals to study non-Gaussian quantum states in the regime of single-photon optomechanics [116, 117].

Motivated by these theoretical and experimental advancements, we shall explore a novel possibility of entangling mechanical and optical modes of two distant cavities [56]. In previous studies squeezed light was used as a resource in order to entangle two distant mirrors, which were either part of the same optical cavity [110, 112] or belonged to two different cavities [64]. In the present work we are interested in a physically different setup, where two distant Fabry-Pérot cavities each fabricated with one movable mirror are coupled by an optical fibre. We show that, as a result of a combination of the optomechanical interaction and an optical-fibre mediated coupling, the two distant optical and mechanical modes become entangled [56]. Moreover, we explicitly study two different regimes of physical interest. First we consider a scenario in which the two cavities are not externally pumped. In this regime the two mechanical modes are found not to be very strongly entangled. The advantage is however that in this physical regime an analytical solution describing the state evolution of the two mirrors can be derived. Thereafter we work in a regime where the coupled cavities are strongly driven. Here we explicitly derive the relevant quantum Langevin equations (QLE) and construct the covariance matrix governing the dynamics of all the optical and mechanical modes.

5.2 Physical setup

We consider a physical setup comprised of two identical Fabry-Pérot cavities, each fabricated with one fixed and one movable mirror, as schematically shown in Fig. 5.1. We assume that only one resonant mode of each cavity is populated, and that these two modes are coupled via an optical fibre. The two modes have the same frequency, $\omega = 2\pi c/L$; where L is the cavity length, and are described by the creation (annihilation) operators $\hat{a}^\dagger(\hat{a})$ and $\hat{b}^\dagger(\hat{b})$, respectively. Furthermore, we assume that each movable mirror has been cooled near to its ground state, so that it is operating in the quantum regime. Under the action of cavity-photon-induced radiation pressure, the movable mirrors will oscillate about their equilibrium positions.

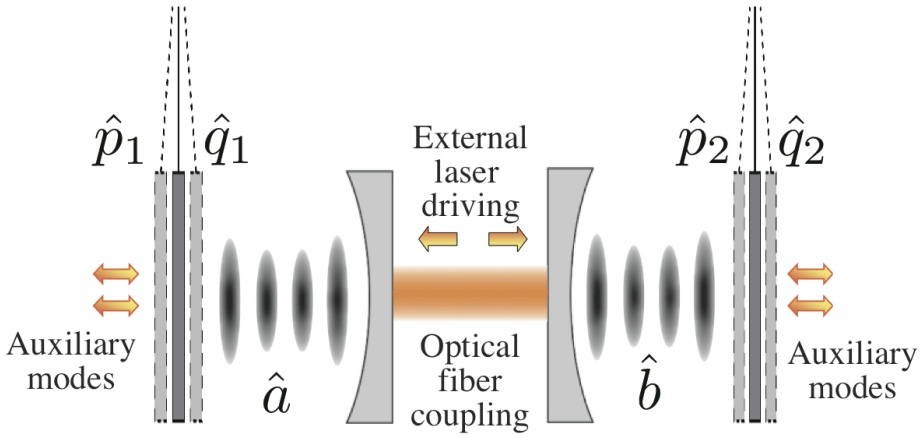

Figure 5.1: Sketch of the physical setup to entangle distant optomechanical modes. Two optomechanical cavities pumped by classical laser fields are coupled to each other by an optical fibre. As a result of indirect coupling mediated by the two cavity modes, the two movable mirrors become entangled. Furthermore, two initially uncorrelated auxiliary cavity modes interact independently with the two entangled movable mirrors, which induces non-local correlations between the two modes. Using standard homodyne measurement techniques non-local correlations between the two auxiliary cavity modes can be read out giving an indirect signature of quantum correlations between the two mirrors.

If we assume that the two mirrors move distances x and y along the respective cavity axes, so that the two displacements are much smaller than the wavelength of each cavity mode in one cavity round-trip time, then scattering of photons to other cavity modes can be safely neglected [99, 118]. The effective lengths of the cavities will then become $L + x$ and $L + y$, with new resonance frequencies $\omega_a = 2\pi c/(L + x)$ and $\omega_b = 2\pi c/(L + y)$, where x and y are the instantaneous displacements of the two cavity mirrors from their equilibrium positions. With the above assumption, i.e. $x/L, y/L \ll 1$, the free evolution of the two optical cavity modes in the adiabatic regime takes the form [118]

$$\begin{aligned} \hat{H}_{\text{free}} &= \hbar\omega_a \hat{a}^\dagger \hat{a} + \hbar\omega_b \hat{b}^\dagger \hat{b} \\ &= \hbar\omega \left(1 + \frac{x}{L}\right)^{-1} \hat{a}^\dagger \hat{a} + \hbar\omega \left(1 + \frac{y}{L}\right)^{-1} \hat{b}^\dagger \hat{b} \\ &\approx \hbar\omega \left(\hat{a}^\dagger \hat{a} + \hat{b}^\dagger \hat{b}\right) - \frac{\hbar\omega}{L} \hat{a}^\dagger \hat{a} x - \frac{\hbar\omega}{L} \hat{b}^\dagger \hat{b} y. \end{aligned} \tag{5.1}$$

Under the action of a weak radiation-pressure force, each movable mirror undergoes small-amplitude oscillations with frequency Ω. In the absence of external driving, the full Hamiltonian of the two coupled cavities thus becomes

$$\hat{H} = \hat{H}_{\text{free}} + \frac{m\Omega^2}{2} x^2 + \frac{p_x^2}{2m} + \frac{m\Omega^2}{2} y^2 + \frac{p_y^2}{2m} + \hbar\lambda \left(\hat{a}^\dagger \hat{b} + \hat{b}^\dagger \hat{a}\right), \tag{5.2}$$

where λ is the inter-mode coupling between the two cavities [1]. This coupling could be mediated by, e.g., an optical fibre connecting the two distant cavities. Introducing dimensionless conjugate variables q_i and p_i for the ith movable mirror, (5.2) can be rewritten as

$$\begin{aligned} \hat{H} &= \hbar\omega \left(\hat{a}^\dagger \hat{a} + \hat{b}^\dagger \hat{b}\right) + \frac{\hbar\Omega}{2} \left(\hat{q_1}^2 + \hat{p_1}^2\right) + \frac{\hbar\Omega}{2} \left(\hat{q_2}^2 + \hat{p_2}^2\right) \\ &\quad + \hbar\lambda \left(\hat{a}^\dagger \hat{b} + \hat{b}^\dagger \hat{a}\right) - \hbar g \left(\hat{a}^\dagger \hat{a} \hat{q_1} + \hat{b}^\dagger \hat{b} \hat{q_2}\right), \end{aligned} \tag{5.3}$$

[1] The two distant cavity modes can be alternatively assumed to be coupled through mode overlap (evanescent coupling) of the two cavity modes and in that case λ will decrease as the spatial distance between the two cavities increases.

where $g = (\omega/L)\sqrt{\hbar/m\Omega}$ is the radiation pressure-induced coupling between the cavity modes and the movable mirrors. The Hamiltonian (5.3) will form the basis for the analysis in the next section.

5.3 Perturbative expansion

The frequency mismatch between optical ($\omega/2\pi \sim 10^{14}$ Hz) and mechanical ($\Omega/2\pi \sim 10^6 - 10^9$ Hz) degrees of freedom is enormous [104]. This suggests a separation of the Hamiltonian (5.3) into two parts, one with very rapidly evolving optical modes and another with slowly varying mechanical modes. In the limit that the mirror coordinates $\hat{q}_1$ and $\hat{q}_2$ remain stationary with respect to the rapidly evolving cavity modes $\hat{a}$ and $\hat{b}$, we can diagonalise the interaction between the two cavity modes of Hamiltonian (5.3).

We first introduce the collective excitation operators $\hat{A}$ and $\hat{B}$ obeying

$$\begin{pmatrix} \hat{a} \\ \hat{b} \end{pmatrix} = \begin{pmatrix} \cos\theta & \sin\theta \\ -\sin\theta & \cos\theta \end{pmatrix} \begin{pmatrix} \hat{A} \\ \hat{B} \end{pmatrix}. \tag{5.4}$$

Choosing $\tan 2\theta = 2\lambda/(g(q_1 - q_2))$ and substituting for the new field modes, the rapidly varying optical part of Hamiltonian (5.3) reduces to

$$\begin{aligned} \hat{H}_{\rm cav} &= \hbar\left(\omega - g\frac{q_1+q_2}{2}\right)(\hat{A}^\dagger\hat{A} + \hat{B}^\dagger\hat{B}) \\ &\quad -\hbar\sqrt{g^2(q_1-q_2)^2 + 4\lambda^2}\frac{(\hat{A}^\dagger\hat{A} - \hat{B}^\dagger\hat{B})}{2}. \end{aligned} \tag{5.5}$$

The Hamiltonian describing the dynamics of the two movable cavity mirrors thus takes the form

$$\hat{H}_{\rm mir} = \frac{\hbar\Omega}{2}\left(\hat{q_1}^2 + \hat{p_1}^2 + \hat{q_2}^2 + \hat{p_2}^2\right) + \hat{H}_{\rm cav}. \tag{5.6}$$

The collective wave function of the cavity-mirror coupled system at time t as

$$|\Psi(t)\rangle = \sum_{n_A,n_B} c(n_A,n_B)|n\rangle|\Phi(n,t)\rangle. \tag{5.7}$$

Here, $P(n_A,n_B) = |c(n_A,n_B)|^2$ is the probability distribution of the collective cavity fields, $|n\rangle$=$|n_A,n_B\rangle$ denotes the time-independent index of the energy levels of the two collective cavity modes $\hat{A}$ and $\hat{B}$, in the adiabatic limit, in which $\hat{A}^\dagger\hat{A}|n\rangle = n_A|n\rangle$ and $\hat{B}^\dagger\hat{B}|n\rangle = n_B|n\rangle$, and $|\Phi(n,t)\rangle = e^{-i\hat{H}_{\rm mir}t/\hbar}|\Phi(n,0)\rangle$ denotes the time-evolved wave function of the two movable mirrors.

Thus the cavity modes can be seen as inducing an effective potential in which the two mirrors evolve,

$$\hat{V}_{\rm eff} = \hbar\left(\omega - g\frac{q_1+q_2}{2}\right)(n_A+n_B) - \hbar\sqrt{g^2(q_1-q_2)^2+4\lambda^2}\frac{n_A-n_B}{2}. \tag{5.8}$$

Since we have assumed that the oscillation amplitudes of the movable mirrors are small, it follows that their relative displacement $\hat{q}_1 - \hat{q}_2$ is also small. Therefore, it is sufficient to expand the second term in the cavity Hamiltonian (5.8) to second (quadratic) order in $\hat{q}_1 - \hat{q}_2$. This can be justified, since for a typical optomechanical cavity with optical frequency $\omega/2\pi \sim 10^{14}$ Hz, length $L \sim 1$ mm, mirror frequency $\Omega/2\pi \sim 10^6$ Hz, and with a zero-point-oscillation amplitude of 0.02 pm, one finds that $g \sim 10^4$ Hz. With the reasonable estimate $\lambda = 10^5$ Hz one gets $(g/2\lambda)^2 \sim 10^{-3}$. This results in an effective Hamiltonian describing the dynamics of two coupled movable mirror in absence of any losses,

$$\hat{H}_{\rm mir} \approx \frac{\hbar\Omega}{2}\left(\hat{q_1}^2 + \hat{p_1}^2 + \hat{q_2}^2 + \hat{p_2}^2\right) - (n_A-n_B)\hbar\lambda\frac{g^2}{8\lambda^2}(\hat{q_1}-\hat{q_2})^2, \tag{5.9}$$

where we have dropped all the constant and terms linear in $\hat{q}_1$ and $\hat{q}_2$ from the Hamiltonian [2]. Dynamical properties of entanglement in a model related to the one of

[2]In the present section we are interested in investigating a possibility of generating non-local behaviour such as entanglement between distant mechanical oscillators in absence of any external driving terms in the Hamiltonian. A more careful analysis which also takes into account all the

equation (5.9) was recently studied for a closed system [119]. Equation (5.9) can be rewritten in terms of

$$\begin{aligned}\hat{q}_1 &= \frac{(\hat{c}^\dagger + \hat{c})}{\sqrt{2}},\\ \hat{p}_1 &= i\frac{(\hat{c}^\dagger - \hat{c})}{\sqrt{2}},\\ \hat{q}_2 &= \frac{(\hat{d}^\dagger + \hat{d})}{\sqrt{2}},\\ \hat{p}_2 &= i\frac{(\hat{d}^\dagger - \hat{d})}{\sqrt{2}},\end{aligned}$$

such that

$$\begin{aligned}\hat{H}_{\rm mir} &= \hbar\Omega\left(\hat{c}^\dagger\hat{c} + \hat{d}^\dagger\hat{d}\right) - (n_A - n_B)\hbar\lambda\left(\frac{g^2}{16\lambda^2}\right)\left(\hat{c}^2 + \hat{c}^{\dagger 2} + 2\hat{c}^\dagger\hat{c}\right) - (n_A - n_B)\hbar\lambda\\ &\left(\frac{g^2}{16\lambda^2}\right)\left(\hat{d}^2 + \hat{d}^{\dagger 2} + 2\hat{d}^\dagger\hat{d}\right) + (n_A - n_B)\hbar\lambda\left(\frac{g^2}{8\lambda^2}\right)\left(\hat{c} + \hat{c}^\dagger\right)\left(\hat{d} + \hat{d}^\dagger\right). \quad (5.10)\end{aligned}$$

Introducing center of mass and relative modes,

$$\hat{C} = \frac{\hat{c} + \hat{d}}{\sqrt{2}}, \qquad \hat{D} = \frac{\hat{c} - \hat{d}}{\sqrt{2}}, \quad (5.11)$$

equation (5.10) becomes

$$\hat{H}_{\rm mir} = \hbar\Omega\hat{C}^\dagger\hat{C} + \hbar(\Omega - 4N\lambda)\hat{D}^\dagger\hat{D} - 2N\hbar\lambda\left(\hat{D}^2 + \hat{D}^{\dagger 2}\right), \quad (5.12)$$

where $N = (n_A - n_B)(g/4\lambda)^2$. The Hamiltonian in the above form is known to generate squeezing in the D-mode [120], which will also be manifested as quantum correlations between the two mirror oscillations.

After arriving at this simplified form of the Hamiltonian governing the dynamics of the two movable mirrors, we now provide a fully analytical treatment describing the

linear terms in the Hamiltonian needs further investigation. However in the Section 5.4.3 we shall provide a full quantum treatment of a physical scenario when the two optical cavities are intensely driven externally, which results in non-zero steady state entanglement between various optical and mechanical modes.

state evolution of the two mirrors. We shall now discuss the unitary dynamics of the system in Section 5.3.1 and provide a closed-form expression for the time-evolved mirror operators $\hat{c}(t)$ and $\hat{d}(t)$ in the Heisenberg picture. This will allow us to solve for the dynamics of initially uncoupled movable mirrors for an arbitrary initial state.

5.3.1 Unitary evolution

The Hamiltonian (5.12) describing the dynamics of the two movable mirrors can be further diagonalised by a Bogoliubov transformation. We define operators $\hat{E}$ and $\hat{E}^\dagger$ such that

$$\begin{pmatrix} \hat{D}^\dagger \\ \hat{D} \end{pmatrix} = \begin{pmatrix} u & v \\ v & u \end{pmatrix} \begin{pmatrix} \hat{E}^\dagger \\ \hat{E} \end{pmatrix}, \tag{5.13}$$

where $u^2 - v^2 = 1$. Setting

$$\begin{aligned} u^2 &= \frac{1}{2}\left(1 + \sqrt{1 + \frac{4M^2}{1-4M^2}}\right), \\ v^2 &= \frac{1}{2}\left(-1 + \sqrt{1 + \frac{4M^2}{1-4M^2}}\right), \end{aligned} \tag{5.14}$$

the Hamiltonian (5.12) reduces to the diagonal form

$$\tilde{H}_{\rm mir} = \hbar\Omega\hat{C}^\dagger\hat{C} + 2\hbar\omega_0\hat{E}^\dagger\hat{E}, \tag{5.15}$$

where

$$\begin{aligned} \omega_0 &= \frac{(\Omega - 8\lambda N)\Omega}{2\sqrt{1-4M^2}(\Omega - 4\lambda N)}, \\ M &= \frac{2N\lambda}{\Omega - 4N\lambda}. \end{aligned} \tag{5.16}$$

We can then straightforwardly solve the equations of motion for the operators $\hat{C}(t)$ and $\hat{E}(t)$,

$$\begin{aligned}\hat{C}(t) &= \hat{C}(0)e^{i\Omega t} \\ \hat{E}(t) &= \hat{E}(0)e^{-i2\omega_0 t},\end{aligned} \tag{5.17}$$

giving the closed-form expressions for the time evolved operators $\hat{c}(t)$ and $\hat{d}(t)$,

$$\begin{aligned}\hat{c}(t) &= \frac{1}{2}\Big[F(t)\hat{c}(0) + G(t)\hat{d}(0) + 2i\sin(2\omega_0 t)uv\,\hat{c}^\dagger(0) - 2i\sin(2\omega_0 t)uv\,\hat{d}^\dagger(0)\Big] \\ \hat{d}(t) &= \frac{1}{2}\Big[G(t)\hat{c}(0) + F(t)\hat{d}(0) - 2i\sin(2\omega_0 t)uv\,\hat{c}^\dagger(0) + 2i\sin(2\omega_0 t)uv\,\hat{d}^\dagger(0)\Big],\end{aligned}$$

where $F(t)$ and $G(t)$ are time-dependent complex functions given by

$$\begin{aligned}F(t) &= e^{-i\Omega t} + u^2 e^{-i2\omega_0 t} - v^2 e^{i2\omega_0 t}, \\ G(t) &= e^{-i\Omega t} + v^2 e^{i2\omega_0 t} - u^2 e^{-i2\omega_0 t}.\end{aligned}$$

With the solution of the operators $\hat{c}(t)$ and $\hat{d}(t)$ now in hand we can faithfully describe the unitary dynamics of the two movable mirrors for any arbitrary initial state. Of particular interest are initial Gaussian states including thermal, coherent, and squeezed states. A Gaussian continuous variable state can be fully described in terms of a real symmetric covariance matrix $\mathbf{V}$ as defined in (2.28). Once we have the covariance matrix, all the quantum statistical properties of Gaussian continuous variable states can be constructed. Also worth mentioning is the important fact that the Hamiltonian (5.10) is quadratic in the position and momentum coordinates of the movable mirrors. An initial Gaussian state of the mirror evolving under (5.10) will therefore maintain its Gaussian character.

A widely used entanglement measure is the logarithmic negativity, which is an entanglement monotone and fairly easy to compute [121]. For a two-mode Gaussian continuous variable state characterised by the covariance matrix $\mathbf{V}$, logarithmic neg-

ativity is defined as

$$\mathcal{N} = \mathrm{Max}[0, \log(2\tilde{\nu}_-)], \tag{5.18}$$

where $\tilde{\nu}_-$ is the smallest of the symplectic eigenvalues of the partially transposed covariance matrix given by

$$\tilde{\nu}_- = \sqrt{\sigma/2 - \sqrt{(\sigma^2 - 4\mathrm{Det}\mathbf{V})/2}} \tag{5.19}$$

and

$$\sigma = \mathrm{Det}\mathbf{A} + \mathrm{Det}\mathbf{B} - 2\mathrm{Det}\mathbf{C}. \tag{5.20}$$

Here

$$\mathbf{V} = \begin{pmatrix} \mathbf{A} & \mathbf{C} \\ \mathbf{C^T} & \mathbf{B} \end{pmatrix},$$

where $\mathbf{A}(\mathbf{B})$ accounts for the local variances of the modes and $\mathbf{C}$ for the inter-mode correlations. We analytically reconstruct the time-dependent covariance matrix, from which it is then straightforward to compute the logarithmic negativity, with a typical solution shown in Fig. 5.2. In these calculations, the logarithmic negativity has been weighted with a coherent state probability distribution for the collective cavity modes A and B such that $P(n_A, n_B) = \exp(-(|\alpha_A|^2 + |\alpha_B|^2))|\alpha_A|^{2n_A}|\alpha_B|^{2n_B}/(n_A! n_B!)$. Such averaging accounts for initial quantum fluctuations in the two cavity modes. A non-zero value of $\mathcal{N}$ quantifies the degree of entanglement between the two movable mirrors. As can be seen from Fig. 5.2, increasing the initial temperature of the mirror degrades the quantum correlations and eventually leads to completely separable states of the two mirrors. The figure also gives a clear example of entanglement sudden death and birth [122], arising from the common coupling of the mirrors to the two cavity modes.

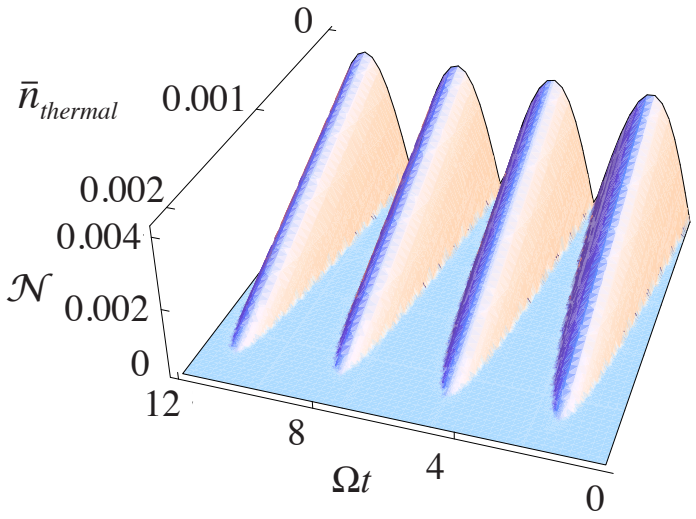

Figure 5.2: Time evolution of the degree of entanglement, as measured by the logarithmic negativity, as a function of initial temperature of the movable mirrors, measured in terms of $\bar{n}_{\rm thermal}$. The dimensionless parameters are chosen such that $\Omega = 1$, $g = 10^{-2}$, $\lambda = 10^{-1}$, $\alpha_A = 4$ and $\alpha_B = 1$. Time is scaled in units of Ω.

5.4 Effect of losses

So far we have not considered the effect of losses in optical and mechanical degrees of freedom in our proposed scheme to generate distant optomechanical correlations. In the present section we shall discuss in detail the influence of inevitable coupling of the system of interest to environmental degrees of freedom. We shall discuss the effect of losses under different physical scenarios of interest.

5.4.1 Adiabatic elimination of cavity modes

In our proposed scheme to generate distant optomechanical correlations, optical and mechanical degrees of freedom evolve on very different time scales. In most practical scenarios, optical degrees of freedom evolves on a very fast time scale and can thus be adiabatically eliminated. Optical degrees of freedom are thus slaved to the mechanical degrees of freedom. In the present section we cater our interest to this particular

regime.

Denoting the two quantized optical modes with creation (destruction) operators $\hat{a}$ ($\hat{a}^\dagger$) and $\hat{b}$ ($\hat{b}^\dagger$) respectively. Representing the quantized motion of each movable mirror by creation (destruction) operators $\hat{m}$ ($\hat{m}^\dagger$) and $\hat{n}$ ($\hat{n}^\dagger$) respectively, the Hamiltonian representing the closed system dynamics of the closed system takes the form

$$H = \omega(\hat{a}^\dagger\hat{a}+\hat{b}^\dagger\hat{b})+\Omega(\hat{m}^\dagger\hat{m}+\hat{n}^\dagger\hat{n})+\lambda(\hat{a}^\dagger\hat{b}+\hat{b}^\dagger\hat{a})-g\hat{a}^\dagger\hat{a}(\hat{m}+\hat{m}^\dagger)-g\hat{b}^\dagger\hat{b}(\hat{n}+\hat{n}^\dagger). \quad (5.21)$$

In the interaction picture of the free evolution of the two optical modes, the above Hamiltonian takes the form

$$H = \Omega(\hat{m}^\dagger\hat{m} + \hat{n}^\dagger\hat{n}) + \lambda(\hat{a}^\dagger\hat{b} + \hat{b}^\dagger\hat{a}) - g\hat{a}^\dagger\hat{a}(\hat{m} + \hat{m}^\dagger) - g\hat{b}^\dagger\hat{b}(\hat{n} + \hat{n}^\dagger). \quad (5.22)$$

Heisenberg equations of motion taking into account cavity losses takes the form

$$\frac{d}{dt}\hat{a} = -i\lambda\hat{b} + ig\hat{a}(\hat{m} + \hat{m}^\dagger) - \kappa\hat{a}, \quad (5.23)$$

$$\frac{d}{dt}\hat{b} = -i\lambda\hat{a} + ig\hat{b}(\hat{n} + \hat{n}^\dagger) - \kappa\hat{b}, \quad (5.24)$$

where κ is the identical decay rate of each cavity mode. Adiabatically eliminating the cavity modes we get

$$\hat{a} = \frac{-i\lambda\hat{b}}{\kappa - ig(\hat{m} + \hat{m}^\dagger)} \quad (5.25)$$

$$\hat{b} = \frac{-i\lambda\hat{a}}{\kappa - ig(\hat{n} + \hat{n}^\dagger)}. \quad (5.26)$$

Truncating the expressions for the cavity modes $\hat{a}$ and $\hat{b}$ only up to linear order in the small parameter g/κ we get

$$\hat{a} = \frac{-i\lambda\hat{b}}{\kappa}(1 + i\frac{g}{\kappa}(\hat{m} + \hat{m}^\dagger)) \quad (5.27)$$

$$\hat{b} = \frac{-i\lambda\hat{a}}{\kappa}(1 + i\frac{g}{\kappa}(\hat{n} + \hat{n}^\dagger)). \quad (5.28)$$

We treat the two cavity modes in the semiclassical limit and thus replace the two cavity mode operators $\hat{a}$ and $\hat{b}$ by their coherent state amplitudes α_a and α_b respectively. In this limit and in absence of mirror's losses, the two distant movable mirrors evolve under the Hamiltonian

$$H = \Omega(\hat{m}^\dagger\hat{m} + \hat{n}^\dagger\hat{n}) + 2\frac{\lambda^3 g^2}{\kappa^4}\alpha_a\alpha_b(\hat{m} + \hat{m}^\dagger)(\hat{n} + \hat{n}^\dagger)$$
$$-\frac{g\alpha_a^2\lambda^2}{\kappa^2}(1 + \frac{g^2}{\kappa^2}(\hat{m} + \hat{m}^\dagger)^2)(\hat{m} + \hat{m}^\dagger) - \frac{g\alpha_b^2\lambda^2}{\kappa^2}(1 + \frac{g^2}{\kappa^2}(\hat{n} + \hat{n}^\dagger)^2)(\hat{n} + \hat{n}^\dagger), \quad (5.29)$$

where for the sake of simplifying the calculations we have assumed that both α_a and α_b are real. Further going in the interaction picture of $\Omega(\hat{m}^\dagger\hat{m} + \hat{n}^\dagger\hat{n})$ and simplifying the above Hamiltonian under the rotating wave approximation [79] we get

$$H = \eta(\hat{c}^\dagger\hat{d} + \hat{d}^\dagger\hat{c}), \quad (5.30)$$

where $\eta = 2g^2\lambda^3/\kappa^4$. The above Hamiltonian can be straightforwardly used to describe the time evolved mechanical modes which takes the form

$$\hat{m}(t) = \hat{c}(0)\cos(\eta t) - i\hat{d}(0)\sin(\eta t), \quad (5.31)$$
$$\hat{n}(t) = \hat{d}(0)\cos(\eta t) - i\hat{c}(0)\sin(\eta t). \quad (5.32)$$

Now it is a straightforward excercise to describe the state evolution of distant mechanical mirrors. For instance, if the two mirrors are are initially prepared in vibrational states close to their quantum ground states so that initially $|\Psi(0)\rangle = |1\rangle_m|0\rangle_n$, the time evolved state of the two coupled mirrors evolves $|\Psi(t)\rangle = \cos(\eta t)|1\rangle_m|0\rangle_n + i\sin(\eta t)|0\rangle_m|1\rangle_n$. Clearly the time evolved state is an entangled state of the two movable mirrors and as a measure of entanglement between the two movable mirrors we plot negativity $\mathcal{N}$ in Fig. 5.3.

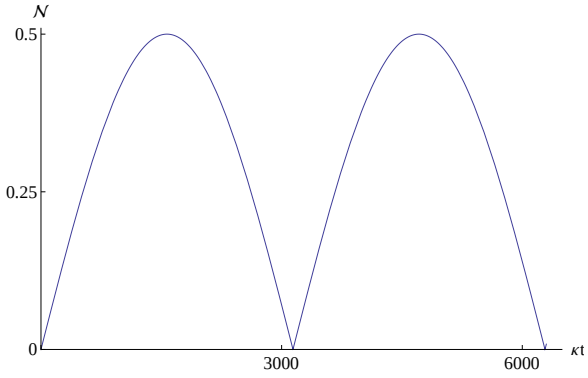

Figure 5.3: Temporal evolution of the degree of entanglement between two indirectly coupled movable mirrors as measured by the negativity. Dimensionless parameters used are chosen such that $\kappa = 1$, $g = 0.05$, $\lambda = 10^{-1}$, $\alpha_a = 10$, $\alpha_b = 10$. Time is scaled in units of κ.

5.4.2 Conditional quantum measurement

In any physical setting, coupling to the environment is inevitable and typically results in decoherence of the quantum state to its classical counterpart. In the scheme of interest to us, there can be two main causes of dissipation. One is the photon leakage through the two cavities, and the other is thermal decay of the states of the movable mirrors due to their coupling to baths of non-zero temperature.

In the present section we will continue treating the two cavity modes in this semiclassical regime and defer the explicit calculations involving reservoir induced quantum fluctuations in the cavity modes till the next section. More precisely, we assign coherent states for the two cavity modes and introduce cavity losses in terms of a non-Hermitian Hamiltonian.

In the presence of a conditional quantum measurement of the excitations in modes A and B that exit into the environment, we introduce cavity losses by shifting the cavity resonance frequency ω by $-i\kappa$ where κ is the cavity decay rate. Then, conditional on seeing no counts at all, the two indirectly coupled movable mirrors evolve according

to the non-Hermitian Hamiltonian

$$\hat{H}_{\rm disp} \approx \hat{H}_{\rm mir} - i\kappa(n_A + n_B), \tag{5.33}$$

where $\hat{H}_{\rm mir}$ is given by (5.10) and we again have neglected all the driving terms in the Hamiltonian. Apart from the cavity losses, the two cavity mirrors might undergo further decoherence due to their inevitable coupling to the external environment. The time evolution of the mixed state of the two movable mirrors obtained by tracing over the cavity field distribution takes the form

$$\hat{\rho}_{\rm mir}(t) = \frac{1}{\sum_{n_A,n_B} N_{n_A,n_B}(t)} \sum_{n_A,n_B} N_{n_A,n_B}(t)\hat{\rho}^{(n)}_{\rm mir}(t), \tag{5.34}$$

where

$$N_{n_A,n_B}(t) = \exp\left(-|\alpha_A e^{-\kappa t}|^2\right) |\alpha_A e^{-\kappa t}|^{2n_A} \exp\left(-|\alpha_B e^{-\kappa t}|^2\right) |\alpha_B e^{-\kappa t}|^{2n_B}/n_A! n_B! \tag{5.35}$$

and $\hat{\rho}^{(n)}_{\rm mir}(t)$ is the time-evolved reduced density matrix of the two movable mirrors with the photon number difference $n = n_A - n_B$. It turns out that if both the collective cavity modes are initially prepared in coherent states, then even when a quantum jump occurs the initial coherent state of the cavity modes is preserved [123]. This is because an initial coherent state evolving in a purely dissipative channel remains a coherent state, although with an exponentially decaying amplitude [3]. In presence of no quantum jump event, the time evolution of $\hat{\rho}^{(n)}_{\rm mir}(t)$ in the Born-Markov approximation is then described by the Lindblad-type master equation [79, 124]

$$\begin{aligned} \frac{\partial}{\partial t}\hat{\rho}^{(n)}_{\rm mir} &= -i\left[\hat{H}_{\rm mir}, \hat{\rho}^{(n)}_{\rm mir}\right] + \frac{\Gamma}{2}\bar{n}\mathcal{L}_{c^\dagger}\hat{\rho}^{(n)}_{\rm mir} + \frac{\Gamma}{2}\bar{n}\mathcal{L}_{d^\dagger}\hat{\rho}^{(n)}_{\rm mir} \\ &\quad + \frac{\Gamma}{2}(\bar{n}+1)\mathcal{L}_c\hat{\rho}^{(n)}_{\rm mir} + \frac{\Gamma}{2}(\bar{n}+1)\mathcal{L}_d\hat{\rho}^{(n)}_{\rm mir}, \end{aligned} \tag{5.36}$$

[3] This follows from noting that an initial coherent state with amplitude α has the quantum characteristic function $\chi(\epsilon) = e^{\epsilon\alpha^* - \text{c.c.}}$. Under purely dissipative time evolution χ satisfies $\frac{\partial\chi}{\partial t} = -\kappa(\epsilon^*\frac{\partial}{\partial\epsilon^*} + \text{c.c.})\chi$, the solution of which is $\chi(\epsilon) = e^{\epsilon\alpha^* e^{-\kappa t} - \text{c.c.}}$.

where Γ is the decay rate of each movable mirror due to its coupling to a heat bath with average thermal occupancy $\bar{n}$, and $\mathcal{L}_x\hat{\rho}^{(n)}_{\rm mir} \equiv 2\hat{x}\hat{\rho}^{(n)}_{\rm mir}\hat{x}^\dagger - \hat{x}^\dagger\hat{x}\hat{\rho}^{(n)}_{\rm mir} - \hat{\rho}^{(n)}_{\rm mir}\hat{x}^\dagger\hat{x}$. In terms of the center of mass mode $\hat{C}$ and relative mode $\hat{D}$, equation (5.36) can be equivalently written as

$$\begin{aligned}\frac{\partial}{\partial t}\hat{\rho}^{(n)}_{\rm mir} &= -i\left[\hat{H}_{\rm mir},\hat{\rho}^{(n)}_{\rm mir}\right] + \frac{\Gamma}{2}\bar{n}\mathcal{L}_{C^\dagger}\hat{\rho}^{(n)}_{\rm mir} + \frac{\Gamma}{2}\bar{n}\mathcal{L}_{D^\dagger}\hat{\rho}^{(n)}_{\rm mir} \\ &\quad + \frac{\Gamma}{2}(\bar{n}+1)\mathcal{L}_C\hat{\rho}^{(n)}_{\rm mir} + \frac{\Gamma}{2}(\bar{n}+1)\mathcal{L}_D\hat{\rho}^{(n)}_{\rm mir}, \end{aligned} \tag{5.37}$$

where $\hat{H}_{\rm mir}$ is given by (5.12). We again stress that *phenomenological* introduction of dissipation is only valid for the case of weakly coupled modes and a careful analysis of this will be presented in greater detail in chapter 6

To solve the master equation (5.37), we define a normal-ordered quantum characteristic function [79, 124] for the two movable mirrors as $\chi(\epsilon,\eta,t) = \langle e^{\epsilon\hat{C}^\dagger}e^{-\epsilon^*\hat{C}}e^{\eta\hat{D}^\dagger}e^{-\eta^*\hat{D}}\rangle$. Using standard quantum optical techniques [79, 124], the master equation (5.37) can be rewritten as a partial differential equation for the quantum characteristic function $\chi(\epsilon,\eta,t)$ of the form

$$\frac{\partial}{\partial t}\chi(\epsilon,\eta,t) = z^T\mathbf{M}\nabla\chi(\epsilon,\eta,t) + 4\lambda z^T\mathbf{K}z\chi(\epsilon,\eta,t), \tag{5.38}$$

where

$$
\begin{aligned}
z^T &= (u_1, u_2, v_1, v_2), \\
\nabla &= \left(\tfrac{\partial}{\partial u_1}, \tfrac{\partial}{\partial u_2}, \tfrac{\partial}{\partial v_1}, \tfrac{\partial}{\partial v_2}\right)^T, \\
u_1 &= \tfrac{\epsilon_c+\epsilon_d+\epsilon_c^*+\epsilon_d^*}{2\sqrt{2}}, \\
u_2 &= \tfrac{\epsilon_c+\epsilon_d-\epsilon_c^*-\epsilon_d^*}{i2\sqrt{2}}, \\
v_1 &= \tfrac{\epsilon_c-\epsilon_d+\epsilon_c^*-\epsilon_d^*}{2\sqrt{2}}, \\
v_2 &= \tfrac{\epsilon_c-\epsilon_d-\epsilon_c^*+\epsilon_d^*}{i2\sqrt{2}},
\end{aligned}
\tag{5.39}
$$

and

$$
\epsilon_c = \frac{\epsilon+\eta}{\sqrt{2}}, \qquad \epsilon_d = \frac{\epsilon-\eta}{\sqrt{2}}. \tag{5.40}
$$

The 4×4 matrix coefficients of equation (5.38) are

$$
\mathbf{M} = \begin{pmatrix} \mathbf{M}_1 & \mathbf{0} \\ \mathbf{0} & \mathbf{M}_2 \end{pmatrix}, \qquad \mathbf{K} = \begin{pmatrix} \mathbf{K}_1 & \mathbf{0} \\ \mathbf{0} & \mathbf{K}_2 \end{pmatrix}, \tag{5.41}
$$

with

$$\mathbf{M}_1 = \begin{pmatrix} -\Gamma/2 & \Omega \\ -\Omega & -\Gamma/2 \end{pmatrix},$$

$$\mathbf{M}_2 = \begin{pmatrix} -\Gamma/2 & \Omega - 8N\lambda \\ -\Omega & -\Gamma/2 \end{pmatrix},$$

$$\mathbf{K}_1 = \begin{pmatrix} -\Gamma\bar{n}/4\lambda & 0 \\ 0 & -\Gamma\bar{n}/4\lambda \end{pmatrix}, \tag{5.42}$$

$$\mathbf{K}_2 = \begin{pmatrix} -\Gamma\bar{n}/4\lambda & N \\ N & -\Gamma\bar{n}/4\lambda \end{pmatrix}.$$

For an initial Gaussian state of the two movable mirrors, it is consistent to make an ansatz for the quantum characteristic function of the form

$$\chi(\epsilon, \eta, t) = \exp\left[-z^T \mathbf{L}(t)\, z + i z^T q(t)\right], \tag{5.43}$$

where $\mathbf{L}(t)$ is a 4×4 time-dependent symmetric matrix and $q(t)$ is a 4×1 time-dependent vector. Using the above ansatz in equation (5.38) results in the coupled matrix differential equations

$$\dot{\mathbf{L}} = \mathbf{M}\mathbf{L} + \mathbf{L}\mathbf{M}^T - 4\lambda\mathbf{K}, \tag{5.44}$$

$$\dot{q} = \mathbf{M}q. \tag{5.45}$$

Making use of the fact that $\mathbf{L}$ is a 4×4 symmetric matrix, it can be decomposed into 2×2 square matrices such that

$$\mathbf{L} = \begin{pmatrix} \mathbf{P} & \mathbf{Q} \\ \mathbf{Q}^T & \mathbf{R} \end{pmatrix}, \tag{5.46}$$

where $\mathbf{P}$ and $\mathbf{R}$ are 2×2 symmetric matrices. Obtaining an explicit form for the time-

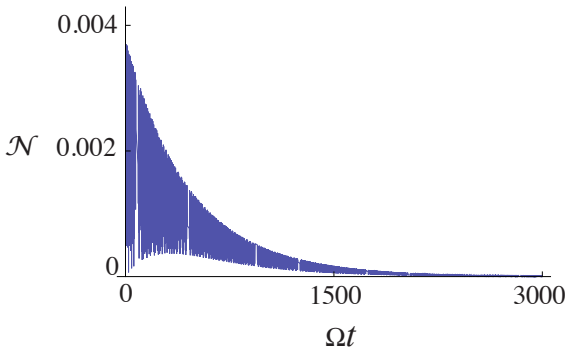

Figure 5.4: Temporal evolution of the degree of entanglement between two indirectly coupled movable mirrors as measured by the logarithmic negativity. Compared with Fig. 5.2, here losses in all modes have been considered and the degree of entanglement is consequently somewhat smaller, but importantly, it survives for a reasonably long time. Each mirror is initially assumed to be in its ground state and the dimensionless parameters used are chosen such that $\Omega = 1$, $g = 10^{-2}$, $\lambda = 10^{-1}$, $\alpha_A = 4$, $\alpha_B = 1$, $\kappa = 10^{-3}$, $\Gamma = 10^{-4}$ and $\bar{n} = 0$. Time is scaled in units of Ω.

dependent quantum characteristic function $\chi(\epsilon, \eta, t)$ now reduces to solving 2×2 coupled matrix differential equations.

Although an exact analytical solution can be arrived at, it is not very illuminating. Nonetheless, the time-dependent covariance matrix $\mathbf{V}$ can be fully reconstructed from the quantum characteristic function $\chi(\epsilon, \eta, t)$. This can be easily seen by noting that from the quantum characteristic function one can obtain the expectation values of quantum mechanical observables, e.g., $\langle \hat{c}^{\dagger m}(t) \hat{d}^{\dagger n}(t) \rangle = (\frac{\partial}{\partial \epsilon_c})^m (\frac{\partial}{\partial \epsilon_d})^n \chi(\epsilon_c, \epsilon_d, t)|_{\epsilon_c=0, \epsilon_d=0}$ and thus all the elements of the covariance matrix can be found.

As a measure of entanglement between the distant cavity mirrors we again compute the logarithmic negativity. The result of such a calculation is shown in Fig. 5.4. As is clear from the figure, under the action of cavity-mediated coupling, the two movable mirrors exhibit entanglement. Although the entanglement generated is not too large, it is sustained over a reasonably long timescale. The degree of inseparability between the two mirrors can be improved significantly either by a conditional measurement of the cavity field or by increasing the difference in the mean number of photons in the field distributions of the two cavity modes. Thus we conclude that the aforementioned

protocol is indeed capable of generating quantum entangled states of two movable mirrors, which are robust with respect to dissipation for a long time. It should be pointed out that the logarithmic negativity approaches zero exponentially for large times due to the decay of photons out of the cavities. In order to have sustainable non-vanishing entanglement, the photon modes must be driven externally to prevent the absence of photons. This will be discussed in the next section of this chapter.

5.4.3 Quantum Langevin approach

The radiation pressure coupling for an undriven cavity with a movable mirror is usually very weak. This problem can be circumvented by driving the cavity with a coherent classical laser field. Driving with an intense laser field enhances the radiation pressure coupling and thus facilitates the observation of non-classical phenomena such as entanglement between mechanical oscillators and light.

In the previous section, cavity driving was not taken into account. Instead the two cavity fields were assumed to be initially in coherent states and the system time-evolution in the presence of the decay of the two cavity fields was studied. In what follows, we shall instead study the situation of cavity driving and show that robust steady state entanglement may exist between different optical and mechanical modes. To this end, we find it more convenient to work in the Heisenberg picture. For our system of two coupled cavities with movable mirrors, the Hamiltonian in the interaction picture of the two driving lasers with identical frequency ω_L now takes the form

$$\begin{aligned}\frac{\hat{H}}{\hbar} &= (\omega-\omega_L)(\hat{a}^\dagger\hat{a}+\hat{b}^\dagger\hat{b})+\frac{\Omega}{2}(\hat{q}_1^2+\hat{p_1}^2)+\frac{\Omega}{2}(\hat{q}_2^2+\hat{p}_2^2)\\ &\quad +\lambda(\hat{a}^\dagger\hat{b}+\hat{b}^\dagger\hat{a})-g\hat{a}^\dagger\hat{a}\hat{q}_1-g\hat{b}^\dagger\hat{b}\hat{q}_2+i\eta(\hat{a}^\dagger-\hat{a})+i\eta(\hat{b}^\dagger-\hat{b}). \qquad (5.47)\end{aligned}$$

Here $\eta=\sqrt{2P_c\kappa/\hbar\omega_c}$ is related to the driving laser, where P_c is the power of the driving laser and κ is the damping rate, identical for both cavities.

The Hamiltonian (5.47) describes the closed-system dynamics of the two driven coupled cavities with movable mirrors. However, as discussed in the previous section, the dynamics of the system is also affected by damping and noise. The main channels of dissipation in our system are the decay in the cavity modes and the coupling of the movable mirrors to their independent thermal baths[4]. One possible way to take into account all the damping and noise processes is to use quantum Langevin equations (QLEs). The QLEs are equivalent to the Heisenberg equations of motion for time-evolving operators, where noise and dissipative processes have been included *phenomenologically* [124].

For the Hamiltonian (5.47), the QLEs for the cavity and the mirror modes become

$$\begin{aligned}
\tfrac{d\hat{a}}{dt} &= -i\lambda\hat{b} + ig\hat{q}_1\hat{a} + \eta - (\kappa + i\tilde{\Delta})\hat{a} + \sqrt{2\kappa}\hat{a}_{in}, \\
\tfrac{d\hat{b}}{dt} &= -i\lambda\hat{a} + ig\hat{q}_2\hat{b} + \eta - (\kappa + i\tilde{\Delta})\hat{b} + \sqrt{2\kappa}\hat{b}_{in}, \\
\tfrac{d\hat{p}_1}{dt} &= -\Omega\hat{q}_1 + g\hat{a}^\dagger\hat{a} - \gamma_m\hat{p}_1 + \hat{\varepsilon}_1(t), \\
\tfrac{d\hat{p}_2}{dt} &= -\Omega\hat{q}_2 + g\hat{b}^\dagger\hat{b} - \gamma_m\hat{p}_2 + \hat{\varepsilon}_2(t), \\
\tfrac{d\hat{q}_1}{dt} &= \Omega\hat{p}_1, \\
\tfrac{d\hat{q}_2}{dt} &= \Omega\hat{p}_2,
\end{aligned} \tag{5.48}$$

where $\tilde{\Delta} = \omega - \omega_L$ is the laser detuning from the cavity resonance frequency ω, κ is the decay rate of each cavity and γ_m is the thermal decay rate, identical for the two movable mirrors subject to independent Brownian motion noise characterised by the operators $\hat{\varepsilon}_1(t)$ and $\hat{\varepsilon}_2(t)$ respectively. The quantum noise operators have the

[4]Assuming independent baths implies neglecting any reservoir-induced correlations, which is supposed to be justified in the present setup of spatially separated oscillators.

quantum statistical properties

$$\begin{aligned} \langle \hat{\varepsilon}_1(t) \rangle &= \langle \hat{\varepsilon}_2(t) \rangle = 0, \\ \langle \hat{\varepsilon}_i(t) \hat{\varepsilon}_j(t') \rangle &= \frac{\gamma_m}{\Omega} \int e^{-i\omega'(t-t')} \omega' \times \left[1 + \coth\left(\frac{\hbar\omega'}{k_B T_i} \right) \right] \frac{d\omega'}{2\pi} \delta_{ij}, \end{aligned} \tag{5.49}$$

where i, $j \in 1, 2$ and δ_{ij} is the Kronecker delta. We have also introduced independent cavity input noise operators, $\hat{a}_{in}(t)$ and $\hat{b}_{in}(t)$ for the first and second cavity respectively. For the case of optical fields, $\hbar\omega/k_B T \gg 1$, and hence the mean number of thermal photons can be safely neglected. In this limit the noise operators $\hat{a}_{in}(t)$ and $\hat{b}_{in}(t)$ satisfy the two-time correlations

$$\begin{aligned} \langle \hat{a}_{in}(t) \hat{a}^{\dagger}_{in}(t') \rangle &= \delta(t - t'), \\ \langle \hat{a}^{\dagger}_{in}(t) \hat{a}_{in}(t') \rangle &= 0, \\ \langle \hat{b}_{in}(t) \hat{b}^{\dagger}_{in}(t') \rangle &= \delta(t - t'), \\ \langle \hat{b}^{\dagger}_{in}(t) \hat{b}_{in}(t') \rangle &= 0. \end{aligned} \tag{5.50}$$

In the present chapter we are interested in investigating a novel possibility of achieving steady-state entanglement between distant optical and mechanical modes. To pursue this aim we have to solve the above set of coupled nonlinear QLEs (5.48). This task is difficult in general, but it is simplified in the presence of strong external driving, in which case linearisation of the above set of QLEs around the steady-state values is justified. Solving the set of QLEs (5.48) for the steady-state amplitudes of the optical

and mechanical modes, we get

$$\begin{aligned}
\langle q_1^s \rangle &= \tfrac{g|\langle a_s \rangle|^2}{\Omega}, \\
\langle q_2^s \rangle &= \tfrac{g|\langle b_s \rangle|^2}{\Omega}, \\
\langle p_1^s \rangle &= 0, \\
\langle p_2^s \rangle &= 0, \\
\langle a_s \rangle &= \tfrac{-i\lambda\eta+\eta(\kappa+i\Delta_b)}{\lambda^2+\kappa^2+i\kappa(\Delta_a+\Delta_b)-\Delta_a\Delta_b}, \\
\langle b_s \rangle &= \tfrac{-i\lambda\eta+\eta(\kappa+i\Delta_a)}{\lambda^2+\kappa^2+i\kappa(\Delta_a+\Delta_b)-\Delta_a\Delta_b}, \\
\Delta_a &= \tilde{\Delta} - g\langle q_1 \rangle^s = \omega - \omega_L - g\langle q_1^s \rangle, \\
\Delta_b &= \tilde{\Delta} - g\langle q_2 \rangle^s = \omega - \omega_L - g\langle q_2^s \rangle.
\end{aligned} \tag{5.51}$$

In the regime where the two cavities are very intensely driven, such that $|\langle a_s \rangle|, |\langle b_s \rangle| \gg 1$, and by expanding the mechanical and optical mode operators as quantum fluctuations around their steady state values ($\hat{a} = \langle a_s \rangle + \delta\hat{a}$, $\hat{b} = \langle b_s \rangle + \delta\hat{b}$, $\hat{q}_i = \langle q_i^s \rangle + \delta\hat{q}_i$ and $\hat{p}_i = \langle p_i^s \rangle + \delta\hat{p}_i$ for $i = 1, 2$) we obtain the following linearised QLEs for the quantum

fluctuations,

$$\begin{aligned}
\tfrac{d\delta\hat{a}}{dt} &= -\delta\hat{a}(\kappa + i\Delta_a) - i\lambda\delta\hat{b} + ig\langle a_s\rangle\delta\hat{x} + \sqrt{2\kappa}\hat{a}_{in}, \\
\tfrac{d\delta\hat{b}}{dt} &= -\delta\hat{b}(\kappa + i\Delta_b) - i\lambda\delta\hat{a} + ig\langle b_s\rangle\delta\hat{y} + \sqrt{2\kappa}\hat{b}_{in}, \\
\tfrac{d\delta\hat{q}_1}{dt} &= \Omega\delta\hat{p}_1, \\
\tfrac{d\delta\hat{q}_2}{dt} &= \Omega\delta\hat{p}_2, \\
\tfrac{d\delta\hat{p}_1}{dt} &= -\Omega\delta\hat{q}_1 + g\left(|\langle a_s\rangle|^2 + \langle a_s\rangle^*\delta\hat{a} + \langle a_s\rangle\delta\hat{a}^\dagger\right), \\
\tfrac{d\delta\hat{p}_2}{dt} &= -\Omega\delta\hat{q}_2 + g\left(|\langle b_s\rangle|^2 + \langle b_s\rangle^*\delta\hat{b} + \langle b_s\rangle\delta\hat{b}^\dagger\right).
\end{aligned} \tag{5.52}$$

By further introducing the position and momentum quadratures for the two cavity

modes and their input noises,

$$\begin{aligned}
\frac{d\delta\hat{X}_a}{dt} &= \frac{d(\delta\hat{a}^\dagger+\delta\hat{a})}{dt},\\
\frac{d\delta\hat{P}_a}{dt} &= i\frac{d(\delta\hat{a}^\dagger-\delta\hat{a})}{dt},\\
\frac{d\delta\hat{X}_b}{dt} &= \frac{d(\delta\hat{b}^\dagger+\delta\hat{b})}{dt},\\
\frac{d\delta\hat{P}_b}{dt} &= i\frac{d(\delta\hat{b}^\dagger-\delta\hat{b})}{dt},\\
\frac{d\delta\hat{X}^a_{in}}{dt} &= \frac{d(\delta\hat{a}^\dagger_{in}+\delta\hat{a}_{in})}{dt},\\
\frac{d\delta\hat{P}^a_{in}}{dt} &= i\frac{d(\delta\hat{a}^\dagger_{in}-\delta\hat{a}_{in})}{dt},\\
\frac{d\delta\hat{X}^b_{in}}{dt} &= \frac{d(\delta\hat{b}^\dagger_{in}+\delta\hat{b}_{in})}{dt},\\
\frac{d\delta\hat{X}^b_{in}}{dt} &= i\frac{d(\delta\hat{b}^\dagger_{in}-\delta\hat{b}_{in})}{dt},
\end{aligned} \tag{5.53}$$

we can rewrite equation (5.52) in the following compact form

$$\frac{dR}{dt} = \mathbf{Z}R + N, \tag{5.54}$$

where

$$\begin{aligned}
R^T &= (\delta\hat{q}_1, \delta\hat{p}_1, \delta\hat{q}_2, \delta\hat{p}_2, \delta\hat{X}_a, \delta\hat{P}_a, \delta\hat{X}_b, \delta\hat{P}_b),\\
N^T &= (0, \epsilon_1(t), 0, \epsilon_2(t), \sqrt{2\kappa}\delta\hat{X}^a_{in}(t), \sqrt{2\kappa}\delta\hat{P}^a_{in}(t), \sqrt{2\kappa}\delta\hat{X}^b_{in}(t), \sqrt{2\kappa}\delta\hat{P}^b_{in}(t)),\\
\mathbf{Z} &= \begin{pmatrix} \mathbf{Z}_1 & \mathbf{Z}_2 \\ \mathbf{Z}_2 & \mathbf{Z}_3 \end{pmatrix},
\end{aligned}$$

and with the 4×4 matrices

$$\mathbf{Z}_1 = \begin{pmatrix} 0 & \Omega & 0 & 0 \\ -\Omega & -\gamma_m & 0 & 0 \\ 0 & 0 & 0 & \Omega \\ 0 & 0 & -\Omega & -\gamma_m \end{pmatrix}, \tag{5.55}$$

$$\mathbf{Z}_2 = \begin{pmatrix} 0 & 0 & 0 & 0 \\ g_a^s & 0 & 0 & 0 \\ 0 & 0 & 0 & 0 \\ 0 & 0 & g_b^s & 0 \end{pmatrix}, \tag{5.56}$$

$$\mathbf{Z}_3 = \begin{pmatrix} -\kappa & \Delta_a & 0 & \lambda \\ -\Delta_a & -\kappa & -\lambda & 0 \\ 0 & \lambda & -\kappa & \Delta_b \\ -\lambda & 0 & -\Delta_b & -\kappa \end{pmatrix}. \tag{5.57}$$

The phase reference has been chosen such that $\langle a_s \rangle$ and $\langle b_s \rangle$ are real with $g_a^s = \sqrt{2} g \langle a_s \rangle$ and $g_b^s = \sqrt{2} g \langle b_s \rangle$. In equation (5.54), $\mathbf{Z}$ is the drift matrix. Stability (in the steady state) demands that the real part of all the eigenvalues of $\mathbf{Z}$ must be negative. We have chosen all the physical parameters such that the system is stable in the steady state.

The dynamics of the coupled cavities with movable mirrors is governed by the first order matrix differential equation (5.54). For an initial Gaussian state of the two cavities and their movable mirrors it is sufficient to fully characterise all the quantum correlations by explicitly evaluating the 8×8 symmetric covariance matrix $\mathbf{V}$ where $V_{i,j}(t) = (\langle R_i(t) R_j(t) + R_j(t) R_i(t) \rangle)/2$. If the system is stable in the steady state, then the covariance matrix takes the form

$$V_{i,j} = \sum_{p,q} \int_0^\infty ds \int_0^\infty ds' W_{i,p}(s) W_{j,q}(s') \Phi_{p,q}(s - s'), \tag{5.58}$$

where $\mathbf{W} = \exp(\mathbf{Z}\mathrm{s})$ and $\Phi_{p,q}(s - s') = (\langle N_p(s) N_q(s') + N_q(s') N_p(s) \rangle)/2$ is the steady-

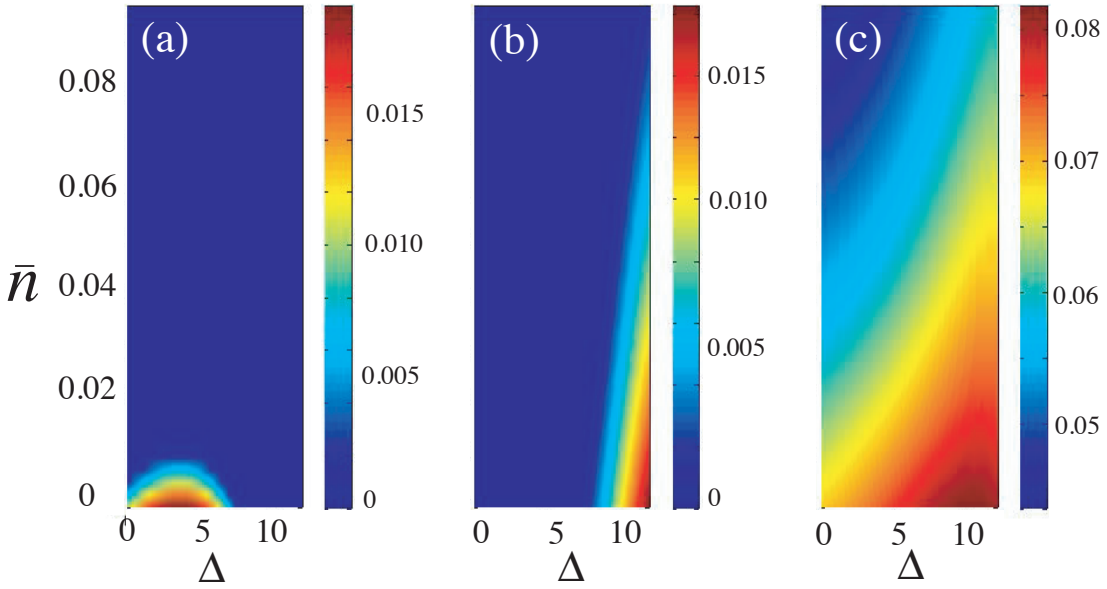

Figure 5.5: Logarithmic negativity as a measure of entanglement between (a) two distant cavity mirrors, (b) a mirror and adjacent cavity mode, and (c) a mirror and distant cavity mode, plotted as a function of detuning Δ and average thermal occupancy of the two mirrors $\bar{n}_1 = \bar{n}_2 = \bar{n}$. We have chosen the different physical parameters such that $\Omega = 1$, $g_a^s = g_b^s = 2.5$, $\lambda = 20$, $\kappa = 0.08$, $\gamma_m = 0.01$, and $\Delta_a = \Delta_b = \Delta$.

state noise correlation matrix. It turns out that in the regime where the mechanical oscillators possess very high Q-values, the quantum Brownian noise becomes approximately δ-correlated and in this limit the noise correlation matrix takes the form

$$\begin{aligned}\Phi_{p,q}(s-s') &= \tilde{N}_{p,q}\delta(s-s'), \\ &= \mathrm{Diag}[0,\gamma_{\mathrm{m}}(2\bar{\mathrm{n}}_1+1)),0,\gamma_{\mathrm{m}}(2\bar{\mathrm{n}}_2+1),\kappa,\kappa,\kappa,\kappa]\delta(\mathrm{s}-\mathrm{s}'), \quad (5.59)\end{aligned}$$

with $\bar{n}_1 = \left[e^{(\hbar\Omega/k_B T_1)}-1\right]^{-1}$ and $\bar{n}_2 = \left[e^{(\hbar\Omega/k_B T_2)}-1\right]^{-1}$. In this limit equation (5.58) simplifies to

$$\mathbf{V} = \int_0^\infty ds \mathbf{W}(s)\tilde{\mathbf{N}}\mathbf{W}^T(s). \quad (5.60)$$

When the system of coupled optomechanical cavities is stable in the steady state, the covariance matrix $\mathbf{V}$ satisfies a Lyapunov equation [133]

$$\mathbf{Z}\mathbf{V} + \mathbf{V}\mathbf{Z}^T = -\tilde{\mathbf{N}}. \quad (5.61)$$

Once again, when we have the solution for the covariance matrix, we can compute various non-classical correlations between the optical and mechanical degrees of freedom. In particular, the degree of entanglement between different optical and mechanical modes can be evaluated by computing the logarithmic negativity as defined in (5.18). We numerically solve equation (5.61) for the covariance matrix $\mathbf{V}$. An example of the numerically calculated logarithmic negativity between various optical and mechanical modes is presented in Fig. 5.5.

For evaluating the entanglement between various optical and mechanical modes we have chosen physical parameters accessible in present experiments. Not surprisingly, the steady-state entanglement is susceptible to thermal fluctuations of the environment. A high temperature of the surrounding reservoirs will result in a completely separable state of the optical and mechanical modes. One should note that the entanglement generated between optical and mechanical modes in the steady state is not very large, but, it does not require any quantum resources, such as additionally

driving the two cavities with squeezed light [64, 110].

Also, it is worth pointing out that with our particular choice of parameters we find that an appreciable entanglement appears between various optical and mechanical modes only when we operate far away from the regime of the red ($\Delta = \Omega$) or blue ($\Delta = -\Omega$) sideband. Although operating in the blue sideband regime is commonly considered ideal for generating entanglement between various optical and mechanical modes, the condition that the steady state should be stable puts serious restrictions on the coupling strength between the mechanical and optical modes [134, 135].

A challenging aspect of any scheme involving entanglement generation between macroscopic mechanical systems is the actual experimental detection of entanglement. There are however some recent promising proposals to create and detect quantum correlations in optomechanical settings [64, 65]. Since it is comparatively easy to detect quantum correlations between optical modes, compared to directly detecting quantum entanglement between mechanical modes, the essence of these proposals is to swap the nonlocal correlations from the mechanical modes back to the optical modes. As shown in Fig. 5.1 this can, for instance, be implemented using two auxiliary light modes, each initially prepared in classical uncorrelated states. These auxiliary modes can be two modes of distant cavities, and the geometry so arranged that each entangled mirror couples independently to the two modes. The non-local correlations may then be transferred from the movable mirrors to the initially uncorrelated auxiliary modes, which may eventually become entangled. Thus, using standard homodyne measurement techniques, the entire correlation matrix of the two optical auxiliary modes can be reconstructed. A presence of non-zero quantum correlations between these optical modes will be an indirect signature of non-zero quantum correlations between the mechanical modes.

5.5 Conclusions

In this chapter we have discussed how to generate non-local quantum correlations between optical and mechanical modes of two spatially separated cavities. Each cavity is assumed to have one fixed and one movable mirror and the two cavities are coupled by an optical fibre. Under the Born-Oppenheimer approximation, relying on separating the dynamics into a fast optical timescale and a slow mechanical timescale, we have analytically worked out the dynamics of the two coupled movable mirrors. Furthermore, within this adiabatic regime, we have also presented a full analytical solution of the master equation governing the open-system dynamics of the two mirrors. We found that the interaction mediated via two optical modes entangles the two distant mirrors. Cavity losses were taken into account in an effective non-Hermitian model, and mirror entanglement was found to be fairly robust against such dissipation.

Using a complementary model, we have also studied the two coupled cavities using the quantum Langevin formalism, by explicitly solving the resulting equations of motion. In the presence of strong driving laser fields we have found that the two coupled cavities exhibit nonlocal quantum correlations between distant optical and mechanical modes. In particular, these optical and mechanical modes exhibit entanglement in the steady state and at finite temperatures. This opens up an interesting possibility to study spatially separated massive Schrödinger cat states.

Of course the biggest challenge in ascertaining any massive quantum superposition lies in the actual detection of non-local quantum correlations. Optomechanics provides us with an alternative for detecting the quantum correlations generated between the mechanical modes by using a state transfer of the mechanical modes to initially uncorrelated auxiliary(optical) modes. Another major hindrance in achieving bigger and bigger quantum superpositions is the inevitable thermal decay of the mechanical modes. Thus the need of the hour is to engineer novel topologies of mechanical systems to minimise their contacts with the external environment. In this direction,

a recent interesting proposal aiming at creating massive quantum superposition of a levitating dielectric sphere is a promising one [136].

CHAPTER 6

STRONGLY COUPLED HARMONIC OSCILLATORS

6.1 Introduction

Entanglement is one of the strangest features of quantum mechanics, and is also a useful resource for quantum information processing [34, 137]. Superposition states, including entangled states, are however extremely sensitive to environmental noise and dissipation. Decoherence induced by an environment commonly reduces quantum coherent superpositions to incoherent mixtures [138], somewhat counter-intuitively, decoherence can also be used to generate entanglement [80, 81, 139]. These schemes typically employ few-level quantum systems coupled to harmonic oscillators, for example atoms coupled to cavity fields.

Apart from entanglement in finite-dimensional discrete systems, attention has also been devoted to entanglement in continuous variable systems [121]. Two-mode Gaussian entangled states are a useful resource for many quantum information processing tasks [53]. There are also proposals to generate entangled states of micro- or nanomechanical oscillators with infinite dimensional Hilbert spaces [15, 40, 140].

One may now ask whether schemes that take advantage of dissipation to prepare

entangled states, similar to those in [80, 81, 139], could be used to generate entanglement among coupled harmonic oscillators initially prepared in classical separable Gaussian states, such as vacuum, coherent or thermal states. Such a scheme could then be applied e.g. to micro- or nanomechanical oscillators coupled to cavity fields. At first sight it would seem that it is not possible to generate entanglement from classical initial states unless few-level quantum systems are included in a cavity QED-like setting. This is because if any number of harmonic oscillator modes are coupled using linear optics, then an initial classical state, with a positive P-function, *always* remains classical [87]. As long as decoherence and noise can be modelled through passive coupling to additional harmonic oscillator modes, this fact does not change [124].

The analogy with linear optics, however, relies on making the rotating-wave approximation (RWA) in modelling the interactions between coupled bosonic modes. The RWA can profoundly affect entanglement properties of a system; in the RWA, the ground state of a chain of harmonic oscillators is separable, while if the RWA is not made, it is entangled [41]. In the present chapter we will show that if the RWA is not made, then entanglement between coupled quantum harmonic oscillators, initially prepared in classical separable Gaussian states, may indeed arise. We will show that modelling the interaction between the oscillators beyond the RWA can significantly affect the dynamics of the coupled system. More generally, if the RWA is not made for linearly coupled oscillators, then generic squeezing interactions remain and the coupling is no longer passive. In this case entanglement between the oscillators, initially prepared in classical separable states, may indeed arise.

The unitary evolution of linearly coupled harmonic oscillators with interactions modelled beyond the RWA can be described analytically, but a complete picture of the dynamics should also take into account the irreversible system-environment coupling. The role of counter-rotating terms in describing the dynamics of coupled oscillators is not only limited to generate quantum correlations between them, but as it turns out,

they are also decisive in governing the dissipative state evolution of the oscillators and thus characterising their steady state behaviour.

In this chapter we investigate the Markovian evolution of strongly coupled harmonic oscillators. We provide an explicit derivation of the master equation for two strongly coupled harmonic oscillators which are subject to individual heat baths modelled by a collection of harmonic oscillators. We compare the results with the evolution obtained by phenomenologically introducing dissipation using local Lindblad terms for each individual oscillator, and discuss the validity of such a model. The difference in the above two approaches may seem innocuous, but will in fact result in different steady state solutions, which may give rise to non-trivial differences in ground state properties especially as far as correlations between the oscillators are concerned.

6.2 Local Lindblad type dissipation

We shall limit our attention to a simpler yet interesting system of two coupled harmonic oscillators interacting under two different physical settings. Firstly we shall embark on a study of two indirectly coupled harmonic oscillators where the indirect interactions are mediated via a third oscillator and then we move on to study another scenario when the two oscillators are directly coupled with bilinear interactions. While the physics of two directly coupled oscillators may be a little simpler to comprehend, the entanglement properties under dissipation are complicated by the fact that the ground state of a harmonic chain has nearest-neighbour entanglement [140]. This ground state has non-zero bipartite entanglement only for nearest neighbours. The next-to-nearest neighbours are always separable in the ground state. This motivates us to explore in somewhat more detail the interaction between coupled harmonic oscillators interacting under these two different physical settings. We shall study in detail both scenarios when the interaction between the oscillators are modelled with or without making the RWA. We shall first consider a case when the two coupled

oscillators are interacting with their local environments and dissipative dynamics is then modelled by *adding* local Lindblad operators for each individual oscillator. We will show that adding such local Lindblad terms to the master equation must be carefully justified, and may in fact lead to incorrect dynamics for the most common heat bath model based on a collection of harmonic oscillators.

6.2.1 Indirectly coupled harmonic oscillators interacting using the rotating wave approximation

As stated above, the ground state of a harmonic chain has non-zero bipartite entanglement only for nearest neighbours. The next-to-nearest neighbours are always separable in the ground state. So in order to see any genuine non-trivial effect of dissipation on the entanglement properties of coupled harmonic oscillators, we shall first embark on a study of an open chain of three coupled harmonic oscillators followed by an investigation of a physical system of two directly coupled harmonic oscillators.

As argued before, an initial classical Gaussian state of coupled harmonic oscillators, with interactions modelled under the RWA, will always remain separable. This result still applies in the presence of decoherence and noise as long as the system-reservoir coupling can be modelled via passive coupling to additional harmonic oscillator modes. Essentially, what one has, both in the presence and absence of dissipation, is equivalent to a linear optical network involving only beam splitters and phase shifters, which cannot generate any entanglement starting from classical states [87]. In what follows, we briefly discuss the dynamics of coupled harmonic oscillators when the interaction Hamiltonian is modelled under the RWA.

We consider an open chain of three coupled harmonic oscillators with quantised modes labelled a, b and c respectively. The time evolution is governed by the Hamiltonian

(with $\hbar = 1$)

$$\hat{H} = \omega(\hat{a}^\dagger\hat{a} + \hat{b}^\dagger\hat{b} + \hat{c}^\dagger\hat{c}) + \kappa(\hat{c}^\dagger + \hat{c})(\hat{a}^\dagger + \hat{a} + \hat{b}^\dagger + \hat{b}), \tag{6.1}$$

where ω is the resonance frequency of each oscillator and κ is the inter-mode coupling strength. In the interaction picture of the free evolution of the three coupled harmonic oscillators of Hamiltonian (6.1), and if $\kappa \ll \omega$, we can make use of the RWA and further simplify the Hamiltonian (6.1). Doing so results in the simplified Hamiltonian

$$\hat{H}_{\text{RWA}} = \kappa\hat{c}^\dagger(\hat{a} + \hat{b}) + h.c.. \tag{6.2}$$

The Hamiltonian in equation (6.2) conserves the total number of excitations and thus can be exactly solved analytically. It is thus straightforward to show that modes $\hat{a}(t)$, $\hat{b}(t)$ and $\hat{c}(t)$ evolves as

$$\begin{aligned}
\hat{a}(t) &= \hat{a}(0)(\tfrac{\cos(\sqrt{2}\kappa t)+1}{2}) + \hat{b}(0)(\tfrac{\cos(\sqrt{2}\kappa t)-1}{2}) - i\tfrac{\hat{c}(0)}{2}\sin(\sqrt{2}\kappa t),\\
\hat{b}(t) &= \hat{b}(0)(\tfrac{\cos(\sqrt{2}\kappa t)+1}{2}) + \hat{a}(0)(\tfrac{\cos(\sqrt{2}\kappa t)-1}{2}) - i\tfrac{\hat{c}(0)}{2}\sin(\sqrt{2}\kappa t),\\
\hat{c}(t) &= \hat{c}(0)\cos(\sqrt{2}\kappa t) - i\tfrac{1}{\sqrt{2}}\sin(\sqrt{2}\kappa t)(\hat{a}(0) + \hat{b}(0)).
\end{aligned} \tag{6.3}$$

It is worth pointing out that the Hamiltonian (6.2) is analogous to a beam splitter interaction Hamiltonian in quantum optics. This is an interesting observation since this allows us to conclude that harmonic oscillators initially prepared in classical Gaussian states and coupled under linear and passive coupling, will *never* become entangled [87].

This argument can be extended to the case when the oscillators are coupled to independent heat baths. This follows by noting that if dissipation of each individual mode is characterised by adding *local* Lindblad operator for each individual mode, then the dynamics of two coupled harmonic oscillators is governed by the following master equation

$$\frac{d}{dt}\hat{\rho} = -i[H', \hat{\rho}] + \sum_{x=a,b} \gamma\mathcal{L}_x\hat{\rho} + \Gamma(\bar{n}+1)\mathcal{L}_c\hat{\rho} + \Gamma\bar{n}\mathcal{L}_{c^\dagger}\hat{\rho}, \tag{6.4}$$

where H' is given by (6.2), $\mathcal{L}_x\hat{\rho} \equiv 2\hat{x}\hat{\rho}\hat{x}^\dagger - \hat{x}^\dagger\hat{x}\hat{\rho} - \hat{\rho}\hat{x}^\dagger\hat{x}$, and $\mathcal{L}_{x^\dagger}\hat{\rho} \equiv 2\hat{x}^\dagger\hat{\rho}\hat{x} - \hat{x}\hat{x}^\dagger\hat{\rho} - \hat{\rho}\hat{x}\hat{x}^\dagger$. For the sake of simplicity, we have assumed that the two end oscillators are coupled to their local zero temperature baths with equal strength γ and the middle oscillator is coupled with strength Γ to a bath with average thermal occupancy $\bar{n}$.

One way to solve the master equation (6.4) is to rewrite it in terms of a partial differential equation for the quantum characteristic function [79]. For the case of three coupled harmonic oscillators, we define a normal ordered characteristic function $\chi(\epsilon, \eta, w) = \langle e^{\epsilon\hat{r}^\dagger} e^{-\epsilon^*\hat{r}} e^{\eta\hat{c}^\dagger} e^{-\eta^*\hat{c}} e^{w\hat{s}^\dagger} e^{-w^*\hat{s}} \rangle$, where $\hat{r} = (\hat{a} + \hat{b})/\sqrt{2}$ and $\hat{s} = (\hat{a} - \hat{b})/\sqrt{2}$. We note that mode $\hat{s}^\dagger$ remains decoupled from the evolution, i.e. $[H', \hat{s}^\dagger] = 0$. This is not surprising since $\hat{s}^\dagger$ is the generator of dark states of the two oscillators [40, 80, 81]. Dark states are examples of decoherence free subspaces and have been used extensively in the context of quantum correlations which are subject to decoherence [40, 80, 81].

For the sake of simplicity we will analyse the case where $\gamma = 0$, which is reasonable since passive coupling of the two end oscillators to their independent baths is not expected to induce entanglement between them. However, what might lead to some more interesting features between coupled harmonic oscillators is instead a nonzero Γ. Moreover studying this special case gives us a recipe to generate a mixture of entangled states. The partial differential equation for $\chi(\epsilon, \eta, w, t)$ is then given by

$$\frac{\partial}{\partial t}\chi(\epsilon, \eta, w, t) = v^T J \nabla \chi(\epsilon, \eta, w, t) - v^T K v \chi(\epsilon, \eta, w, t), \tag{6.5}$$

where $v^T = (\eta, \eta^*, \epsilon, \epsilon^*)$, $\nabla = (\frac{\partial}{\partial\eta}, \frac{\partial}{\partial\eta^*}, \frac{\partial}{\partial\epsilon}, \frac{\partial}{\partial\epsilon^*})^T$ and

$$K = \begin{pmatrix} \mathbf{0} & \mathbf{0} \\ \mathbf{0} & b\mathbf{X} \end{pmatrix}, J = \begin{pmatrix} \mathbf{0} & i\mathbf{Z} \\ i\mathbf{Z} & -a\mathbf{I} \end{pmatrix}. \tag{6.6}$$

Here $\mathbf{X}$ and $\mathbf{Z}$ are the 2×2 Pauli matrices, $\mathbf{0}$ the 2×2 null matrix, $a = \Gamma/(2\sqrt{2}\kappa)$ and $b = \bar{n}\Gamma/(2\sqrt{2}\kappa)$.

To solve the partial differential equation (6.5) for an initial Gaussian state of each

coupled oscillator, we make an ansatz of the form $\chi(\epsilon,\eta,w) = f(w)e^{-v^T Av}$ where A is a 4×4 time-dependent symmetric matrix. Using this ansatz it easily follows that

$$\frac{\partial}{\partial t}\chi(\epsilon,\eta,w,t) = -v^T\frac{d\mathbf{A}}{dt}v\chi(\epsilon,\eta,w,t) \tag{6.7}$$

and

$$\nabla\chi(\epsilon,\eta,w,t) = -2\mathbf{A}z\chi(\epsilon,\eta,w,t). \tag{6.8}$$

Thus (6.5) takes the form

$$v^T\frac{d\mathbf{A}}{dt}v = 2v^T\mathbf{J}\mathbf{A}v + v^T\mathbf{K}v. \tag{6.9}$$

Since $\mathbf{A}$ is a symmetric matrix (6.9) reduces to

$$\frac{d\mathbf{A}}{dt} = \mathbf{J}\mathbf{A} + \mathbf{A}\mathbf{J} + \mathbf{K}. \tag{6.10}$$

We can write $\mathbf{A}$ in terms of 2×2 square matrices $\mathbf{P},\mathbf{Q}$ and $\mathbf{R}$ such that

$$\mathbf{A} \;=\; \begin{pmatrix} \mathbf{P} & \mathbf{R} \\ \mathbf{R}^T & \mathbf{Q} \end{pmatrix}. \tag{6.11}$$

The evaluation of the characteristic function now reduces to solving the following coupled matrix differential equations

$$\begin{aligned} \dot{\mathbf{P}} &= i(\mathbf{R}\mathbf{Z} + \mathbf{Z}\mathbf{R}^T), \\ \dot{\mathbf{R}} &= i(\mathbf{P}\mathbf{Z} + \mathbf{Z}\mathbf{Q}) - a\mathbf{R}, \\ \dot{\mathbf{Q}} &= i(\mathbf{Z}\mathbf{R} + \mathbf{R}^T\mathbf{Z}) - 2a\mathbf{Q} + b\mathbf{X}. \end{aligned} \tag{6.12}$$

Although an exact analytical solution for the above coupled matrix differential equations can be obtained, it is rather lengthy and not very illuminating. However, the solution is greatly simplified if one considers the steady state solution only. For the

equilibrium state $\dot{\mathbf{P}}$, $\dot{\mathbf{R}}$ and $\dot{\mathbf{Q}}$ must vanish. It then easily follows that

$$\begin{aligned} \mathbf{P} &= \frac{b}{2a}\mathbf{X} \\ \mathbf{Q} &= \frac{b}{2a}\mathbf{X} \\ \mathbf{R} &= \mathbf{0}. \end{aligned} \tag{6.13}$$

In the steady state the quantum characteristic function takes the form

$$\chi(\epsilon, \eta, w) = f(w) e^{-\bar{n}(|\epsilon|^2 + |\eta|^2)}, \tag{6.14}$$

where $f(w)$ is determined by the particular initial state of the coupled harmonic oscillators.

In particular, if the end oscillators are prepared in thermal states with mean phonon occupancy $\bar{n}'$ and the mediating oscillator is prepared in its ground state, then the corresponding quantum characteristic function is

$$\begin{aligned} \chi(\epsilon, \eta, w) &= \mathrm{Tr}(e^{\epsilon \hat{r}^\dagger} e^{-\epsilon^* \hat{r}} e^{\eta \hat{c}^\dagger} e^{-\eta^* \hat{c}} e^{w \hat{s}^\dagger} e^{-w^* \hat{s}} \sum_{n,m=0}^{\infty} P(n) P(m) |n\rangle\langle n|_a |m\rangle\langle m|_b \otimes |0\rangle\langle 0|_c) \\ &= \mathrm{Tr}(\sum_{n=0}^{\infty} P(n) |n\rangle\langle n|_a e^{\epsilon_a \hat{a}^\dagger} e^{-\epsilon_a^* \hat{a}}) \otimes \mathrm{Tr}(\sum_{m=0}^{\infty} P(m) |m\rangle\langle m|_b e^{\epsilon_b \hat{b}^\dagger} e^{-\epsilon_b^* \hat{b}}) \otimes \\ &\quad \mathrm{Tr}(|0\rangle\langle 0|_c e^{\eta \hat{c}^\dagger} e^{-\eta^* \hat{c}}) \chi(\epsilon, \eta, w) \\ &= e^{-\bar{n}'(|\epsilon|^2 + |w|^2)}, \end{aligned}$$

where $P(n) = \bar{n}'^n/(\bar{n}'+1)^{n+1}$ and $P(m) = \bar{n}'^m/(\bar{n}'+1)^{m+1}$. As noted above, the $\hat{s}$ mode remains decoupled from the dissipative evolution of the three oscillators and thus $f(w)$ will maintain its initial value. The steady state for an initial thermal state therefore takes the form

$$\chi(\epsilon, \eta, w, t \to \infty) = e^{-\bar{n}'(|w|^2)} e^{-\bar{n}(|\epsilon|^2 + |\eta|^2)}. \tag{6.15}$$

For the case of three coupled harmonic oscillators, a dark state is a state for which

excitations are shared only between the two end oscillators. When $\gamma = 0$, this state is immune to dissipation in the middle oscillator and thus called a dark state. For instance, in a subspace with n excitations, the dark state of the two end oscillators with modes a and b is of the form

$$|\Psi_{\rm dark}\rangle = \frac{(\hat{s}^\dagger)^n}{\sqrt{n!}}|0\rangle_a|0\rangle_b|0\rangle_c. \tag{6.16}$$

In the limit $\bar{n} \to 0$, the steady state (6.15) corresponds to a thermal mixture of dark states. This can be seen by noting that a thermal mixture of dark states can be written as

$$\hat{\tilde{\rho}} = \sum_{n=0}^{\infty} \frac{\bar{n'}^n}{(\bar{n'}+1)^{n+1}}|\Psi_{\rm dark}\rangle\langle\Psi_{\rm dark}| \otimes |0_c\rangle\langle 0_c|, \tag{6.17}$$

where $|\Psi_{\rm dark}\rangle$ is given by (6.16). The individual dark states are the entangled states of the two oscillators a and b and exist in subspaces with different excitations. For a thermal mixture of dark states the quantum characteristic function takes the form

$$\chi(\epsilon,\eta,w) = \sum_{n=0}^{\infty} \frac{\bar{n'}^n}{(\bar{n'}+1)^{n+1}}\frac{1}{n!}e^{(|\epsilon|^2+|\eta|^2+|w|^2)}\langle 0_a|\langle 0_b|\langle 0_c|(\hat{s})^n\tilde{\zeta}(\epsilon,\eta,w)(\hat{s}^\dagger)^n|0_a\rangle|0_b\rangle|0_c\rangle, \tag{6.18}$$

where $\tilde{\zeta}(\epsilon,\eta,w) = e^{-\epsilon^*\hat{r}}e^{\epsilon\hat{r}^\dagger}e^{-\eta^*\hat{c}}e^{\eta\hat{c}^\dagger}e^{-w^*\hat{s}}e^{w\hat{s}^\dagger}$. Making use of the fact that $\hat{s}(\hat{s}^\dagger)$ commutes with the operators $\hat{r}^\dagger(\hat{r})$ and $\hat{c}^\dagger(\hat{c})$, equation (6.18) can be rewritten as

$$\begin{aligned}\chi(\epsilon,\eta,w) &= \sum_{p=0}^{\infty} \frac{\bar{n}'^p}{(\bar{n}'+1)^{p+1}}\frac{1}{p!}(-\frac{\partial}{\partial w^*})^p(\frac{\partial}{\partial w})^p\langle 0_a|\langle 0_b|\langle 0_c|e^{-\epsilon^*\hat{r}}e^{\epsilon\hat{r}^\dagger}e^{-\eta^*\hat{c}}e^{\eta\hat{c}^\dagger}e^{-w^*\hat{s}}e^{w\hat{s}^\dagger} \\ &\quad |0_a\rangle|0_b\rangle|0_c\rangle e^{(|\epsilon|^2+|\eta|^2+|w|^2)}.\end{aligned} \tag{6.19}$$

Using the relation $\langle 0_c|e^{-\eta\hat{c}}e^{\eta\hat{c}^\dagger}|0_c\rangle = e^{-|\eta|^2}$, equation (6.19) simplifies to

$$\chi(\epsilon,\eta,w) = \sum_{n=0}^{\infty} \frac{\bar{n'}^n}{(\bar{n'}+1)^{n+1}}\frac{1}{n!}(-\frac{\partial}{\partial w^*})^n(\frac{\partial}{\partial w})^n\langle 0_a|\langle 0_b|e^{-\epsilon^*\hat{r}}e^{\epsilon\hat{r}^\dagger}e^{-w^*\hat{s}}e^{w\hat{s}^\dagger}|0_a\rangle|0_b\rangle e^{(|\epsilon|^2+|w|^2)}.$$

After some manipulations, the above equation can be further simplified to

$$\chi(\epsilon,\eta,w) = \sum_{n=0}^{\infty} \frac{\bar{n'}^n}{(\bar{n'}+1)^{n+1}}L_n(|w|^2), \tag{6.20}$$

where $L_n(|w|^2)$ is the Laguerre polynomial of order n. By making use of the identity $e^{xz/(z-1)}=(1-z)\sum_{n=0}^{\infty} z^n L_n(x)$ the characteristic function (6.20) takes the compact form

$$\chi(\epsilon,\eta,w) = e^{-\bar{n'}|w|^2}. \tag{6.21}$$

Thus it follows that if $\bar{n} \to 0$ then equation (6.15) reduces to equation (6.21). Hence we conclude that the steady state of two indirectly coupled harmonic oscillators, initially prepared in thermal states and evolving under (6.4) (with $\gamma = 0$), generates a thermal mixture of dark states. Each dark state is an individually entangled state of the two oscillators existing in subspaces with different excitations.

To check if any non-classical correlations are present in the steady state (6.21), we will compute the Glauber-Sudarshan P representation or the P-function [124]. Any two-mode state represented by a density operator $\hat{\rho}$ can be written in terms of a two-mode P function $P(\alpha,\beta)$ as $\hat{\rho} = \int d^2\alpha d^2\beta P(\alpha,\beta)|\alpha\rangle\langle\alpha| \otimes |\beta\rangle\langle\beta|$. For a classical state, the P function is positive. If $P(\alpha,\beta)$ is not a probability distribution, the state ceases to be classical and a quantum description is required. Negativity of the P function is a signature of non-classical correlations in the system [141]. For the state described by the quantum characteristic function (6.21), the following two-mode P function representation exists

$$P(\alpha,\beta) = \frac{2}{\pi\bar{n}'}\delta(\alpha_i+\beta_i)\delta(\alpha_r+\beta_r)e^{-\frac{2}{\bar{n}'}|\beta|^2}, \tag{6.22}$$

where $\alpha_r(\beta_r)$ and $\alpha_i(\beta_i)$ are the real and imaginary parts of $\alpha(\beta)$ respectively. The non-negativity of $P(\alpha,\beta)$ implies that the state described by (6.21) is classical. It exemplifies that a mixture of individually entangled states is not always necessarily entangled, which is somewhat counter-intuitive, since the individually entangled states in the mixture all live in mutually orthogonal parts of the Hilbert space. On the other hand, the result is analogous to the fact that even though a number state is nonclassical, a mixture of number states need not be non-classical (it can e.g. be a coherent state or a thermal state). However, we have found that a finite mixture of

dark states does exhibit non-classical features.

Through a similar calculation we have confirmed that if the RWA is made and the two end oscillators are initially prepared in coherent states, then the steady state is classical. To characterise entanglement in a two-mode Gaussian continuous variable state, there exists a necessary and sufficient criteria for inseparability [142]. A two-mode Gaussian continuous variable state is completely described by the first and second order moments only, and is inseparable iff

$$d = \begin{vmatrix} 1 & \langle\hat{a}\rangle & \langle\hat{a}^\dagger\rangle & \langle\hat{b}^\dagger\rangle & \langle\hat{b}\rangle \\ \langle\hat{a}^\dagger\rangle & \langle\hat{a}^\dagger\hat{a}\rangle & \langle\hat{a}^{\dagger 2}\rangle & \langle\hat{a}^\dagger\hat{b}^\dagger\rangle & \langle\hat{a}^\dagger\hat{b}\rangle \\ \langle\hat{a}\rangle & \langle\hat{a}^2\rangle & \langle\hat{a}\hat{a}^\dagger\rangle & \langle\hat{a}\hat{b}^\dagger\rangle & \langle\hat{a}\hat{b}\rangle \\ \langle\hat{b}\rangle & \langle\hat{a}\hat{b}\rangle & \langle\hat{a}^\dagger\hat{b}\rangle & \langle\hat{b}^\dagger\hat{b}\rangle & \langle\hat{b}^2\rangle \\ \langle\hat{b}^\dagger\rangle & \langle\hat{a}\hat{b}^\dagger\rangle & \langle\hat{a}^\dagger b^\dagger\rangle & \langle\hat{b}^{\dagger 2}\rangle & \langle\hat{b}\hat{b}^\dagger\rangle \end{vmatrix} < 0. \tag{6.23}$$

Through a numerical evaluation of the determinant (6.23), we have verified that the time-evolved state of passively coupled harmonic oscillators initially prepared in two-mode classical Gaussian states, *always* remain separable.

To get a more physical insight we note that in the interaction picture of Hamiltonian (6.2), the density matrix describing the state of three coupled bosonic modes evolves as

$$\frac{d}{dt}\hat{\rho}_I = \sum_{x=a,b} \gamma\mathcal{L}_{x(t)}\hat{\rho}_I + \Gamma(\bar{n}+1)\mathcal{L}_{c(t)}\hat{\rho}_I + \Gamma\bar{n}\mathcal{L}_{c^\dagger(t)}\hat{\rho}_I, \tag{6.24}$$

where $\mathcal{L}_{x(t)}\hat{\rho}_I = e^{-iH't}\mathcal{L}_x\hat{\rho}e^{iH't}$, $x \in (a,b,c)$ and $\mathcal{L}_{c^\dagger(t)}\hat{\rho}_I = e^{-iH't}\mathcal{L}_{c^\dagger}\hat{\rho}e^{iH't}$. Using the solution for the time dependent operators $\hat{a}(t)$, $\hat{b}(t)$ and $\hat{c}(t)$ obtained from (6.3), it follows that

$$[\hat{a}_I(t), \hat{b}_I(t), \hat{c}_I(t)]^T = \mathbf{G}\cdot[\hat{a}(0), \hat{b}(0), \hat{c}(0)]^T, \tag{6.25}$$

where G is a 3×3 time dependent complex matrix. It is easy to verify that the Lindblad operators in the master equation (6.24) can only have one creation and one

destruction operator of the bosonic modes a, b and c. In other words, even under dissipation, linearity of the interaction Hamiltonian (6.2) is preserved and no squeezing is generated between the coupled harmonic oscillators. This verifies our previous assertion that solely under the action of passive linear interactions, harmonic oscillators initially prepared in classical Gaussian states, will always remain separable. In the next section we shall begin with investigating the dynamics of an open chain of three coupled oscillators, when the interactions between the oscillators are modelled beyond the RWA.

6.2.2 Indirectly coupled harmonic oscillators interacting without the rotating wave approximation

In the previous section we modelled the interaction between the oscillators using the RWA. If the coupling strength κ is of the order of ω, then the RWA breaks down and one has to consider the full Hamiltonian (6.1). In this section we will show a detailed calculation of the dynamics governed by the master equation (6.4) with H' now given by (6.1).

As before, we define a normal ordered quantum characteristic function $\chi(u, v, w, t)$ $=\langle e^{u\hat{a}^\dagger} e^{-u^*\hat{a}} e^{v\hat{b}^\dagger} e^{-v^*\hat{b}} e^{w\hat{c}^\dagger} e^{-w^*\hat{c}} \rangle$, describing the state of the three coupled harmonic oscillators. The master equation (6.4) can consequently be converted into a partial differential equation for $\chi(u, v, w, t)$. For an initial Gaussian ansatz $\chi(u, v, w, t) =$ $\exp[-z^T \mathbf{A}(t)\, z + i$
$z^T h(t)]$, where $z^T = (x_1, x_2, w_2, w_1)$ with $x_1 = (u + u^* + v + v^*)/4$, $x_2 = (u - u^* + v - v^*)/4i$ and $w = w_1 + iw_2$, the corresponding partial differential equation for $\chi(u, v, w, t)$ becomes

$$(\frac{\partial}{\partial t} + 2\kappa z^T \mathbf{N} z)\chi(u, v, w, t) = z^T \mathbf{M} \nabla \chi(u, v, w, t), \tag{6.26}$$

where $\nabla = (\frac{\partial}{\partial x_1}, \frac{\partial}{\partial x_2}, \frac{\partial}{\partial w_2}, \frac{\partial}{\partial w_1})^T$ and

$$\mathbf{N} = \begin{pmatrix} \mathbf{0} & \mathbf{I} \\ \mathbf{I} & \bar{n}\Gamma/\kappa\mathbf{I} \end{pmatrix}, \quad \mathbf{M} = \begin{pmatrix} -\gamma\mathbf{I} + \omega\mathbf{S} & \mathbf{U} \\ \mathbf{V} & -\Gamma\mathbf{I} - \omega\mathbf{S} \end{pmatrix}. \tag{6.27}$$

Here $\mathbf{0}$ is the 2×2 null matrix, $\mathbf{I}$ is the 2×2 identity matrix, and

$$\mathbf{S} = \begin{pmatrix} 0 & 1 \\ -1 & 0 \end{pmatrix}, \quad \mathbf{U} = \begin{pmatrix} 4\kappa & 0 \\ 0 & 0 \end{pmatrix}, \quad \mathbf{V} = \begin{pmatrix} 0 & 0 \\ 0 & 2\kappa \end{pmatrix}. \tag{6.28}$$

Using the Gaussian ansatz for the quantum characteristic function $\chi(u, v, w, t)$, it easily follows that

$$\frac{\partial \chi}{\partial t} = -z^{\mathrm{T}} \frac{d\mathbf{A}}{dt} z\chi + iz^{\mathrm{T}} \frac{dh}{dt}\chi \tag{6.29}$$

$$\nabla\chi = -2\mathbf{A}z\chi + ih\chi. \tag{6.30}$$

Using the above two equations, the partial differential equation (6.26) for χ becomes

$$-z^{\mathrm{T}} \frac{d\mathbf{A}}{dt} z + iz^{\mathrm{T}} \frac{dh}{dt}\chi + 2\kappa z^{\mathrm{T}}\mathbf{N}z\chi = -2z^{\mathrm{T}}\mathbf{M}\mathbf{A}z\chi + iz^{\mathrm{T}}\mathbf{M}h\chi. \tag{6.31}$$

Recalling that $\mathbf{A}(t)$ is a symmetric matrix, we can write

$$\mathbf{A}(t) = \begin{pmatrix} \mathbf{P}(t) & \mathbf{Q}(t) \\ \mathbf{Q}(t)^T & \mathbf{R}(t) \end{pmatrix}, \tag{6.32}$$

where $\mathbf{P}(t)$ and $\mathbf{R}(t)$ are 2×2 symmetric matrices. Then taking the symmetric part of equation (6.31) one gets

$$-\frac{d\mathbf{A}(t)}{dt} + 2\kappa\mathbf{N} = -\mathbf{M}\mathbf{A} - \mathbf{A}\mathbf{M}^{\mathrm{T}} \tag{6.33}$$

$$\frac{dh}{dt} = \mathbf{M}h. \tag{6.34}$$

Using the above form of $\mathbf{A}(t)$, equation (6.33) reduces to the three coupled matrix

differential equations

$$\begin{aligned}\dot{\mathbf{P}} &= \omega(\mathbf{SP}-\mathbf{PS})-2\gamma\mathbf{P}+\mathbf{UQ}^T+\mathbf{QU} \\ \dot{\mathbf{R}} &= \omega(\mathbf{RS}-\mathbf{SR})-2\Gamma\mathbf{R}+\mathbf{VQ}+\mathbf{Q}^T\mathbf{V}+2\bar{n}\Gamma\mathbf{I} \\ \dot{\mathbf{Q}} &= \omega(\mathbf{SQ}+\mathbf{QS})-(\Gamma+\gamma)\mathbf{Q}+\mathbf{PV}+\mathbf{UR}+2\kappa\mathbf{I}.\end{aligned} \tag{6.35}$$

The above set of equations can be numerically solved for the time dependent matrices $\mathbf{P}(t)$, $\mathbf{R}(t)$ and $\mathbf{Q}(t)$, which together with the solution $h(t)=\exp(\mathbf{M}t)h(0)$ allows us to obtain the two-mode quantum characteristic function $\chi(u,v,w,t)$.

6.2.3 Directly coupled harmonic oscillators

We consider two coupled harmonic oscillators with modes labelled a and b and interacting bilinearly with a position-dependent coupling. The unitary evolution of the oscillators is then described by the Hamiltonian

$$H=\omega(\hat{a}^\dagger\hat{a}+\hat{b}^\dagger\hat{b})+\kappa(\hat{a}+\hat{a}^\dagger)(\hat{b}+\hat{b}^\dagger), \tag{6.36}$$

where ω is the identical resonance frequency of each oscillator and κ is the coupling strength between the two oscillators. We can generalise the Hamiltonian (6.36) as

$$H_{\text{sys}}=\omega(\hat{a}^\dagger\hat{a}+\hat{b}^\dagger\hat{b})+\kappa(\hat{a}\hat{b}+\hat{b}^\dagger\hat{a}^\dagger)+\epsilon(\hat{a}^\dagger\hat{b}+\hat{b}^\dagger\hat{a}), \tag{6.37}$$

and as can be seen when $\kappa=\epsilon$, equation (6.37) reduces to (6.36).

If the two coupled oscillators interact with an environment which itself can be described by a Gaussian state, then even under the resulting dissipative evolution, the two coupled oscillators maintain their initial Gaussian character.

Assume that the time evolution of the system in the Born-Markov approximation is

described by a Lindblad-type master equation of the form

$$\frac{\partial \rho}{\partial t} = -i[H_{\rm sys}, \rho] + \frac{1}{2}\sum_{j=a,b}[(\Gamma_j(\bar{n}_j+1)\mathcal{L}_j\rho + \Gamma_j\bar{n}_j\mathcal{L}_{j^\dagger}\rho)], \tag{6.38}$$

where Γ_j is the decay rates of the jth oscillator, coupled to a heat bath with average thermal occupancy $\bar{n}_j$.

One way to solve the master equation (6.38) is to rewrite it in terms of a partial differential equation for the two-mode quantum characteristic function. We define a normal ordered characteristic function as $\chi(\epsilon_a, \eta_b, t) = \langle e^{\epsilon_a \hat{a}^\dagger} e^{-\epsilon_a^* \hat{a}} e^{\eta_b \hat{b}^\dagger} e^{-\eta_b^* \hat{b}} \rangle$ and make a Gaussian ansatz for the time-evolved characteristic function, $\chi(\epsilon_a, \eta_b, t) = \exp\left[-y^T \mathbf{L}(t)\, y + i y^T h(t)\right]$. Here $\mathbf{L}(t)$ is a time dependent 4×4 symmetric matrix, $h(t)$ is a 4×1 time dependent vector and $y^T = (\epsilon_a, \epsilon_a^*, \eta_b, \eta_b^*)$. The corresponding partial differential equation for $\chi(\epsilon_a, \epsilon_a^*, \eta_b, \epsilon_b^*, t)$ then becomes [79]

$$\frac{\partial}{\partial t}\chi = z^T \mathbf{M} z \chi + z^T \mathbf{N} \nabla \chi, \tag{6.39}$$

where $\nabla = (\frac{\partial}{\partial \epsilon_a}, \frac{\partial}{\partial \epsilon_a^*}, \frac{\partial}{\partial \epsilon_b}, \frac{\partial}{\partial \epsilon_b^*})^T$ and

$$\mathbf{N} = \begin{pmatrix} i\omega - \Gamma_a & 0 & i\epsilon & -i\kappa \\ 0 & -i\omega - \Gamma_a & i\kappa & -i\epsilon \\ i\epsilon & -i\kappa & i\omega - \Gamma_b & 0 \\ i\kappa & -i\epsilon & 0 & -i\omega - \Gamma_b \end{pmatrix}, \tag{6.40}$$

$$\mathbf{M} = \begin{pmatrix} 0 & -\Gamma_a\bar{n}_a & i\kappa/2 & 0 \\ -\Gamma_a\bar{n}_a & 0 & 0 & -i\kappa/2 \\ i\kappa/2 & 0 & 0 & -\Gamma_b\bar{n}_b \\ 0 & -i\kappa/2 & -\Gamma_b\bar{n}_b & 0 \end{pmatrix}. \tag{6.41}$$

From the Gaussian ansatz for the quantum characteristic function $\chi(u, v, w, t)$, it

follows that

$$\frac{\partial \chi}{\partial t} = -z^{\mathrm{T}} \frac{d\mathbf{L}}{dt} z\chi + iz^{\mathrm{T}} \frac{dh}{dt}\chi \tag{6.42}$$

$$\nabla\chi = -2\mathbf{L}z\chi + ih\chi. \tag{6.43}$$

Using the above relations, the partial differential equation (6.39) for χ becomes

$$-z^{\mathrm{T}} \frac{d\mathbf{L}}{dt} z + iz^{\mathrm{T}} \frac{dh}{dt}\chi = z^{\mathrm{T}}\mathbf{M}z\chi - 2z^{\mathrm{T}}\mathbf{N}\mathbf{L}z\chi + iz^{\mathrm{T}}\mathbf{N}h\chi. \tag{6.44}$$

Recalling that $\mathbf{L}(t)$ is symmetric, we can write

$$\mathbf{L}(t) = \begin{pmatrix} \mathbf{P}(t) & \mathbf{Q}(t) \\ \mathbf{Q}(t)^T & \mathbf{R}(t) \end{pmatrix} \tag{6.45}$$

where $\mathbf{P}(t)$ and $\mathbf{R}(t)$ are 2×2 symmetric matrices. Taking the symmetric part of (6.44) results in two matrix differential equations

$$\frac{d\mathbf{L}(t)}{dt} + \mathbf{M} = \mathbf{N}\mathbf{L} + \mathbf{L}\mathbf{N}^{\mathrm{T}} \tag{6.46}$$

$$\frac{dh}{dt} = \mathbf{N}h. \tag{6.47}$$

Thus solving the master equation (6.38) reduces to solving the above coupled matrix differential equations. Before providing details of the results obtained by the numerical solution of above coupled matrix differential equations, in the next section we shall derive a master equation describing the dynamics of two strongly coupled harmonic oscillators where their individual environments are modelled as collections of harmonic oscillators.

6.3 Bath induced dissipation

A master equation of standard Lindblad form guarantees the positivity of the time-evolved density matrix. It may seem justified to simply add local Lindblad terms

acting on the individual coupled oscillators a and b, as was done in the previous section, but as we will show next, this is fraught with pitfalls. In what follows we shall derive a Markovian master equation for two strongly coupled harmonic oscillators which are harmonically coupled to their local heat baths.The result is a master equation of Lindblad form, but the Lindblad superoperators $\mathcal{L}$ do not act locally on each individual oscillator.

The oscillators are as before labelled a and b and their coupled dynamics is governed by the Hamiltonian (6.37). We consider a scenario where the two oscillators are irreversibly coupled to local heat baths, each of which is modelled as a collection of many harmonic oscillators. The Hamiltonian corresponding to the two independent local heat baths is given by

$$H_{\text{env}} = \sum_{\Omega} \Omega \hat{c}_{\Omega}^{\dagger} \hat{c}_{\Omega} + \sum_{\Omega'} \Omega' \hat{d}_{\Omega'}^{\dagger} \hat{d}_{\Omega'}, \tag{6.48}$$

where $\hat{c}_{\Omega}$ and $\hat{d}_{\Omega'}$ represent the destruction operators for the bosonic modes of the local heat baths for oscillators a and b, respectively. Assuming a bilinear coupling between the position quadratures of each oscillator and the modes of their local heat baths, the system-environment interaction takes the form

$$H_{\text{int}} = \sum_{\Omega} \zeta_{\Omega} (\hat{c}_{\Omega}^{\dagger} + \hat{c}_{\Omega})(\hat{a} + \hat{a}^{\dagger}) + \sum_{\Omega'} \eta_{\Omega'} (\hat{d}_{\Omega'}^{\dagger} + \hat{d}_{\Omega'})(\hat{b} + \hat{b}^{\dagger}), \tag{6.49}$$

where ζ_{Ω} and $\eta_{\Omega'}$ are the coupling strengths between each individual oscillator and the corresponding environment [**143**]. The two coupled oscillators undergo unitary evolution described by the Hamiltonian

$$H = H_{\text{sys}} + H_{\text{env}} + H_{\text{int}}. \tag{6.50}$$

Using the Hamiltonian (6.50), a master equation describing the dissipative evolution of the two coupled oscillators will now be derived.

6.3.1 Derivation of the coupled oscillator master equation

In order to derive a master equation for the two coupled harmonic oscillators we shall first diagonalise the Hamiltonian (6.37) by defining the centre of mass and relative modes,

$$\hat{e} = \frac{\hat{a}+\hat{b}}{\sqrt{2}} \tag{6.51}$$

$$\hat{f} = \frac{\hat{a}-\hat{b}}{\sqrt{2}}. \tag{6.52}$$

The Hamiltonian (6.37) now takes the form

$$H_{\rm sys} = \omega(\hat{e}^\dagger\hat{e} + \hat{f}^\dagger\hat{f}) + \frac{\kappa}{2}(\hat{e}^2 + \hat{e}^{\dagger 2} - \hat{f}^2 - \hat{f}^{\dagger 2}) + \frac{\epsilon}{2}(\hat{e}\hat{e}^\dagger + \hat{e}^\dagger\hat{e} - \hat{f}\hat{f}^\dagger - \hat{f}^\dagger\hat{f}) \tag{6.53}$$

which can be diagonalised using a Bogoliubov transformation

$$\begin{pmatrix} \hat{e} \\ \hat{e}^\dagger \end{pmatrix} = \begin{pmatrix} \alpha_1 & -\beta_1 \\ -\beta_1 & \alpha_1 \end{pmatrix} \begin{pmatrix} \hat{l} \\ \hat{l}^\dagger \end{pmatrix}, \tag{6.54}$$

$$\begin{pmatrix} \hat{f} \\ \hat{f}^\dagger \end{pmatrix} = \begin{pmatrix} \alpha_2 & -\beta_2 \\ -\beta_2 & \alpha_2 \end{pmatrix} \begin{pmatrix} \hat{m} \\ \hat{m}^\dagger \end{pmatrix}. \tag{6.55}$$

The Hamiltonian (6.53) then takes the simplified form

$$H_{\rm sys} = (\alpha_{11} + \alpha_{22})\hat{l}^\dagger\hat{l} + (\beta_{11} + \beta_{22})\hat{m}^\dagger\hat{m}, \tag{6.56}$$

with

$$\alpha_{11} = \frac{(2\omega+\epsilon)\alpha_1^2 - 2\kappa\alpha_1\beta_1 + \epsilon\beta_1^2}{2} \tag{6.57}$$

$$\alpha_{22} = \frac{(2\omega+\epsilon)\beta_1^2 - 2\kappa\alpha_1\beta_1 + \epsilon\alpha_1^2}{2} \tag{6.58}$$

$$\beta_{11} = \frac{(2\omega-\epsilon)\alpha_2^2 + 2\kappa\alpha_2\beta_2 - \epsilon\beta_2^2}{2} \tag{6.59}$$

$$\beta_{22} = \frac{(2\omega-\epsilon)\beta_2^2 + 2\kappa\alpha_2\beta_2 - \epsilon\alpha_2^2}{2}, \tag{6.60}$$

where α_i and β_i are of the form

$$\alpha_1^2 = \frac{1}{2} + \frac{1}{2}\frac{\epsilon+\omega}{\sqrt{(\epsilon+\omega)^2-\kappa^2}} \tag{6.61}$$

$$\beta_1^2 = -\frac{1}{2} + \frac{1}{2}\frac{\epsilon+\omega}{\sqrt{(\epsilon+\omega)^2-\kappa^2}} \tag{6.62}$$

$$\alpha_2^2 = \frac{1}{2} + \frac{1}{2}\frac{-\epsilon+\omega}{\sqrt{(-\epsilon+\omega)^2-\kappa^2}} \tag{6.63}$$

$$\beta_2^2 = -\frac{1}{2} + \frac{1}{2}\frac{-\epsilon+\omega}{\sqrt{(-\epsilon+\omega)^2-\kappa^2}}. \tag{6.64}$$

Thus the free evolution of the two coupled oscillators and their local environments is given by

$$\begin{aligned} H_{\rm sys} + H_{\rm env} &= (\alpha_{11}+\alpha_{22})\hat{l}^\dagger\hat{l} + (\beta_{11}+\beta_{22})\hat{m}^\dagger\hat{m} \\ &\quad + \sum_\Omega \Omega\hat{c}_\Omega^\dagger\hat{c}_\Omega + \sum_{\Omega'}\Omega'\hat{d}_{\Omega'}^\dagger\hat{d}_\Omega. \end{aligned} \tag{6.65}$$

Re-expressing the bare modes a and b in terms of $\hat{l}$ and $\hat{m}$, the Hamiltonian (6.50) in the interaction picture with $H_0 = H_{\rm sys} + H_{\rm env}$ becomes

$$\begin{aligned} H_I(t) = \sum_{\Omega,\Omega'}[&\zeta_\Omega(\hat{c}_I + \hat{c}_I^\dagger)(\alpha_1\hat{l}_I - \beta_1\hat{l}_I^\dagger + \alpha_1\hat{l}_I^\dagger - \beta_1\hat{l}_I + \alpha_2\hat{m}_I - \beta_2\hat{m}_I^\dagger + \alpha_2\hat{m}_I^\dagger - \beta_2\hat{m}_I) \\ &+\eta_{\Omega'}(\hat{d}_I + \hat{d}_I^\dagger)(\alpha_1\hat{l}_I - \beta_1\hat{l}_I^\dagger + \alpha_1\hat{l}_I^\dagger - \beta_1\hat{l}_I - \alpha_2\hat{m}_I + \beta_2\hat{m}_I^\dagger - \alpha_2\hat{m}_I^\dagger + \beta_2\hat{m}_I)], \end{aligned} \tag{6.66}$$

where $H_I(t) = e^{-iH_0t}H_{\rm int}e^{iH_0t}$, $\hat{l}_I{=}\hat{l}\ e^{-i(\alpha_{11}+\alpha_{22})t}$, $\hat{m}_I = \hat{m}\ e^{-i(\beta_{11}+\beta_{22})t}$, $\hat{c}_I = \hat{c}\ e^{-i\Omega t}$, $\hat{d}_I = \hat{d}\ e^{-i\Omega t}$ and a factor of $1/\sqrt{2}$ has been absorbed into the definition of g_Ω and $\eta_{\Omega'}$.

If the system-reservoir coupling is weak we can simplify the interaction Hamiltonian (6.66) using the rotating wave approximation (RWA). Invoking the RWA essentially amounts to dropping the fast oscillating terms proportional to $\hat{c}_I\hat{l}_I, \hat{c}_I\hat{m}_I, \hat{d}_I\hat{l}_I, \hat{d}_I\hat{m}_I$ and their Hermitian conjugates from the Hamiltonian (6.66), which results in

$$H_I(t) = \hat{l}_I\hat{F}^\dagger(t) + \hat{m}_I\hat{Q}^\dagger(t) + h.c., \tag{6.67}$$

where the noise operators are given by

$$\hat{F}^\dagger(t) = \sum_{\Omega,\Omega'}(\alpha_1 - \beta_1)(\zeta_\Omega\hat{c}^\dagger_\Omega e^{i\Omega t} + \eta_{\Omega'}\hat{d}^\dagger_{\Omega'}e^{i\Omega' t}), \tag{6.68}$$

$$\hat{Q}^\dagger(t) = \sum_{\Omega,\Omega'}(\alpha_2 - \beta_2)(\zeta_\Omega\hat{c}^\dagger_\Omega e^{i\Omega t} - \eta_{\Omega'}\hat{d}^\dagger_{\Omega'}e^{i\Omega' t}). \tag{6.69}$$

Using the RWA and in the interaction picture with $H_0 = H_{\rm sys} + H_{\rm env}$, the total density matrix ρ_I representing the joint state of the two oscillators and their local environments, evolves according to

$$\dot{\rho}_I(t) = -i[H_I(t), \rho_I(t)], \tag{6.70}$$

where $H_I(t)$ is given by Eq. (6.67). We assume that at $t = 0$ the joint state of the system and environments is factorisable so that $\rho_I(t = 0) = \rho_{\rm e}(0) \otimes \rho_{\rm sys}(0)$ where $\rho_{\rm e}(0)$ is the joint initial state of the two local baths and $\rho_{\rm sys}(0)$ is the density matrix of the two coupled harmonic oscillators.

The evolution of the density matrix $\rho_{\rm sys}$ representing the state of the two oscillators is given by

$$\dot{\rho}_{\rm sys}(t) = {\rm Tr}_{\rm e}\dot{\rho}_I(t) = -i{\rm Tr}_{\rm e}[H_I(t), \rho_I(t)], \tag{6.71}$$

where ${\rm Tr}_{\rm e}$ denotes the trace over the environmental degrees of freedom. If we also assume that the state of the environment for each oscillator remains unaffected as a result of the coupling, then the joint state of the system evolves as $\rho_I(t) = \rho_{\rm e}(0) \otimes$

$\rho_{\rm sys}(t)$. Formally integrating (6.70) gives

$$\rho_I(t) = \rho_I(0) - i\int_0^t [H_I(t'), \rho_I(t')]dt', \tag{6.72}$$

which when substituted in (6.71) gives an integro-differential equation for the state of the oscillators,

$$\dot{\rho}_{\rm sys}(t) = -i{\rm Tr}_{\rm e}[H_I(t), \rho_I(0)] - \int_0^t {\rm Tr}_{\rm e}[H_I(t), [H_I(t'), \rho_I(t')]]dt'. \tag{6.73}$$

For an environment in thermal equilibrium the first term in (6.73) is identically zero. Using (6.67) the above integro-differential equation takes the form

$$\dot{\rho}_{\rm sys}(t) = -\int_0^t {\rm Tr}_{\rm e}\big[\tilde{\hat{l}}\hat{F}^\dagger + \tilde{\hat{m}}\hat{Q}^\dagger + h.c., [\tilde{\hat{l}}\hat{F}^\dagger + \tilde{\hat{m}}\hat{Q}^\dagger + h.c., \rho_{\rm e}(0)\otimes\rho_{\rm sys}(t')]\big]dt'. \tag{6.74}$$

Equation (6.74) can be rearranged as

$$\begin{aligned}\dot{\rho}_{\rm sys}(t) = -\int_0^t {\rm Tr}_{\rm e}[&H_I(t)H_I(t')\rho_{\rm e}(0)\otimes\rho_{\rm sys}(t') - H_I(t)\rho_{\rm e}(0)\otimes\rho_{\rm sys}(t')H_I(t') \\ &-H_I(t')\rho_{\rm e}(0)\otimes\rho_{\rm sys}(t')H_I(t) + \rho_{\rm e}(0)\otimes\rho_{\rm sys}(t')H_I(t')H_I(t)]dt'.\end{aligned}$$

For environments in thermal equilibrium with flat spectral densities such that $\zeta_\Omega = \zeta$ and $\eta_{\Omega'} = \eta$, together with the Markov approximation, one obtains

$$\sum_\Omega \zeta_\Omega^2 e^{i\Omega(t'-t)} = \zeta^2 2\pi\delta(t'-t), \tag{6.75}$$

$$\sum_\Omega \eta_{\Omega'}^2 e^{i\Omega'(t'-t)} = \eta^2 2\pi\delta(t'-t). \tag{6.76}$$

One can easily verify that in the case of symmetric coupling of each oscillator to its own environment at zero temperature such that $\pi\zeta^2 = \pi\eta^2 = \Gamma$, one obtains the following master equation in the Schrödinger picture,

$$\begin{aligned}\dot{\rho}(t) = &-i[(\alpha_{11}+\alpha_{22})\hat{l}^\dagger\hat{l} + (\beta_{11}+\beta_{22})\hat{m}^\dagger\hat{m}, \rho(t)] + \langle\hat{F}\hat{F}^\dagger\rangle[2\hat{l}\rho(t)\hat{l}^\dagger - \hat{l}^\dagger\hat{l}\rho(t) - \rho(t)\hat{l}^\dagger\hat{l}] \\ &+\langle\hat{Q}\hat{Q}^\dagger\rangle[2\hat{m}\rho(t)\hat{m}^\dagger - \hat{m}^\dagger\hat{m}\rho(t) - \rho(t)\hat{m}^\dagger\hat{m}],\end{aligned} \tag{6.77}$$

where $\rho(t) = e^{-iH_{\rm sys}t}\rho_{\rm sys}(t)e^{iH_{\rm sys}t}$ is the density matrix representing the state of the two coupled oscillators in the Schrödinger picture and the only non-zero two-time noise correlation functions are of the form

$$\langle \hat{F}\hat{F}^\dagger \rangle = 2\Gamma(\alpha_1 - \beta_1)^2 \tag{6.78}$$

$$\langle \hat{Q}\hat{Q}^\dagger \rangle = 2\Gamma(\alpha_2 - \beta_2)^2. \tag{6.79}$$

Reverting back to the bare modes a and b, the master equation (6.77) takes the form

$$\begin{aligned}
\dot{\rho}(t) = & -i[H_{\rm sys}, \rho(t)] \\
& +\Gamma_1[2\hat{a}\rho(t)\hat{a}^\dagger - \hat{a}^\dagger\hat{a}\rho(t) - \rho(t)\hat{a}^\dagger\hat{a}] \\
& +\Gamma_2[2\hat{a}^\dagger\rho(t)\hat{a} - \hat{a}\hat{a}^\dagger\rho(t) - \rho(t)\hat{a}\hat{a}^\dagger] \\
& +\Gamma_3[2\hat{a}\rho(t)\hat{a} - \hat{a}\hat{a}\rho(t) - \rho(t)\hat{a}\hat{a}] \\
& +\Gamma_3[2\hat{a}^\dagger\rho(t)\hat{a}^\dagger - \hat{a}^\dagger\hat{a}^\dagger\rho(t) - \rho(t)\hat{a}^\dagger\hat{a}^\dagger] \\
& +\Gamma_1[2\hat{b}\rho(t)\hat{b}^\dagger - \hat{b}^\dagger\hat{b}\rho(t) - \rho(t)\hat{b}^\dagger\hat{b}] \\
& +\Gamma_2[2\hat{b}^\dagger\rho(t)\hat{b} - \hat{b}\hat{b}^\dagger\rho(t) - \rho(t)\hat{b}\hat{b}^\dagger] \\
& +\Gamma_3[2\hat{b}\rho(t)\hat{b} - \hat{b}\hat{b}\rho(t) - \rho(t)\hat{b}\hat{b}] \\
& +\Gamma_3[2\hat{b}^\dagger\rho(t)\hat{b}^\dagger - \hat{b}^\dagger\hat{b}^\dagger\rho(t) - \rho(t)\hat{b}^\dagger\hat{b}^\dagger] \\
& +\Gamma_4[2\hat{a}\rho(t)\hat{b}^\dagger - \hat{b}^\dagger\hat{a}\rho(t) - \rho(t)\hat{b}^\dagger\hat{a}] \\
& +\Gamma_5[2\hat{a}^\dagger\rho(t)\hat{b} - \hat{b}\hat{a}^\dagger\rho(t) - \rho(t)\hat{b}\hat{a}^\dagger] \\
& +\Gamma_4[2\hat{b}\rho(t)\hat{a}^\dagger - \hat{a}^\dagger\hat{b}\rho(t) - \rho(t)\hat{a}^\dagger\hat{b}] \\
& +\Gamma_5[2\hat{b}^\dagger\rho(t)\hat{a} - \hat{a}\hat{b}^\dagger\rho(t) - \rho(t)\hat{a}\hat{b}^\dagger] \\
& +\Gamma_6[2\hat{b}\rho(t)\hat{a} - \hat{a}\hat{b}\rho(t) - \rho(t)\hat{a}\hat{b}] \\
& +\Gamma_6[2\hat{a}\rho(t)\hat{b} - \hat{a}\hat{b}\rho(t) - \rho(t)\hat{a}\hat{b}] \\
& +\Gamma_6[2\hat{b}^\dagger\rho(t)\hat{a}^\dagger - \hat{a}^\dagger\hat{b}^\dagger\rho(t) - \rho(t)\hat{a}^\dagger\hat{b}^\dagger] \\
& +\Gamma_6[2\hat{a}^\dagger\rho(t)\hat{b}^\dagger - \hat{b}^\dagger\hat{a}^\dagger\rho(t) - \rho(t)\hat{a}^\dagger\hat{b}^\dagger],
\end{aligned} \tag{6.80}$$

where the Γ_i are given by

$$\begin{aligned}
\Gamma_1 &= (\langle \hat{F}\hat{F}^\dagger \rangle \alpha_1^2 + \langle \hat{Q}\hat{Q}^\dagger \rangle \alpha_2^2)/2 \\
\Gamma_2 &= (\langle \hat{F}\hat{F}^\dagger \rangle \beta_1^2 + \langle \hat{Q}\hat{Q}^\dagger \rangle \beta_2^2)/2 \\
\Gamma_3 &= (\langle \hat{F}\hat{F}^\dagger \rangle \alpha_1\beta_1 + \langle \hat{Q}\hat{Q}^\dagger \rangle \alpha_2\beta_2)/2 \\
\Gamma_4 &= (\langle \hat{F}\hat{F}^\dagger \rangle \alpha_1^2 - \langle \hat{Q}\hat{Q}^\dagger \rangle \alpha_2^2)/2 \\
\Gamma_5 &= (\langle \hat{F}\hat{F}^\dagger \rangle \beta_1^2 - \langle \hat{Q}\hat{Q}^\dagger \rangle \beta_2^2)/2 \\
\Gamma_6 &= (\langle \hat{F}\hat{F}^\dagger \rangle \alpha_1\beta_1 - \langle \hat{Q}\hat{Q}^\dagger \rangle \alpha_2\beta_2)/2.
\end{aligned}$$

Equation (6.80) is the final form of the master equation describing the dynamics of the two coupled harmonic oscillators interacting with independent zero temperature baths with flat spectral densities.

6.3.2 The characteristic function

From the master equation (6.80) we obtain a partial differential equation for the two-mode quantum characteristic function,

$$\frac{\partial}{\partial t}\chi = z^T \mathbf{M}_1 z\chi + z^T \mathbf{N}_1 \nabla\chi, \tag{6.81}$$

where $\nabla = (\frac{\partial}{\partial \epsilon_a}, \frac{\partial}{\partial \epsilon_a^*}, \frac{\partial}{\partial \epsilon_b}, \frac{\partial}{\partial \epsilon_b^*})^T$ and

$$\mathbf{N}_1 = \begin{pmatrix} i\omega + \Gamma_2 - \Gamma_1 & 0 & \Gamma_5 - \Gamma_4 + i\epsilon & -i\kappa \\ 0 & -i\omega + \Gamma_2 - \Gamma_1 & i\kappa & -i\epsilon + \Gamma_5 - \Gamma_4 \\ i\epsilon + \Gamma_5 - \Gamma_4 & -i\kappa & i\omega + \Gamma_2 - \Gamma_1 & 0 \\ i\kappa & -i\epsilon + \Gamma_5 - \Gamma_4 & 0 & -i\omega + \Gamma_2 - \Gamma_1 \end{pmatrix} \tag{6.82}$$

$$\mathbf{M}_1 = \begin{pmatrix} -\Gamma_3 & -\Gamma_2 & \tilde{\Gamma}_x & -\Gamma_5 \\ -\Gamma_2 & -\Gamma_3 & -\Gamma_5 & \tilde{\Gamma}_y \\ \tilde{\Gamma}_x & -\Gamma_5 & -\Gamma_3 & -\Gamma_2 \\ -\Gamma_5 & \tilde{\Gamma}_y & -\Gamma_2 & -\Gamma_3 \end{pmatrix}, \tag{6.83}$$

with $\tilde{\Gamma}_x = i\kappa/2 - \Gamma_6$ and $\tilde{\Gamma}_y = -i\kappa/2 - \Gamma_6$. Using the numerical solution of equations (6.39) and (6.81), or equivalently, equations (6.38) and (6.80), we can compare the time evolution of the state of the two coupled oscillators initially prepared in Gaussian states. This is the subject of the next section.

6.4 Time evolution

By numerically solving the master equations obtained in sections 6.2 and 6.3, we can now compare the results of the two approaches. We are interested in studying the time evolution of the oscillators initially prepared in Gaussian states. The state of the oscillators can therefore be fully characterised in terms of the covariance matrix. Figures 6.1(a) and 6.1(b) show the average number of excitations for each oscillator evolving according to equations (6.38) (with $\bar{n}_a = \bar{n}_b = 0$) and (6.80). One can clearly see that the dissipative dynamics is different depending on which master equation and model for dissipation is used. As will be discussed later, the mismatch between the two approaches will become even stronger when one looks at the steady-state solutions of the two different master equations obtained through the above two approaches.

To quantify the quantum correlations between the two oscillators, we investigate

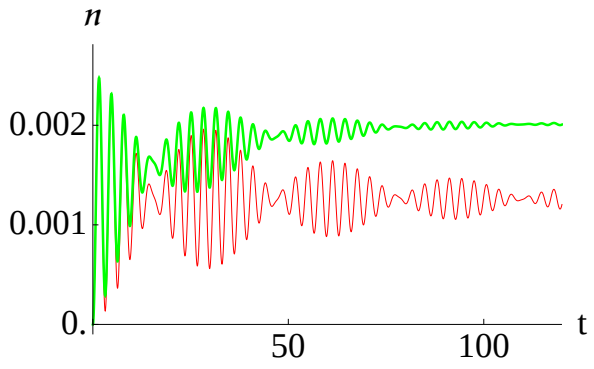

(a)

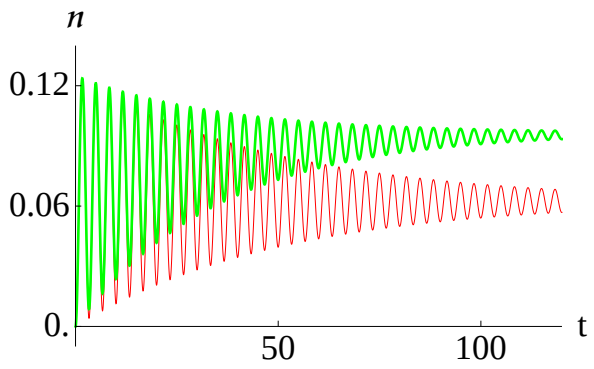

(b)

Figure 6.1: Average number of excitation quanta $n = \langle \hat{a}^\dagger(t)\hat{a}(t)\rangle = \langle \hat{b}^\dagger(t)\hat{b}(t)\rangle$ for each identically coupled oscillator, calculated using the master equations (6.38) (red, solid) and (6.80) (green, thick solid), plotted as a function of time. Each oscillator is initially in a vacuum state, and $\Gamma_a = \Gamma_b = \omega/100$. In (a), $\epsilon = \kappa = \omega/20$, and in (b) $\kappa = \omega/3$ and $\epsilon = 0$. Time is in units of $1/\omega$.

the entanglement between the oscillators initially prepared in Gaussian states, and evolving according to the master equations (6.38) and (6.80). For the case of two-mode Gaussian states, the covariance matrix $\mathbf{V}$ is a 4×4 symmetric matrix with $V_{ij} = (\langle R_i R_j + R_j R_i \rangle)/2$ where $i, j \epsilon \{a, b\}$ and $R^T = (\hat{q}_a, \hat{p}_a, \hat{q}_b, \hat{p}_b)$. Here $\hat{q}_i$ and $\hat{p}_i$ are the position and momentum quadratures of the ith oscillator. As before, to characterise the entanglement dynamics we use the logarithmic negativity (see Section 5.3.1). Using the numerical solutions of the partial differential equations (6.39) and (6.81) we compute the logarithmic negativity, shown in Fig. 6.2(a) and Fig. 6.2(b). As can be seen from these figures, the two different approaches for modelling the system-reservoir interactions, discussed in Sections 6.2 and 6.3, yield quantitatively very different results as far as quantum correlations between the two oscillators are concerned.

The difference in the dynamics can be further illustrated by computing the quantum fidelity between the time-evolved state of the two oscillators. In general, finding the fidelity between two quantum states is difficult, but for Gaussian states it is possible to arrive at a closed-form expression for the quantum fidelity in terms of the covariance matrix. We trace over the state of one of the oscillators, and compute the fidelity between the two different single-oscillator states resulting from the numerical solutions of equations (6.39) and (6.81).

The one-mode quantum characteristic function $\chi(\epsilon_a)$ can be deduced from the two-mode quantum characteristic function $\chi(\epsilon_a, \epsilon_b)$ through the identity $\chi(\epsilon_a, t) = \chi(\epsilon_a, \epsilon_b = 0, t)$. In this way a one-mode Gaussian state of the pair of oscillators can be defined, which is used for calculating the corresponding fidelity.

The quantum fidelity between two one-mode Gaussian states can be computed from

$$\mathcal{F} = \frac{2}{(\sqrt{\mathrm{Det}[\mathbf{A_1} + \mathbf{A_2}] + \mathcal{P}} - \sqrt{\mathcal{P}}} \tag{6.84}$$

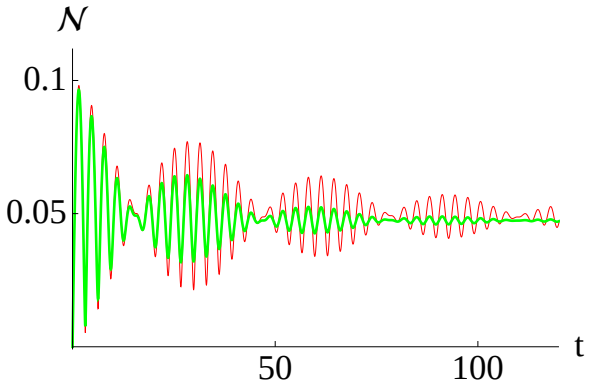

(a)

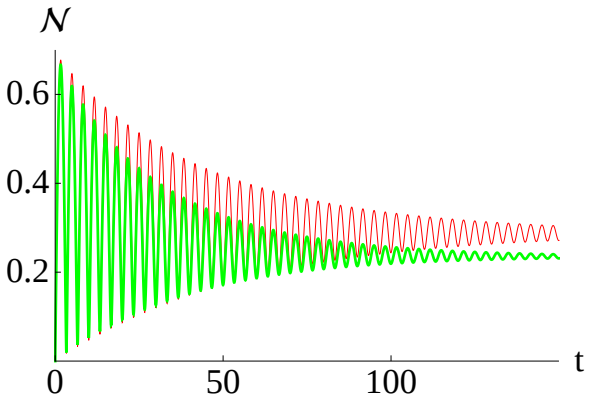

(b)

Figure 6.2: The logarithmic negativity plotted as a function of time, calculated using numerical solutions of the master equations (6.38) (red, solid) and (6.80) (green, thick solid). Each oscillator is initially in a vacuum state, and $\Gamma_a = \Gamma_b = \omega/100$. In (a) $\epsilon = \kappa = \omega/20$, and in (b) $\kappa = \omega/3$ and $\epsilon = 0$. Time is in units of $1/\omega$.

where

$$\mathcal{P} = (\mathrm{Det}[\mathbf{A_1}] - \mathbf{1})(\mathrm{Det}[\mathbf{A_2}] - \mathbf{1}), \tag{6.85}$$

and where $\mathbf{A_i}$ is the 2×2 covariance matrix corresponding to the i:th mode [144, 145]. The time evolution of the fidelity between the solutions of Sections 6.2 and 6.3 is shown in Fig. 6.3(a) and Fig. 6.3(b), where the initial state was chosen to be the ground state of each oscillator. As can be seen from these figures, when the inter-mode coupling strength between the oscillators increases, the fidelity between the time-evolved one-mode Gaussian states of each oscillator obtained through the solution of master equations (6.38) and (6.80) decreases. Thus it is evident that if the oscillators are strongly coupled then the solution of the master equation (6.38) starts to disagree with the solution of the master equation (6.80). Nonetheless the fidelity between the two solutions stays much above 99 % for a wide range of coupling strengths ϵ, κ. It should be noted from Fig. 6.3(a) and 6.3(b) that the mismatch between the solution of the master equations (6.38) and (6.80) becomes more prominent when increasing the two-mode squeezing interaction strength κ.

One of the main differences in the dissipative evolution is brought to light when one looks at the steady-state solutions of the master equations (6.38) and (6.77) respectively. Re-expressing the coupled oscillator operators $\hat{a}$ and $\hat{b}$ and their Hermitian conjugates in terms of the operators for the normal modes $\hat{l}$, $\hat{m}$ and their Hermitian conjugates, for identical heat baths ($\Gamma_a = \Gamma_b = \Gamma$) at zero temperature ($\bar{n}_a$=$\bar{n}_b$=0), the master equation (6.38) can be re-written as

$$\begin{aligned}\dot{\rho}(t) &= -i[(\alpha_{11}+\alpha_{22})\hat{l}^\dagger\hat{l} + (\beta_{11}+\beta_{22})\hat{m}^\dagger\hat{m}, \rho(t)] \\ &\quad + \frac{\alpha_1^2}{2}\Gamma\mathcal{L}_{\hat{l}} + \frac{\alpha_2^2}{2}\Gamma\mathcal{L}_{\hat{m}} + \frac{\beta_1^2}{2}\Gamma\mathcal{L}_{\hat{l}^\dagger} + \frac{\beta_2^2}{2}\Gamma\mathcal{L}_{\hat{m}^\dagger} \\ &\quad - \frac{\alpha_1\beta_1}{2}\Gamma\tilde{\mathcal{L}}_{\hat{l}} - \frac{\alpha_1\beta_1}{2}\Gamma\tilde{\mathcal{L}}_{\hat{l}^\dagger} - \frac{\alpha_2\beta_2}{2}\Gamma\tilde{\mathcal{L}}_{\hat{m}} - \frac{\alpha_2\beta_2}{2}\Gamma\tilde{\mathcal{L}}_{\hat{m}^\dagger},\end{aligned} \tag{6.86}$$

where $\mathcal{L}_{\hat{x}}$=$2\hat{x}\rho\hat{x}^\dagger - \hat{x}^\dagger\hat{x}\rho - \rho\hat{x}^\dagger\hat{x}$ and $\tilde{\mathcal{L}}_{\hat{x}}$=$2\hat{x}\rho\hat{x} - \hat{x}\hat{x}\rho - \rho\hat{x}\hat{x}$. Now it is a simple matter to verify that the steady state of master equation (6.77) is ρ_{ss}=$|0\rangle_{ee}\langle 0| \otimes |0\rangle_{ff}\langle 0|$

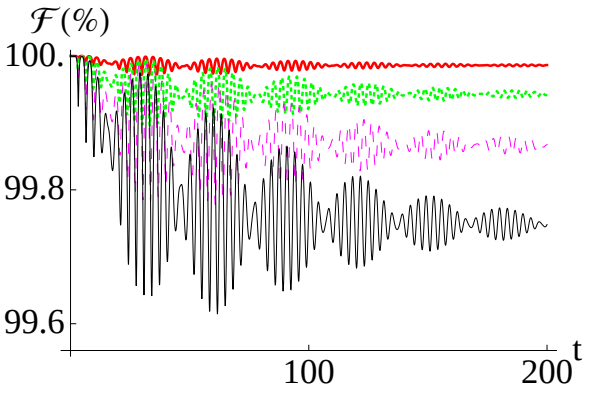

(a)

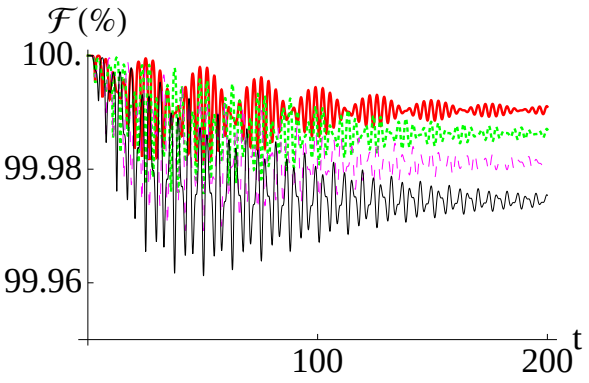

(b)

Figure 6.3: Time dependence of the quantum fidelity between the two one-mode states of each oscillator computed from the numerical solutions of equations (6.38) and (6.80) for $\Gamma_a = \Gamma_b = \omega/100$, when (a) $\epsilon = \omega/20$ and $\kappa = 6\omega/100$ (red, thick solid), $\kappa = 10\omega/100$ (green, thick dashed), $\kappa = 18\omega/100$ (pink, thin broken) and $\kappa = 25\omega/100$ (black, thin solid), and (b) $\kappa = \omega/20$ and $\epsilon = 6\omega/100$ (red, thick solid), $\epsilon = 10\omega/100$ (green, thick dashed), $\epsilon = 18\omega/100$ (pink, thin broken) and $\epsilon = 25\omega/100$ (black, thin solid). Each oscillator is initially in the vacuum state, and time is in units of $1/\omega$.

but that this is *not* the steady state of the master equation (6.86). This is one of the crucial findings of the present work, and may be of great significance in understanding the entanglement properties of the ground state of coupled harmonic oscillators.

6.5 Conclusions

We have discussed in detail the ubiquitous physical system of two coupled harmonic oscillators and the possibility of generating quantum entanglement in coupled harmonic oscillators under two different physical settings. Firstly, when the oscillators are interacting indirectly through a middle oscillator and secondly, when the two oscillators are directly coupled. We have investigated the quantum dynamics of the oscillators when the interactions are modelled with and without making the rotating wave approximation.

We have found that if the RWA is made then under the action of passive linear interactions the coupled harmonic oscillators, initially prepared in classical Gaussian states, will always remain separable. This has been found to hold true both in the presence and absence of dissipation. On the other hand, if the RWA is not made then quantum entanglement does build up between coupled harmonic oscillators.

We have derived a Markovian master equation where the interaction between the oscillators is modelled beyond the RWA. We compared two situations. First, the dissipation of each oscillator was modelled as a harmonic coupling to a bath of harmonic oscillators. This situation was then compared with the resulting dynamics when dissipation in the form of Lindblad terms in the master equation was added phenomenologically to each individual oscillator.

CHAPTER 7

CONCLUSIONS AND OUTLOOK

Entanglement is one of the major cornerstones of quantum theory and it endows a multi-partite state with the strange possibility to simultaneously exist *and* not exist among its different partitions at the same time. Entanglement is a unique attribute of the quantum world which could be held responsible for its entire departure from the classical world. Different subsystems of an entangled state are so strongly quantum correlated that even in the case of space-like separation between them, the quantum correlations persists.

The existence of quantum correlations is strange even at the microscopic scale, but the mystery gets deeper if one tries to see quantum effects in the macroscopic or even in the mesoscopic world. If one believes that quantum theory should be applicable to our 'classical' world, then a big challenge is to see non-classical features in the mesoscopic domain. Preparing bigger and bigger objects in non-classical states will clearly ascertain the validity of the quantum theory to the mesoscopic domain. Such investigations could also prove to be important benchmarks studies to investigate different decoherence mechanisms and thus could help us in understanding the arising of classicality at the macroscopic scale.

Thus, the main motivation behind the theoretical work carried out in this thesis is to investigate novel possibilities of preparing mesoscopic mechanical objects in non-classical states. We hope that the theoretical analysis carried out in this thesis could be a small step in bridging the gap between the quantum and the classical world. The work might pave the way to improve our understanding of the quantum-classical 'divide' along with helping to realise novel applications of mesoscopic mechanical systems for quantum information processing purposes.

Coupled harmonic oscillators capture the essential physics of many physical systems which are accessible in laboratories these days. These include very different physical systems such as coupled cavity modes, coupled nano- or micromechanical oscillators, or even the interactions between quantum fluctuations of the optical and the mechanical modes in the linearised regime in an optomechanical setup, just to name a few. Thus, a major part of the thesis is devoted to understand quantum features in continuous variable systems with truly infinite-dimensional Hilbert spaces.

We have investigated genuine quantum features in coupled harmonic oscillators initially prepared in Gaussian states. A simplest possible physical system is two bilinearly coupled harmonic oscillators. For instance, classically this coupling arises when two oscillators are coupled by an elastic spring. So far most of the studies that explore the quantum physics of such systems have centred their attention on two directly coupled oscillators. In the present work we have also extended this idea to explore a slightly different scenario with two indirectly coupled oscillators, where the indirect coupling between the two oscillators is mediated via another oscillator. This apparently similar looking physical system is found to have its own interesting physics embedded in it.

In the thesis we have centred our attention on the case when the harmonic oscillators are interacting under the action of a position-dependent coupling between their coordinates. As long as the coupling between the oscillators is weak, the interaction between the oscillators can be further approximated using the rotating-wave approx-

imation (RWA). Under the RWA, the bilinear interaction between the oscillators is simplified by dropping the two-mode squeezing terms from the Hamiltonian. For the case of two resonant oscillators with characteristic frequency ω, the RWA works very well as long as the inter-mode coupling strength between the oscillators κ is much smaller than ω. We have compared in detail the effect of making or not making the RWA. We have shown that for coupled harmonic oscillators initially prepared in *classical* Gaussian states and evolving under the RWA Hamiltonian, there is no possibility whatsoever of generating quantum correlations. This argument has been extended to a more practical scenario when the two oscillators are coupled to their local heat baths. On the other hand, on modelling the interaction between the oscillators beyond the RWA, the state of the two oscillators does become inseparable for initial classical separable states.

The main results reported in this thesis can be summarised as follows

- The thesis begins with encapsulating the physics of two indirectly coupled nanocantilevers where the indirect interaction between the oscillators is mediated via the cloud of an ultra-cold atomic ensemble. The interaction between the collective magnetic dipole moment of the atomic ensemble with the time-dependent magnetic field generated due to the motion of the nanocantilevers formed the basis of the scheme. The dynamics of the system was analysed both in the Schrödinger and Heisenberg pictures. The entanglement present in the system of two nanocantilevers is quantified in terms of negativity ($\mathcal{N}$) and tangle (τ). The robustness of our proposal lies in the fact that entangled states of nanomechanical systems could be generated even if the nanocantilevers are initially prepared in mixed states. The scheme is further investigated if the two nanocantilevers interact with the atomic ensemble in the dispersive regime and also if the interaction between the two nanocantilevers and the ultra-cold atoms is described beyond the commonly used rotating wave approximation. The chapter is then further expanded to include the effect of unavoidable cou-

pling with the external environment. It is then shown that by a suitable choice of physical parameters, it is possible to engineer the reservoir to generate robust entangled states of the two nanocantilevers.

- The theoretical investigations are extended to the case when the harmonic potential of coupled oscillators is modulated with an external nonlinearity. In particular, we investigated the dynamics of coupled oscillators when the harmonic potential is modulated with an anharmonic potential proportional to the fourth power of the oscillation amplitude of each oscillator from its equilibrium position. The presence of external nonlinearity is found to strongly affect the quantum dynamics of the oscillators. This is corroborated with a theoretical investigation carried out for two different physical scenarios. One in which the two nonlinear oscillators are interacting indirectly via a harmonic oscillator. In a second scenario a physical setup is envisaged where a movable mirror modelled as a nonlinear oscillator interacts with a quantised cavity mode. A physical scheme to induce quartic nonlinearity to the motion of a mechanical oscillator is also outlined.

- The theoretical analysis presented in the thesis is extended to a scheme to generate quantum correlations between two distant optomechanical cavities. With analytical calculations augmented with numerical investigations, quantum correlations are found to exist between various optical and mechanical modes in the steady state at finite temperature.

- In the concluding chapter of the thesis, we have theoretically investigated the quantum dynamics of strongly coupled bosonic modes. A master equation is derived and the solution is compared with the case when the dissipation in different modes is added *phenomenologically*. The dissipative evolution turned out to be quite different in the above two cases. We find that introducing dissipation through *adding* Lindblad operators corresponding to local heat baths results in a steady state which is different from the one obtained as a solution of

the master equation which takes into account the inter-mode coupling strength, and thus correctly describes the dynamics of strongly coupled bosonic modes.

APPENDICES

APPENDIX A

BOGOLIUBOV TRANSFORMATION

Equation (3.50) can be diagonalised by the Bogoliubov transformations

$$\begin{bmatrix} \hat{f} \\ \hat{f}^\dagger \end{bmatrix} = \begin{bmatrix} \alpha_1 & -\beta_1 \\ -\beta_1 & \alpha_1 \end{bmatrix} \begin{bmatrix} \hat{D}_1 \\ \hat{D}_1^\dagger \end{bmatrix} \tag{A.1}$$

$$\begin{bmatrix} \hat{g} \\ \hat{g}^\dagger \end{bmatrix} = \begin{bmatrix} \alpha_2 & -\beta_2 \\ -\beta_2 & \alpha_2 \end{bmatrix} \begin{bmatrix} \hat{D}_2 \\ \hat{D}_2^\dagger \end{bmatrix}, \tag{A.2}$$

where $\alpha_i^2 - \beta_i^2 = 1$ and $[\hat{D}_i, \hat{D}_i^\dagger] = 1$ for $i = 1, 2$. Under the above transformations, the diagonalised Hamiltonian takes the form

$$\begin{aligned} H &= \begin{bmatrix} \hat{D}_1^\dagger & \hat{D}_1 \end{bmatrix} \begin{bmatrix} D_{11} & 0 \\ 0 & D_{22} \end{bmatrix} \begin{bmatrix} \hat{D}_1 \\ \hat{D}_1^\dagger \end{bmatrix} + \begin{bmatrix} \hat{D}_2^\dagger & \hat{D}_2 \end{bmatrix} \begin{bmatrix} \widetilde{D}_{11} & 0 \\ 0 & \widetilde{D}_{22} \end{bmatrix} \begin{bmatrix} \hat{D}_2 \\ \hat{D}_2^\dagger \end{bmatrix} \\ &\quad + \begin{bmatrix} \hat{s}^\dagger & \hat{s} \end{bmatrix} \begin{bmatrix} \omega/2 & 0 \\ 0 & \omega/2 \end{bmatrix} \begin{bmatrix} \hat{s} \\ \hat{s}^\dagger \end{bmatrix} \end{aligned} \tag{A.3}$$

where

$$D_{11} = (\omega + \kappa/\sqrt{2})\alpha_1^2 + (\kappa/\sqrt{2})\beta_1^2 - \sqrt{2}\kappa\alpha_1\beta_1 \quad (A.4)$$

$$D_{22} = (\omega + \kappa/\sqrt{2})\beta_1^2 + (\kappa/\sqrt{2})\alpha_1^2 - \sqrt{2}\kappa\alpha_1\beta_1 \quad (A.5)$$

$$\widetilde{D}_{11} = (\omega - \kappa/\sqrt{2})\alpha_2^2 - (\kappa/\sqrt{2})\beta_2^2 + \sqrt{2}\kappa\alpha_2\beta_2 \quad (A.6)$$

$$\widetilde{D}_{22} = (\omega - \kappa/\sqrt{2})\beta_2^2 - (\kappa/\sqrt{2})\alpha_2^2 + \sqrt{2}\kappa\alpha_2\beta_2 \quad (A.7)$$

$$\alpha_1^2 = \frac{1}{2} + \frac{1}{2}\frac{(\omega + \sqrt{2}\kappa)}{\sqrt{(\omega + \sqrt{2}\kappa)^2 - 2\kappa^2}} \quad (A.8)$$

$$\beta_1^2 = -\frac{1}{2} + \frac{1}{2}\frac{(\omega + \sqrt{2}\kappa)}{\sqrt{(\omega + \sqrt{2}\kappa)^2 - 2\kappa^2}} \quad (A.9)$$

$$\alpha_2^2 = \frac{1}{2} + \frac{1}{2}\frac{(\omega - \sqrt{2}\kappa)}{\sqrt{(\omega - \sqrt{2}\kappa)^2 - 2\kappa^2}} \quad (A.10)$$

$$\beta_2^2 = -\frac{1}{2} + \frac{1}{2}\frac{(\omega - \sqrt{2}\kappa)}{\sqrt{(\omega - \sqrt{2}\kappa)^2 - 2\kappa^2}}. \quad (A.11)$$

Using the diagonalised Hamiltonian (A.3), the Heisenberg equations of motion for the time-evolved operators $\hat{D}_1^\dagger(t)$, $\hat{D}_2^\dagger(t)$ and $\hat{s}^\dagger(t)$ are

$$\frac{d}{dt}\hat{D}_1^\dagger = i[\hat{H}, \hat{D}_1^\dagger], \quad (A.12)$$

$$\frac{d}{dt}\hat{D}_2^\dagger = i[\hat{H}, \hat{D}_2^\dagger], \quad (A.13)$$

$$\frac{d}{dt}\hat{s}^\dagger = i[\hat{H}, \hat{s}^\dagger]. \quad (A.14)$$

Making use of the fact that $[\hat{D}_i, \hat{D}_j^\dagger] = \delta_{ij}$ we get

$$\hat{D}_1^\dagger(t) = e^{iK_1 t}\hat{D}_1^\dagger(0) \quad (A.15)$$

$$\hat{D}_2^\dagger(t) = e^{iK_2 t}\hat{D}_2^\dagger(0) \quad (A.16)$$

$$\hat{s}^\dagger(t) = e^{i\omega t}\hat{s}^\dagger(0), \quad (A.17)$$

where

$$K_1 = (\omega + \kappa/\sqrt{2})(\alpha_1^2 + \beta_1^2) - 2\sqrt{2}\kappa\alpha_1\beta_1 + (\kappa/\sqrt{2})(\alpha_1^2 + \beta_1^2), \tag{A.18}$$

$$K_2 = (\omega - \kappa/\sqrt{2})(\alpha_2^2 + \beta_2^2) + 2\sqrt{2}\kappa\alpha_2\beta_2 - (\kappa/\sqrt{2})(\alpha_2^2 + \beta_2^2). \tag{A.19}$$

Now the explicit form of **F** can be constructed by expressing $\hat{a}(t)$, $\hat{b}(t)$, $\hat{c}(t)$ in terms of $\hat{f}(t)$, $\hat{g}(t)$, $\hat{s}(t)$. For instance, the time-evolved operator $\hat{a}(t)$ can be reexpressed as

$$\hat{a}(t) = \frac{1}{2}(\hat{f}(t) + \hat{g}(t)) + \frac{\hat{s}(t)}{\sqrt{2}}. \tag{A.20}$$

Rewriting $\hat{f}(t)$ and $\hat{g}(t)$ in terms of $\hat{D}_1(t)$, $\hat{D}_2(t)$ and their Hermitian conjugates, equation (A.20) takes the form

$$\begin{aligned}\hat{a}(t) &= [\frac{\alpha_1^2}{2}\hat{f}(0) + \frac{\alpha_1\beta_1}{2}\hat{f}^\dagger(0)]e^{-iK_1t} - [\frac{\beta_1^2}{2}\hat{f}(0) + \frac{\alpha_1\beta_1}{2}\hat{f}^\dagger(0)]e^{iK_1t} \\ &\quad +[\frac{\alpha_2^2}{2}\hat{g}(0) + \frac{\alpha_2\beta_2}{2}\hat{g}^\dagger(0)]e^{-iK_2t} - [\frac{\beta_2^2}{2}\hat{g}(0) + \frac{\alpha_2\beta_2}{2}\hat{g}^\dagger(0)]e^{iK_2t} + \frac{\hat{s}(0)}{\sqrt{2}}e^{-i\omega t}\end{aligned} \tag{A.21}$$

In a similar manner the time-evolved expressions for the other mode operators can also be obtained. Finally $\hat{f}(0)$, $\hat{g}(0)$ and $\hat{s}(0)$ can be reexpressed in terms of $\hat{a}(0)$, $\hat{b}(0)$ and $\hat{c}(0)$ allowing us to get closed form analytical solutions for the time evolved Heisenberg operators $\hat{a}(t)$, $\hat{b}(t)$, $\hat{c}(t)$ and their hermitian conjugates.

APPENDIX B

UNITARY OPERATOR

The unitary operator $\hat{S}$ in (4.13) which is used to transform the Hamiltonian $\hat{H}_2$ in (4.17) gives the corresponding transformed time evolution operator

$$\hat{U}_{\rm trans}(t) = \exp\left[-i\omega_k t\hat{k}^\dagger\hat{k} + i\frac{g_k^2\omega_m}{\zeta^2}t(\hat{k}^\dagger\hat{k})^2\right]\exp\left[-i\zeta t\hat{a}^\dagger\hat{a} - i\beta t(\hat{a}^\dagger\hat{a})^2\right], \qquad \text{(B.1)}$$

where $\zeta = \omega_m + \beta$. The untransformed operator $\hat{U}(t)$ then becomes

$$\begin{aligned}\hat{U}(t) &= e^{-\hat{S}}\hat{U}_{\rm trans}(t)e^{\hat{S}} = \exp\left[-i\omega_k t\hat{k}^\dagger\hat{k} + i\frac{g_k^2\omega_m}{\zeta^2}t(\hat{k}^\dagger\hat{k})^2\right] \\ &\quad \exp(-\hat{S})\exp\left[-i\zeta t\hat{a}^\dagger\hat{a} - i\beta t(\hat{a}^\dagger\hat{a})^2\right]\exp(\hat{S}). \qquad \text{(B.2)}\end{aligned}$$

Using the Baker-Campbell-Hausdorff expansion [79] together with making the rotating wave approximation, and also neglecting quadratic and higher order terms in g_c/ζ, (B.2) simplifies to

$$\begin{aligned}\hat{U}(t) &= \exp\left\{-i[\omega_k t\hat{k}^\dagger\hat{k} - \frac{g_k^2}{\zeta^2}\left[\omega_m t - \sin(\zeta t)\right](\hat{k}^\dagger\hat{k})^2 + \beta t(\hat{a}^\dagger\hat{a})^2\right]\right\} \\ &\quad \times\exp\left[\frac{g_k}{\zeta}\hat{k}^\dagger\hat{k}(\hat{a}^\dagger - \hat{a}) - \frac{g_k}{\zeta}\hat{k}^\dagger\hat{k}(\hat{a}^\dagger e^{-i\zeta t} - \hat{a}e^{i\zeta t})\right]\exp\left[-i\zeta t\hat{a}^\dagger\hat{a}\right]. \qquad \text{(B.3)}\end{aligned}$$

BIBLIOGRAPHY

[1] R. Penrose, in Mathematical Physics 2000, edited by A. Fokas et al. (Imperial College, London).

[2] W. H. Zurek: Decoherence and the transition from quantum to classical, *Phys. Today* **44** (10), 36 (1991).

[3] See http://discovermagazine.com/2005/jun/cover/article.

[4] L. Hackermüller, K. Hornberger, B. Brezger, A. Zellinger and M. Arndt: Decoherence of matter waves by thermal emission of radiation, *Nature* (London) **427**, 711 (2004).

[5] M. Brune, E. Hagley, J. Dreyer, X. Maître, A. Maali, C. Wunderlich, J. M. Raimond and S. Haroche: Observing the progressive decoherence of the "meter" in a quantum measurement, *Phys. Rev. Lett.* **77**, 4887 (1996).

[6] C. Monroe, D. M. Meekhof, B. E. King and D. J. Wineland: A "Schrödinger cat" superposition state of an atom, *Science* **272**, 1131 (1996).

[7] B. Deb and G. S. Agarwal: Entangling two Bose-Einstein condensates by stimulated Bragg scattering, *Phys Rev. A* **67**, 023603 (2003).

[8] G. S. Agarwal, P. Lougovski and H. Walther: Multiparticle entanglement and the Schrödinger cat state using ground-state coherences, *J. Mod. Opt.* **52**, 1397 (2005).

[9] K. C. Schwab and M. L. Roukes: Putting mechanics into quantum mechanics, *Phys. Today* **58** (7), 36 (2005).

[10] T. Rocheleau, T. Ndukum, C. Macklin, J. B. Hertzberg, A. A. Clerk and K. C. Schwab: Preparation and detection of a mechanical resonator near the ground state of motion, *Nature* (London) **463**, 72 (2010).

[11] F. Khalili, S. Danilishin, H. Miao, H. Müller-Ebhardt, H. Yang and Y. Chen: Preparing a mechanical oscillator in non-Gaussian quantum states, *Phys. Rev. Lett.* **105**, 070403 (2010).

[12] A. Kolkiran and G. S. Agarwal: Amplitude noise reduction in a nano-mechanical oscillator, *Mathematical and Computational Applications*, **16**, 290 (2011).

[13] P. Rabl, A. Shnirman and P. Zoller: Generation of squeezed states of nanomechanical resonators by reservoir engineering, *Phys. Rev. B* **70**, 205304 (2004).

[14] E. Schrödinger: Die gegenwartige situation in der quantenmechanik, Naturwissenschaften **23**, 807-812; 823-823; 844-849 (1935).

[15] A.D. Armour, M. P. Blencowe and K. C. Schwab: Entanglement and decoherence of a micromechanical resonator via coupling to a Cooper-pair box, *Phys Rev. Lett.* **88**, 148301 (2002).

[16] W. Marhsall, C. Simon, R. Penrose and D. Bouwmeester: Towards quantum superpositions of a mirror, *Phys Rev. Lett.* **91**, 130401 (2003).

[17] C. H. Metzger and K. Karrai: Cavity cooling of a microlever, *Nature* (London) **432**, 1002 (2004).

[18] I. Wilson-Rae, N. Nooshi, J. Dobrindt, T. J. Kippenberg and W. Zwerger: Cavity-assisted backaction cooling of mechanical resonators, *New J. Phys* **10**, 095007 (2008).

[19] S. Gröblacher, J. B. Hertzberg, M. R. Vanner, G. D. Cole, S. Gigan, K. C. Schwab and M. Aspelmeyer: Demonstration of an ultracold micro-optomechanical oscillator in a cryogenic cavity, *Nature Phys.* **5**, 485 (2009).

[20] I. Favero, C. Metzger, S. Camerer, D. König, H. Lorenz, J. P. Kotthaus and K. Karrai: Optical cooling of a micromirror of wavelength size, *Appl. Phys. Lett.* **90**, 104101 (2007).

[21] A. D. O'Connell, M. Hofheinz, M. Ansmann, R. C. Bialczak, M. Lenander, E. Lucero, M. Neeley, D. Sank, H. Wang, M. Weides, J. Wenner, J. M. Martinis and A. N. Cleland: Quantum ground state and single-phonon control of a mechanical resonator, *Nature* (London) **464**, 697 (2010).

[22] J. Chan, T. P. Mayer Alegre, A. H. Safavi-Naeini, J. T. Hill, A. Krause, S. Gröblacher, M. Aspelmeyer and O. Painter: Laser cooling of a nanomechanical oscillator into its quantum ground state, *Nature* (London) **478**, 89 (2011).

[23] L. Tian and P. Zoller: Coupled ion-nanomechanical systems, *Phys. Rev. Lett.* **93**, 266403 (2004).

[24] P. Treutlein, D. Hunger, S. Camerer, T. W. Hänsch and J. Reichel: Bose-Einstein condensate coupled to a nanomechanical resonator on an atom ahip, *Phys. Rev. Lett.* **99**, 140403 (2007).

[25] S. Bose and G. S. Agarwal: Entangling pairs of nano-cantilevers, Cooper-pair boxes and mesoscopic teleportation, *New Journal of Physics* **8**, 34 (2006).

[26] P. Rabl, P. Cappellaro, M. V. Gurudev Dutt, L. Jiang, J. R. Maze and M. D. Lukin: Strong magnetic coupling between an electronic spin qubit and a mechanical resonator, *Phys. Rev. B* **79**, 041302(R) (2009).

[27] M. R. Geller and A. N. Cleland: Superconducting qubits coupled to nanoelectromechanical resonators: An architecture for solid-state quantum-information processing, *Phys. Rev. A* **71**, 032311 (2005).

[28] For a review, see M. Wallquist, K. Hammerer, P. Rabl, M. Lukin and P. Zoller: Hybrid quantum devices and quantum engineering, *Phys. Scr.,* **T137**, 014001 (2009).

[29] Y.-J. Wang, M. Eardley, S. Knappe, J. Moreland, L. Hollberg and J. Kitching: Magnetic resonance in an atomic vapor excited by a mechanical resonator, *Phys. Rev. Lett.* **97**, 227602 (2006).

[30] A. Einstein, B. Podolsky and N. Rosen: Can quantum-mechanical description of physical reality be considered complete ?, *Phys. Rev.* **47**, 777 (1935).

[31] John S. Bell: On the Einstein Podolsky Rosen paradox, *Physics* **1**, 195 (1964).

[32] C. H. Bennett, G. Brassard, C. Crépeau, R. Jozsa, A. Peres and W. K. Wootters: Teleporting an unknown quantum state via dual classical and Einstein-Podolsky-Rosen channels, *Phys. Rev. Lett.* **70**, 1895 (1993).

[33] N. Gisin, G. Ribordy, W. Tittel and H. Zbinden: Quantum cryptography, *Rev. Mod. Phys.* **74**, 145 (2002).

[34] M. A. Nielsen and I. L. Chuang, 2000, *Quantum Computation and Quantum Information* (Cambridge University Press).

[35] M. Arndt, O. Nairz, J. Vos-Andreae, C. Keller, G. van der Zouw and A. Zellinger: Waveparticle duality of C_{60} molecules, *Nature* (London) **401**, 680 (1999).

[36] B. Julsgaard, A. Kozhekin and E. S. Polzik: Experimental long-lived entanglement of two macroscopic objects, *Nature* (London) **413**, 400 (2001).

[37] S. Singh, M. Bhattacharya, O. Dutta and P. Meystre: Coupling nanomechanical cantilevers to dipolar molecules, *Phys. Rev. Lett.* **101**, 263603 (2008).

[38] C. A. Regal, J. D. Teufel and K. W. Lehnert: Measuring nanomechanical motion with a microwave cavity interferometer, *Nature Phys.* **4**, 555 (2008).

[39] J. D. Thompson, B. M. Zwickl, A. M. Jayich, F. Marquardt, S. M. Girvin and J. G. E. Harris: Strong dispersive coupling of a high-finesse cavity to a micromechanical membrane, *Nature* (London) **452**, 72 (2008).

[40] C. Joshi, A. Hutter, F. E. Zimmer, M. Jonson, E. Andersson and P. Öhberg: Quantum entanglement of nanocantilevers, *Phys. Rev. A* **82**, 043846 (2010).

[41] J. Anders: Thermal state entanglement in harmonic lattices, *Phys. Rev. A* **77**, 062102 (2008).

[42] P. Rabl, S. J. Kolkowitz, F. H. L. Koppens, J. G. E. Harris, P. Zoller and M. D. Lukin: A quantum spin transducer based on nanoelectromechanical resonator arrays, *Nature Phys.* **6**, 602 (2010).

[43] E. T. Jaynes and F. W. Cummings: Comparison of quantum and semiclassical radiation theories with application to the beam maser, Proc. IEEE **51**, 89 (1963).

[44] M. Tavis and F. W. Cummings: Exact solution for an N-molecule-radiation-field Hamiltonian, *Phys. Rev.* **170**, 379 (1968).

[45] J. S. Aldridge and A. N. Cleland: Noise-enabled precision measurements of a Duffing nanomechanical resonator, *Phys. Rev. Lett.* **94**, 156403 (2005).

[46] I. Katz, A. Retzker, R. Straub and R. Lifshitz: Signatures for a classical to quantum transition of a driven nonlinear nanomechanical resonator, *Phys. Rev. Lett.* **99**, 040404 (2007).

[47] K. K. Lehmann: On the relation of Child and Lawton's harmonically coupled anharmonic-oscillator model and Darling-Dennison coupling, *J. Chem. Phys.* **79**, 1098 (1983).

[48] G. J. Milburn and C. A. Holmes: Dissipative quantum and classical Liouville mechanics of the anharmonic oscillator, *Phys. Rev. Lett.* **56**, 2237 (1996).

[49] V. Peano and M. Thorwart: Nonlinear response of a driven vibrating nanobeam in the quantum regime, *New J. Phys.* **8**, 21 (2006).

[50] L. Chotorlishvili, A. Ugulava, G. Mchedlishvili, A. Komnik, S. Wimberger and J. Berakdar: Nonlinear dynamics of two coupled nano-electromechanical resonators, arXiv 1106.5201 (2011).

[51] M. Kurpas, J. Dajka and E. Zipper: Entanglement of qubits via a nonlinear resonator, *J. Phys.: Condes. Matter* **21**, 235602 (2009).

[52] R. Almog, S. Zaitsev, O. Shtempluck and E. Buks: Noise squeezing in a nanomechanical Duffing resonator, *Phys. Rev. Lett.* **98**, 078103 (2007).

[53] S. L. Braunstein and H. J. Kimble: Dense coding for continuous variables, *Phys. Rev. A* **61**, 042302 (2000); T. Tyc and B. C. Sanders: How to share a continuous-variable quantum secret by optical interferometry, *Phys. Rev. A* **65**, 042310 (2002); S. L. Braunstein and H. J. Kimble: Teleportation of continuous quantum variables, *Phys. Rev. Lett.* **80**, 869 (1998); R. E. S. Polkinghorne and T. C. Ralph: Continuous variable entanglement swapping, *Phys. Rev. Lett.* **83**, 2095 (1999).

[54] C. Joshi, M. Jonson, E. Andersson and P. Öhberg: Quantum entanglement of anharmonic oscillators, *J. Phys. B: At. Mol. Opt. Phys.* **44**, 245503 (2011).

[55] F. Marquardt and S. M. Girvin: Trend: Optomechanics, *Physics* **2**, 40 (2009).

[56] C. Joshi, J. Larson, M. Jonson, E. Andersson and P. Öhberg: Entanglement of distant optomechanical systems, *Phys. Rev. A* **85**, 033805 (2012).

[57] W.K. Wootters: Entanglement of formation of an arbitrary state of two qubits, *Phys. Rev. Lett.* **80**, 2245 (1998).

[58] G. Vidal and R. F. Werner: Computable measure of entanglement, *Phys. Rev. A* **65**, 032314 (2002).

[59] S. P. Walborn, P. H. Souto Ribeiro, L. Davidovich, F. Mintert and A. Buchleitner: Experimental determination of entanglement with a single measurement, *Nature* (London) **440**, 1022 (2006).

[60] H. Jeong, W. Son, M. S. Kim, D. Ahn and Č. Brukner: Quantum nonlocality test for continuous-variable states with dichotomic observables, *Phys. Rev. A* **67**, 012106 (2003).

[61] U. Leonhardt, 2003, *Measuring the Quantum State of Light* (Cambridge University Press).

[62] D. Girolami and G. Adesso: Observable measure of bipartite quantum correlations, *Phys. Rev. Lett.* **108**, 150403 (2012).

[63] S. Singh and P. Meystre: Atomic probe Wigner tomography of a nanomechanical system, *Phys. Rev. A* **81**, 041804(R) (2010).

[64] L. Mazzola and M. Paternostro: Distributing fully optomechanical quantum correlations, *Phys. Rev. A* **83**, 062335 (2011).

[65] D. Vitali, S. Gigan, A. Ferreira, H. R. Böhm, P. Tombesi, A. Guerreiro, V. Vedral, A Zeilinger and M. Aspelmeyer: Optomechanical entanglement between a movable mirror and a cavity Field, *Phys. Rev. Lett.* **98**, 030405 (2007).

[66] K. B. Davis, M. -O. Mewes, M. R. Andrews, N. J. van Druten, D. S. Durfee, D. M. Kurn and W. Ketterle: Bose-Einstein condensation in a gas of sodium atoms, *Phys. Rev. Lett.* **75**, 3969 (1995); D. S. Jin, J. R. Ensher, M. R. Matthews, C. E. Wieman and E. A. Cornell: Collective excitations of a Bose-Einstein condensate in a dilute gas, *ibid* **77**, 420 (1996).

[67] M. Greiner, O. Mandel, T. Esslinger, T. W. Hänsch and I. Bloch: Quantum phase transition from a superfluid to a Mott insulator in a gas of ultracold atoms,

Nature (London) **415**, 39 (2002).

[68] J. Simon, W. S. Bakr, R. Ma, M. E. Tai, P. M. Preiss and M. Greiner: Quantum simulation of antiferromagnetic spin chains in an optical lattice, *Nature* (London) **472**, 307 (2011).

[69] I. Bloch, J. Dalibard and W. Zwerger: Many-body physics with ultracold gases, *Rev. Mod. Phys.* **80**, 885 (2008).

[70] A. Wallraff, D. I. Schuster, A. Blais, L. Frunzio, R.- S. Huang, J. Majer, S. Kumar, S. M. Girvin and R. J. Schoelkopf: Strong coupling of a single photon to a superconducting qubit using circuit quantum electrodynamics, *Nature* **431**, 162 (2004).

[71] A. Naik, O. Buu, M.D. LaHaye, A. D. Armour, A. A. Clerk, M. P. Blencowe and K. C. Schwab: Cooling a nanomechanical resonator with quantum back-action, *Nature* (London) **443**, 193 (2006).

[72] J. D. Teufel, T. Donner, D. Li, J. W. Harlow, M. S. Allman, K. Cicak, A. J. Sirois, J. D. Whittaker, K. W. Lehnert and R. W. Simmonds: Sideband cooling of micromechanical motion to the quantum ground state, *Nature* (London) **475**, 359 (2011).

[73] M. Poot and Herre S. J. van der Zant: Mechanical systems in the quantum regime, *Physics Reports* **511**(5), 273 (2012).

[74] K. L. Ekinci and M.L. Roukes: Nanoelectromechanical systems, *Rev. Sci. Instrum.* **76**, 061101 (2005).

[75] R. H. Dicke: Coherence in spontaneous radiation processes, *Phys. Rev.* **93**, 99 (1954).

[76] Y. Yamamoto and A. Imamoglu, 1999, *Mesoscopic Quantum Optics* (John Wiley and Sons).

[77] T. Kishimoto, H. Hachisu, J. Fujiki, K. Nagato, M. Yasuda and H. Katori: Electrodynamic trapping of spinless neutral atoms with an atom chip, *Phys. Rev. Lett.* **96**, 123001 (2006).

[78] P. Treutlein, T. W. Hänsch, J. Reichel, A. Negretti, M. A. Cirone and T. Calarco: Microwave potentials and optimal control for robust quantum gates on an atom chip, *Phys. Rev. A* **74**, 022312 (2006).

[79] S. M. Barnett and P. M. Radmore, 1997, *Methods in Theoretical Quantum Optics* (Oxford University Press).

[80] M. B. Plenio, S. F. Huelga, A. Beige and P. L. Knight: Cavity-loss-induced generation of entangled atoms, *Phys. Rev. A* **59**, 2468 (1999).

[81] See A. Beige, S. Bose, D. Braun, S. F. Huelga, P. L. Knight, M. B. Plenio and V. Vedral: Entangling atoms and ions in dissipative environments, *J. Mod. Opt.* **47**, 2583 (2000) and references therein.

[82] A. Peres: Separability criterion for density matrices, *Phys. Rev. Lett.* **77,** 1413 (1996).

[83] T. E. Tessier, I. H. Deutsch, A. Delgado and I. Fuentes-Guridi: Entanglement sharing in the two-atom Tavis-Cummings model, *Phys. Rev. A* **68,** 062316 (2003).

[84] P. Rungta, V. Bužek, C. M. Caves, M. Hillery and G. J. Milburn: Universal state inversion and concurrence in arbitrary dimensions, *Phys. Rev. A* **64,** 042315 (2001).

[85] T. Holstein and H. Primakoff: Field dependence of the intrinsic domain magnetization of a ferromagnet, Phys. Rev. **58,** 1098 (1940).

[86] H. Haug and S. W. Koch, 1994, *Quantum theory of the optical and electronic properties of semiconductors* (World Scientific, Singapore).

[87] M. S. Kim, W. Son, V. Bužek and P. L. Knight: Entanglement by a beam splitter: Nonclassicality as a prerequisite for entanglement, *Phys. Rev. A* **65,** 032323 (2002).

[88] D. Zueco, G. M. Reuther, S. Kohler and P. Hänggi: Qubit-oscillator dynamics in the dispersive regime: Analytical theory beyond the rotating-wave approximation, *Phys. Rev. A* **80,** 033846 (2009).

[89] D. Braak: Integrability of the Rabi Model, *Phys. Rev. Lett.* **107,** 100401 (2011).

[90] T. Niemczyk, F. Deppe, H. Huebl, E. P. Menzel, F. Hocke, M. J. Schwarz, J. J. Garcia-Ripoll, D. Zueco, T. Hümmer, E. Solano, A. Marx and R. Gross: Circuit quantum electrodynamics in the ultrastrong-coupling regime, *Nature Physics* **6**, 772 (2010).

[91] A. E. Leanhardt, Y. Shin, A. P. Chikkatur, D. Kielpinski, W. Ketterle and D. E. Pritchard: Bose-Einstein condensates near a microfabricated surface, *Phys. Rev. Lett.* **90**, 100404 (2003).

[92] M. P. A. Jones, C. J. Vale, D. Sahagun, B. V. Hall and E. A. Hinds: Spin coupling between cold atoms and the thermal fluctuations of a metal surface, *Phys. Rev. Lett.* **91**, 080401 (2003).

[93] H.-P. Breuer and F. Petruccione, 2002, *The Theory of Open Quantum Systems* (Oxford University Press).

[94] J. Larson: Anomalous decoherence and absence of thermalization in a photonic many-body system, *Phys. Rev. A* **83**, 052103 (2011).

[95] G. P. Berman and G. M. Zaslavsky: Theory of quantum nonlinear resonance, *Phys. Lett. A* **61**, 295 (1977).

[96] L. Chotorlishvili and A. Ugulava: Quantum chaos and its kinetic stage of evolution, *Physica D* **239**, 103 (2010).

[97] S. Mancini, V. I. Man'ko and P. Tombesi: Ponderomotive control of quantum macroscopic coherence, *Phys. Rev. A.* **55**, 3042 (1997).

[98] S. Bose, K. Jacobs and P. L. Knight: Preparation of nonclassical states in cavities with a moving mirror, *Phys. Rev. A* **56**, 4175 (1997).

[99] A. F. Pace, M. J. Collett and D. F. Walls: Quantum limits in interferometric detection of gravitational radiation, *Phys. Rev. A* **47**, 3173 (1993).

[100] S. Singh, G. A. Phelps, D. S. Goldbaum, E. P. Wright and P. Meystre: All-optical optomechanics: An optical spring mirror, *Phys. Rev. Lett.* **105**, 213602 (2010).

[101] J. R. Friedman, V. Patel, W. Chen, S. K. Tolpygo and J. E. Lukens: Quantum superposition of distinct macroscopic states, *Nature* (London) **406**, 43 (2000).

[102] H. M. Wiseman and G. J. Milburn, *Quantum Measurement and Control*, (Cambridge University Press, Cambridge, 2009).

[103] T. J. Kippenberg and K. J. Vahala: Cavity optomechanics: Back-action at the mesoscale, *Science* **321**, 1172 (2008).

[104] T. J. Kippenberg and K. J. Vahala: Cavity opto-mechanics, *Optics Express* **15**, 17172 (2007).

[105] T. J. Kippenberg, H. Rokhsari, T. Carmon, A. Scherer and K. J. Vahala: Analysis of radiation-pressure induced mechanical oscillation of an optical microcavity, *Phys. Rev. Lett.* **95**, 033901 (2005).

[106] A. Dorsel, J. D. McCullen, P. Meystre, E. Vignes and H. Walther: Optical bistability and mirror confinement induced by radiation pressure, *Phys. Rev. Lett.* **51**, 1550 (1983).

[107] S. Gröblacher, K. Hammerer, M. R. Vanner and M. Aspelmeyer: Observation of strong coupling between a micromechanical resonator and an optical cavity

field, *Nature* (London) **460**, 724 (2009).

[108] J. D. Teufel, D. Li, M. S. Allman, K. Cicak, A. J. Sirois, J. D. Whittaker and R. W. Simmonds: Circuit cavity electromechanics in the strong-coupling regime, *Nature* (London) **471**, 204 (2011).

[109] S. Mancini, V. Giovannetti, D. Vitali and P. Tombesi: Entangling macroscopic oscillators exploiting radiation pressure, *Phys. Rev. Lett.* **88**, 120401 (2002); W. Marshall, C. Simon, R. Penrose and D. Bouwmeester: Towards quantum superpositions of a mirror, *ibid* **91**, 130401 (2003).

[110] S. Huang and G. S. Agarwal: Entangling nanomechanical oscillators in a ring cavity by feeding squeezed light, *New J. Phys.* **11**, 103044 (2009).

[111] Sh. Barzanjeh, D. Vitali, P. Tombesi and G. J. Milburn: Entangling optical and microwave cavity modes by means of a nanomechanical resonator, *Phys. Rev. A* **84**, 042342 (2011).

[112] M. Pinard, A. Dantan, D. Vitali, O. Arcizet, T. Briant and A. Heidmann: Entangling movable mirrors in a double-cavity system, *Europhys. Lett.* **72**, 747 (2005).

[113] M. J. Hartmann and M. B. Plenio: Steady state entanglement in the mechanical vibrations of two dielectric membranes, *Phys. Rev. Lett.* **101**, 200503 (2008).

[114] M. Bhattacharya and P. Meystre: Multiple membrane cavity optomechanics, *Phys. Rev. A* **78**, 041801(R) (2008).

[115] J. Larson and M. Horsdal: Photonic Josephson effect, phase transitions, and chaos in optomechanical systems, *Phys. Rev. A* **84**, 021804(R) (2011).

[116] U. Akram, N. Kiesel, M. Aspelmeyer and G. J. Milburn: Single-photon optomechanics in the strong coupling regime, *New J. Phys.* **12**, 083030 (2010).

[117] P. Rabl: Photon blockade effect in optomechanical systems, *Phys. Rev. Lett.* **107**, 063601 (2011); A. Nunnenkamp, K. Børkje and S. M. Girvin: Single-photon optomechanics, *Phys. Rev. Lett.* **107**, 063602 (2011).

[118] C. K. Law: Interaction between a moving mirror and radiation pressure: A Hamiltonian formulation, Phys. Rev. A **51**, 2537 (1995).

[119] F. Pinheiro and A. F. R. de Toledo Piza: Quantum entanglement of bound particles under free center of mass dispersion, *Phys. Scr.* **85**, 065002 (2012).

[120] H. P. Yuen: Two-photon coherent states of the radiation field, *Phys. Rev. A* **13**, 2226 (1976).

[121] G. Adesso and F. Illuminati: Entanglement in continuous-variable systems: recent advances and current perspectives, *J. Phys. A: Math. Theor.* **40**, 7821 (2007).

[122] T. Yu and J. H. Eberly: Finite-time disentanglement via spontaneous emission, *Phys. Rev. Lett.* **93**, 140404 (2004); T. Yu and J. H. Eberly: Sudden death of entanglement, *Science* **323**, 598 (2009).

[123] K. Mølmer, Y. Castin and J. Dalibard: Monte Carlo wave-function method in quantum optics, *J. Opt. Soc. Am. B* **10**, 524 (1993).

[124] D. F. Walls and G. J. Milburn, *Quantum Optics* (Springer-Verlag, Heidelberg, 2008).

[125] M. V. Berry: Quantal phase factors accompanying adiabatic changes, *Proc. R. Soc. Lond. A* **392**, 45 (1984).

[126] A. Bohm, A. Mostafazadeh, H. Koizumi, Q. Niu and J. Zwanziger, *The Geometric Phase in Quantum Systems*, (Springer, Berlin, 2003); J. Larson and S. Levin: Effective abelian and non-abelian gauge potentials in cavity QED, *Phys. Rev. Lett.* **103**, 013602 (2009); J. Dalibard, F. Gerbier, G. Juzeliūnas and P. Öhberg:

Colloquium: Artificial gauge potentials for neutral atoms, Rev. Mod. Phys. **83**, 1523 (2011).

[127] J. A. Jones, V. Vedral, A. Ekert and G. Castagnoli: Geometric quantum computation using nuclear magnetic resonance, *Nature* (London) **403**, 869 (2000).

[128] Q.-H. Duan and P.-X. Chen: Realization of universal adiabatic quantum computation with fewer physical resources, *Phys. Rev. A* **84**, 042332 (2011).

[129] K.-P. Marzlin and B. C. Sanders: Inconsistency in the application of the adiabatic theorem, *Phys. Rev. Lett.* **93**, 160408 (2004).

[130] D. M. Tong, K. Singh., L. C. Kwek and C. H. Oh: Quantitative conditions do not guarantee the validity of the adiabatic approximation, *Phys. Rev. Lett.* **95**, 110407 (2005).

[131] M. H. S. Amin: Consistency of the adiabatic theorem, *Phys. Rev. Lett.* **102**, 220401 (2009).

[132] X.L. Huang, S. L. Wu., L. C. Wang and X. X. Yi: Born-Oppenheimer approximation for open quantum systems within the quantum trajectory approach, *Phys. Rev. A* **81**, 052113 (2010).

[133] M. Paternostro, D. Vitali, S. Gigan, M. S. Kim, C. Brukner, J. Eisert and M. Aspelmeyer: Creating and probing multipartite macroscopic entanglement with light, *Phys. Rev. Lett.* **99**, 250401 (2007).

[134] C. Genes, A. Mari, D. Vitali and P. Tombesi: Quantum effects in optomechanical systems, *Adv. At. Mol. Opt. Phys.* **57**, 33 (2009).

[135] U. Akram and G. J. Milburn: Photon phonon entanglement in coupled optomechanical arrays, arXiv:1109.0790.

[136] O. Romero-Isart, A. C. Pflanzer, F. Blaser, R. Kaltenbaek, N. Kiesel, M. Aspelmeyer and J. I. Cirac: Large quantum superpositions and interference of mas-

sive nanometer-sized objects, *Phys. Rev. Lett.* **107**, 020405 (2011).

[137] R. Horodecki, P. Horodecki, M. Horodecki and K. Horodecki: Quantum entanglement, *Rev. Mod. Phys.* **81**, 865 (2009).

[138] W. H. Zurek: Decoherence, einselection, and the quantum origins of the classical, *Rev. Mod. Phys.* **75**, 715 (2003).

[139] M. B. Plenio and S. F. Huelga: Entangled light from white noise, *Phys. Rev. Lett.* **88**, 197901 (2002).

[140] J. Eisert, M. B. Plenio, S. Bose and J. Hartley: Towards quantum entanglement in nanoelectromechanical devices, *Phys. Rev. Lett.* **93**, 190402 (2004).

[141] L. Mandel: Non-classical states of the electromagnetic field, *Phys. Scrip* **T12**, 34 (1986).

[142] E. Shchukin and W. Vogel: Inseparability criteria for continuous bipartite quantum states, *Phys. Rev. Lett.* **95**, 230502 (2005).

[143] A. O. Caldeira and A. J. Leggett: Path integral approach to quantum Brownian motion, *Physica A* **121**, 587 (1983); A. O. Caldeira and A. J. Leggett: Quantum Tunnelling in a Dissipative System, *Annals of Physics*, **149**, 374 (1983); R. P. Feynman and F. L. Vernon: The theory of a general quantum system interacting with a linear dissipative system, *Annals of Physics* **24**, 1208 (1963).

[144] H. Scutaru: Fidelity for displaced squeezed thermal states and the oscillator semigroup, *J. Phys. A: Math. Gen.* **31**, 3659 (1998).

[145] Gh.-S. Paraoanu and H. Scutaru: Fidelity for multimode thermal squeezed states, *Phys. Rev. A* **61**, 022306 (2000).